EQUINE SKELETAL MUSCLE MITOCHONDRIAL FUNCTION AND REGENERATION CAPACITY WITH AGING

By

CHENGCHENG LI

A DISSERTATION PRESENTED TO THE GRADUATE SCHOOL
OF THE UNIVERSITY OF FLORIDA IN PARTIAL FULFILLMENT
OF THE REQUIREMENTS FOR THE DEGREE OF
DOCTOR OF PHILOSOPHY

UNIVERSITY OF FLORIDA

2017

To my family

ACKNOWLEDGMENTS

I would like to thank numerous wonderful people who have supported me throughout my PhD life. I must thank my advisor Dr. Stephanie Wohlgemuth, a great scientist I will never forget. She is very knowledgeable and has taught me many great skills regarding to muscle physiology. Without her excellent guidance and dedication, I would never complete my dissertation. I want to give Dr. Wohlgemuth one more thanks for giving me her friendship and life-advice. She has been taking care of me through all these years. Moreover, she has never forgotten to prepare cute presents for my little girl. I would also like to thank the rest of my graduate committee Dr. Lori Warren, Dr. John Driver and Dr. Christiaan Leeuwenburgh for their invaluable academic support. Dr. Warren has been so helpful with planning and designing all the horse studies, and guided me through the experiments. Dr. Driver and Dr. Leeuwenburgh have made themselves so approachable to help me to develop my background in physiology and molecular biology.

There are also so many faculty members that have made me complete my projects. I thank Dr. John Bromfield, Dr. Corwin Nelson, Dr. Peter Hansen and Dr. Timothy Hackman for letting me use their equipment. I thank Dr. Tracy Scheffler and Dr. Jason Scheffler for helping me troubleshooting experimental issues. Special thanks goes to Dr. David Julian from Department of Biology, who was willing to train me how to use fluorescent equipment. Warm thanks to Ted Broome for devoting so much time to help me with developing experimental protocols. Additionally, I also would like to express my appreciation to all graduate students that helped me with sample collection and generously gave me support through my life at UF. I thank a former graduate student Sarah White, who is currently an assistant professor of equine physiology at

Texas A&M University. Sarah has taught me muscle biopsy skills that I could never imagine I can do on my own now. To my lab mate Ariane Sousa: thank you for donating your time to assist with sample collection. Thank Paula Tribulo, Verónica Negrón-Pérez, Sofia Ortega and numerous graduate students who shared ideas and gave advice during my program. I also would like to thank the staff, including Justin Callaham and Nick Carden, and students at the University of Florida's Equine Sciences Center and Horse Teaching Unit, for assistance.

Lastly, my warmest thanks must be to my family. I must thank my parents and my parents-in-law for making my life sweet and wonderful. Thank them for coming to take care of my daughter to make me concentrate on my research. Their love and support made me who I am today. To my beloved little girl, Emilia: you are the best daughter I could ever have, and your smiles encourage me. I also thank my dear husband, Peng Liu, for his continued love. I consider myself to be truly fortunate to have him stand by to support and encourage me during the challenges of graduate program to make the completion of my dissertation possible.

TABLE OF CONTENTS

LIST OF TABLES

LIST OF FIGURES

LIST OF ABBREVIATIONS

ADP	Adenosine diphosphate
ANT	Adenine nucleotide transporter
ATP	Adenosine triphosphate
COX	Cytochrome *c* oxidase
CS	Citrate synthase
ER	Endoplasmic reticulum
ETS	Electron transport system
$FADH_2$	Flavin adenine dinucleotide
FGF	Fibroblast growth factors
3-HADH	3-OH acyl CoA dehydrogenase
HGF	Hepatocyte growth factor
LC3	Microtubule-associated proteins 1A/B light chain 3
MRF	Myogenic regulatory factor
MyHC	Myosin heavy chain
NADH	Nicotinamide adenine dinucleotide
OXPHOS	Oxidative phosphorylation
Pax3	Paired box protein 3
Pax7	Paired box protein 7
PCr	Phosphocreatine
PGC-1α	Peroxisome proliferator-activated receptor-γ coactivator 1α
ROS	Reactive oxygen species
SDS-PAGE	Sodium dodecyl sulfate polyacrylamide gel electrophoresis
TCA	Tricarboxylic acid
TFAM	Mitochondrial transcription factor A

TGF-β1	Transforming growth factor beta 1
UCP	Uncoupling protein

Abstract of Dissertation Presented to the Graduate School
of the University of Florida in Partial Fulfillment of the
Requirements for the Degree of Doctor of Philosophy

EQUINE SKELETAL MUSCLE MITOCHONDRIAL FUNCTION AND REGENERATION CAPACITY WITH AGING

By

Chengcheng Li

August 2017

Chair: Stephanie E. Wohlgemuth
Major: Animal Molecular and Cellular Biology

Skeletal muscle aerobic capacity, mitochondrial function and regenerative capacity have been found to decline with age in humans and rodents. However, not much is known about age-related changes in mitochondrial function in equine skeletal muscle. The objectives of this dissertation were to: 1) evaluate differences in skeletal muscle mitochondrial function between young and aged horses; 2) address underlying mechanisms for the age-related alterations in mitochondrial function; and 3) examine differences in the intrinsic regenerative capacity of muscle stem cells isolated from skeletal muscle of young and aged horses.

We first compared muscle aerobic capacity, especially mitochodnrial density and function in *gluteus medius* (GLU) and *triceps brachii* (TRI) muscle between young and aged American Quarter Horses. Equine skeletal muscle aging was accompanied by a shift in fiber type composition towards a higher percentage of type I and IIA muscle fibers, decrease in mitochondrial density and cytochrome *c* oxidase activity, but preserved mitochodnrial respiratory function.

To further understand the underlying cause for the age-associated decrement of mitochondrial density and function in equine skeletal muscle, expression of factors involved in mitochondrial biogenesis and mitochondrial-selective autophagy pathways, two of the most prominent quality control mechanisms that have been described, were analyzed. Our data suggest that mitochondrial content and biogenesis markers were reduced in aged-TRI, and that autophagic activity was impaired in both muscles with age, albeit more pronounced in the TRI muscle.

Myogenic stem cells, commonly referred to as satellite cells, are responsible for muscle growth and repair after birth. However, the ability to regenerate muscle and replace damaged myofibers declines with age. We then asked whether the intrinsic changes within an aged satellite cell would cause alteration in regenerative capacity in equines. *In vitro* studies with primary satellite cell cultures under standard conditions suggest that satellite cells isolated from aged horses displayed compromised proliferative, differentiation and fusion capacity *in vitro*. In line with compromised myogenic potential of aged muscle-derived satellite cells, there were age-related alterations in mitochondrial biogenesis and autophagy pathways, with satellite cells derived from TRI muscle being more susceptible to impairments with age.

CHAPTER 1
LITERATURE REVIEW

Introduction

Biological aging is a natural phenomenon that occurs in every living species. With age, tissues and organs begin to lose their ability to function correctly, or to function at all. However, the rate of aging can vary between individuals, depending on fitness levels and environmental factors. Furthermore, not all tissues experience aging at the same rate and to the same extent. Some systems may change slowly and exhibit minor dysfunctions, while others show dramatic decline and impairment to a greater extent. The exact cause of aging is not completely understood yet. The theories of aging are many, and one of the most popular explanations is that as cells age they gradually become unable to get rid of the wastes and toxins, and eventually, they are no longer able to function properly. For this reason, post-mitotic tissues such as heart, skeletal muscle, and brain are more likely to be affected by aging (Kwong & Sohal, 2000). Cells within these tissues are not or only to a minor extent mitotically active, and therefore rarely or not at all replaced. Together with increasingly insufficient cellular quality control, damage to macromolecules accumulates, leading to cellular dysfunction. Skeletal muscle is profoundly affected by aging, and its functional decline is characterized by a progressive loss of muscle mass and strength (Delmonico *et al.*, 2009). Previous studies in humans have shown that leg muscle mass was reduced by ~30% (Janssen *et al.*, 2000), and that thigh muscle cross-sectional area declined by ~25% with aging (Klitgaard *et al.*, 1990). In line with the age-related decline in thigh muscle mass, the overall physical function was also decreased (Buford *et al.*, 2012). Similarly, muscle torque, an indicator of muscle quality or function, was 30-40% lower in

sedentary elderly compared to young subjects (Klitgaard *et al.*, 1990). The gradual loss of muscle mass is also linked to a progressive reduction in the regenerative capacity of skeletal muscle. Regeneration of adult skeletal muscle mainly depends on muscle stem cells, also known as satellite cells, located between the basal lamina and muscle fiber membrane (Mauro, 1961). Under normal conditions, satellite cells are rapidly activated by muscle damage and other stimuli (such as exercise), and mediate quick and complete repair or growth by either forming new fibers or fusing with existing fibers. With age, however, skeletal muscle regenerative capacity declines (Carlson & Conboy, 2007), which can be partially explained by a decline in satellite cell function, as reported for mice (Conboy *et al.*, 2005; Chakkalakal *et al.*, 2012;) and humans (Roth *et al.*, 2000b). For this reason, repair or replacement of damaged muscle fibers is attenuated in elderly individuals. This impairment in regenerative and growth capacity contributes to the decline in muscle mass and strength observed with aging (Jang *et al.*, 2011).

Although numerous factors have been implicated in the age-associated decline in skeletal muscle mass, function, and repair capacity, dysfunctional mitochondria in particular are thought to play a primary role in this process. The mitochondria are the main generators of cellular energy. At the same time, they produce and release free radicals, which can cause damage to mitochondria themselves as well as other cellular constituents. For this reason, the mitochondrial theory of aging proposes that the progressive accumulation of damage to mitochondria is the underlying cause for aging of humans and other animals. The relationship between mitochondrial dysfunction and skeletal muscle aging has been supported by numerous studies, which found that skeletal muscle aging is accompanied by a decline in mitochondrial density and

function, and dysregulation of mitochondrial quality control processes such as mitochondrial biogenesis, fission and fusion, and mitophagy, the selective autophagic removal and degradation of damaged mitochondria (reviewed by Seo *et al.*, 2010 and Johnson *et al.*, 2013). The goal of this review is to summarize the current knowledge about the age-related skeletal muscle dysfunction, with specific focus on mitochondrial dysfunction, and some potential mechanisms underlying the decline in mitochondrial content and function.

Aging Related Decline in Skeletal Muscle Mass and Function

Skeletal muscle is one of the largest organs in the body, comprising nearly 40-50% of total body mass in non-obese mammals. It is an exceptionally plastic tissue that can undergo adaptive changes to meet new challenges imposed on it. For example, muscle mass can either increase or decrease in response to metabolic demands like exercise or following a period of inactivity, respectively (Romanello & Sandri, 2015). As we age skeletal muscle undergoes progressive changes, primarily involving loss of muscle mass and strength, known as sarcopenia (reviewed by Buford *et al.*, 2010), which becomes more severe with increasing age and can lead to mobility impairment and frailty (Cruz-Jentoft *et al.*, 2010; Marzetti *et al.*, 2013). In humans, skeletal muscle mass declines as much as 3-10% per decade after the age of 25 (Rogers *et al.*, 1990; Short *et al.*, 2005; Johnson *et al.*, 2013), with a dramatic acceleration of decline after the age of 65 (Nair, 2005). Postmortem examination of healthy individuals who died in accidents revealed that both muscle area and fiber numbers started to decrease as early as the fourth decade of life when compared across all ages (Lexell *et al.*, 1988). This seems to be in line with other studies reporting age-related decrease in muscle area starting at about 30 yr in healthy human subjects ranging in age from 18 to 88 yr

(Short *et al.*, 2003; Short *et al.*, 2004). Moreover, increasing evidence shows the decline in muscle mass is accompanied by a decrease in muscle strength and power. As we age, humans lose approximately 1% of leg lean mass per year and approximately 2.5-4% in leg strength (Goodpaster *et al.*, 2006). Similarly, Short *et al.* (Short *et al.*, 2003; Short *et al.*, 2004) demonstrated a loss of muscle strength (knee extension) concomitant with the decrease in muscle mass between the ages of 20 and 80 yr. This indicates that not only muscle mass declines with age but the muscle quality does as well. However, age-related changes vary substantially among individuals likely due to different fitness levels and other environmental factors (reviewed by Marzetti *et al.*, 2017).

Muscle aging is noted in various species from invertebrates to higher organisms. In the nematode *Caenorhabditis elegans*, aging is accompanied by muscle deterioration and reduced muscle function, which resembled human sarcopenia (Herndon *et al.*, 2002). As *C. elegans* age, muscle mass significantly shrinks and sarcomeres progressively disintegrate and become disorganized (Herndon *et al.*, 2002). A recent study in flies demonstrated similar age-related changes in muscle morphology and function (Miller *et al.*, 2008). For example, myofibrils in striated muscle from old flies displayed reduced sarcomere length and increased disorganization, indicating a loss of sarcomere integrity and acute sarcopenia. Despite vastly different longevity of invertebrate and humans, and essential differences in their muscle fiber types and innervation, similar features of muscle aging have been described. Notwithstanding, only limited data are available for equine skeletal muscle aging. In a study performed on horses of 1 to 21 years of age, the cross-sectional area of the longissimus muscle was

smaller in aged (≥ 16 yr) compared to adult horses (Reed *et al.*, 2015). Seemingly in accordance, Betros *et al.* (Betros *et al.*, 2002) measured lower whole body oxygen consumption (Vo_2 max) and maximum heart rate in aged compared to young horses. It is possible that the decreased aerobic performance capacity of the older horses was related to decreased muscle mass and function, but many other factors contribute to whole body aerobic performance, and none were investigated in that study.

Changes in Skeletal Muscle Fiber Type Composition with Aging

Mammalian skeletal muscle is an extremely heterogeneous tissue. It is composed of muscle fibers as well as connective and adipose tissue, and within muscle fibers there are different types that exert specific contractile and metabolic properties. The overall performance and function of a muscle are mainly dependent on the individual properties of different fiber types and their proportions within the muscle. Major differences between muscle fiber types are related to the contractile element myosin and the different isoforms of its heavy chain component (MyHC). The different MyHC isoforms are characterized by specific modes of energy production and muscle fiber function. In large animals, skeletal muscle fibers are classified based on the MyHC isoform expressed. Type I fibers, or slow-twitch fibers, are associated with predominantly oxidative energy metabolism; type IIX (or historically IIB) fibers, or fast-twitch fibers, are associated with predominantly glycolytic energy metabolism; and type IIA fibers, an intermediate fiber type, exploit both oxidative and glycolytic energy production. Of note, the number of MyHC isoforms expressed in skeletal muscle varies between species, and small mammals are reported to express a forth isoform (type IID) (Talmadge and Roy, 1993). In addition to pure fiber types, expressing only one MyHC isoform, hybrid fibers exist, which express more than one isoform. Those are more

prevalent in muscles undergoing transition, such as during aging or adaptation to exercise (Pette & Staron, 2000). Further, muscle groups very rarely express only one fiber type; instead, they are comprised of a combination of the three fiber types.

Aging has been associated with a decline in muscle fiber number, which is thought to be the principle cause of age-related loss of muscle mass. A significant decline in the number of muscle fibers was observed in elderly humans. By counting the number of fibers in vastus lateralis muscle of men aged from 30 to 74 yr, Lexell and colleagues (Lexell *et al.*, 1986; Lexell *et al.*, 1988) reported that the number of muscle fibers in the oldest man was ~25% less compared to the youngest. In humans, the decline in muscle fiber number is more profound in type II fibers. It has previously been reported that type IIX and IIA fiber numbers decline with age (Lexell *et al.*, 1988), whereas the type I fibers are less affected. Moreover, the preferential atrophy of type II fibers, that is the loss of fibers, is likely to cause a concomitant increase in percentage of type I fibers. Studies on human skeletal muscle aging suggested that the percentage of type I fibers increases with aging, with ~40% type I fibers in individuals in their twenties, and ~70% type I fibers in individuals in their sixties (Gollnick *et al.*, 1972; Larsson & Karlsson, 1978). In addition to fiber number, muscle fiber size is also affected by age, with 10-40% smaller type II fibers observed in elderly compared to young individuals (Frontera *et al.*, 2000).

A number of studies investigated the association of muscle fiber atrophy and loss of motor neurons. This idea was first suggested by Gutmann and Hanzlikova (Gutmann & Hanzlikova, 1966), who reported age-associated alterations in the motor endplate morphology at the neuromuscular junction. Since that time, evidence has accumulated

showing that functional denervation occurs during the aging process, including a progressive decline in the number of spinal cord motor neurons, a process considered irreversible, and of functioning motor units (Roth *et al.*, 2000a; Roubenoff, 2001). A motor unit consists of one motor neuron innervating a group of muscle fibers. With age, motor neurons die and cause a denervation of the muscle fibers within the motor unit, which subsequently leads to muscle fiber atrophy and death.

Another factor causing muscle fiber atrophy with age is believed to be the impairment of skeletal muscle protein turnover. Muscle mass is determined by coordinated balance between protein synthesis and degradation. This balance was disrupted in aged humans, driven by an overall decrease in muscle protein synthesis rate, including that of specific contractile and mitochondrial proteins (Yarasheski *et al.*, 2002; Short *et al.*, 2004). The synthesis of mixed skeletal muscle proteins was described to decline by 4% per decade after the age of 20 (Short *et al.*, 2004). A significantly lower synthesis rate of myofibrillar proteins and MyHC was observed with age (Welle *et al.*, 1993; Hasten *et al.*, 2000), which may be related to age-associated reduction in either or both gene transcription and translation of MyHC-IIX and MyHC-IIA (Balagopal *et al.*, 2001). Furthermore, the exercise-stimulated response in myofibrillar and mitochondrial protein synthesis following resistance or endurance training (Moore *et al.*, 2009) was attenuated in older humans (Kumar *et al.*, 2009). The reduction in synthesis of specific contractile proteins is likely to contribute to a decline in locomotor function.

Besides loss of muscle fibers, aging skeletal muscle is characterized by a fiber type transition. Skeletal muscle is highly malleable and able to adapt to altered

functional demands and stimuli (Flück, 2006). A common adaptation is a change in muscle metabolism through modifying fiber type composition. Under certain conditions, fiber type transitions occur between fast and slow fiber types, either from fast to slow or vice versa. In general, increased neuromuscular activity or overload induces fast-to-slow transitions, whereas reduced neuromuscular activity or unloading causes transitions in the opposite direction (Pette, 2002). Aging is associated with a fast-to-slow shift of muscle fibers, which was demonstrated by Gannon *et al.* (Gannon *et al.*, 2009), who observed a drastic increase in slow myosin light chain in aged rat muscle. Similarly, a proteomic study of human skeletal muscle indicated a slower-contracting mode of senescent muscle fibers (Gelfi *et al.*, 2006). Of note, this fast-to-slow fiber type shift is affecting mostly IIX fibers, which can be explained by the age-related remodeling of motor units that more likely result in denervation of type II muscle fibers (D'Antona *et al.*, 2003; Kostek & Delmonico, 2011), whereas type I fibers are less affected. However, the fast-to-slow fiber type shift does not increase oxidative capacity in older muscle, which could be due to the reduction in oxidative enzyme activity with age (Boffoli *et al.*, 1994; Rooyackers *et al.*, 1996). Fiber type distribution in skeletal muscle from untrained horses appears to reflect alterations in muscle function with advancing age (Rivero *et al.*, 1993; Lehnhard *et al.*, 2004; Kim *et al.*, 2005). However, the data are contradictory, with some studies reporting an increase in oxidative, slow-twitch fibers (Rivero *et al.*, 1993), and others suggesting an age-related shift from oxidative to glycolytic fibers (Lehnhard *et al.*, 2004; Kim *et al.*, 2005). In addition, whether an age-related alteration in muscle fiber type composition is associated with changes in muscle oxidative

capacity has not been well investigated in the horse (Rivero *et al.*, 1993; Kim *et al.*, 2005).

Changes in Muscle Energy Metabolism with Aging

Skeletal muscle plays a central role in locomotion and thereby in many activities of daily living, and its action, muscle contraction, depends on the presence of the energy-rich molecule adenosine triphosphate (ATP). There are several pathways for generating ATP in skeletal muscle, such as 1) hydrolysis of phosphocreatine (PCr) through creatine kinase reaction, 2) anaerobic glycolysis, and 3) citric acid cycle (TCA cycle) and oxidative phosphorylation (OXPHOS). The former pathways are located in the cytosol, while the TCA cycle and OXPHOS are located in the mitochondria. Muscle aging is commonly accompanied by alteration in bioenergetics. Recent microarray data indicated a reduction in mRNA level of 55 genes involved in energy metabolism by more than 2-fold during the aging process, which may have negative implications for the bioenergetic capacity of human skeletal muscle. In general, these 55 genes were associated with glycolysis, glycogen metabolism and mitochondrial function (Lee *et al.*, 1999). However, the effect of aging on bioenergetic capacity remains controversial, which is probably due to differences in physical activity levels of the individuals assessed.

Muscle cells store some ATP that can be used for muscle contraction immediately, but this is usually only enough to last for a few seconds. During short-term, intense activities, after these ATP stores are depleted, the phosphocreatine (PCr) system (also called the ATP-creatine phosphate system) can provide fuel for an additional 4-6 seconds. The PCr system serves as the quickest way to replenish ATP levels by directly transferring a phosphate group from creatine phosphate to ADP to

form ATP. After cellular uptake, about two-thirds of the creatine in skeletal muscle is phosphorylated to PCr by creatine kinase, with the remaining one third remaining as free creatine. As muscle works, PCr is used to replenish ATP, preventing a depletion of ATP levels. Aging is associated with alteration in the PCr system. Möller *et al.*, (Möller *et al.*, 1980) found that intramuscular PCr levels were approximately 5% lower in elderly (52-79 yr) when compared to younger (18-36 yr) adults, while intramuscular free creatine levels were 5% higher in older adults. At the same time, elderly individuals exhibited significantly reduced total adenine nucleotides. Subsequently, it was found that the activity of the key enzyme catalyzing the phosphorylation of creatine, creatine kinase, in heart tissue was lower in older compared to middle-aged adults (Kaczor *et al.*, 2006). Aksenov *et al.* (Aksenov *et al.*, 1997) concluded that the activity of creatine kinase was reduced by reactive oxygen species (ROS) damage. Given that generation of ROS increases with age (Chabi *et al.*, 2008), formation of phosphocreatine may be decreased in the aged population due to an oxidatively damaged creatine kinase.

Glycolysis is the second-fastest way to regenerate ATP and acts as the predominant source of energy provision to support explosive exercise lasting from about 30 seconds to 2 min. This metabolic process produces a net sum of 2 ATP molecules per molecule of glucose (Baker *et al.*, 2010) by converting a glucose molecule into 2 molecules of pyruvate, 2 molecules of H_2O, and 2 molecules of NADH. In subsequent steps, pyruvate is either converted to lactate through the so-called lactic acid system, or transported into the mitochondria, where it is further oxidized by in the reactions of the TCA cycle. Lanza *et al.* (Lanza *et al.*, 2005) reported an age-related decline in glycolytic flux in skeletal muscle, which is consistent with reduced glycolytic enzyme contents

(Gelfi *et al.*, 2006; Capitanio *et al.*, 2009) and/or activities (Larsson *et al.* 1978; Pastoris *et al.* 2000) observed in older muscle. For example, the activity of glycolytic enzymes, such as lactate dehydrogenase and hexokinase are markedly decreased in elderly humans (Pastoris *et al.*, 2000; Kaczor *et al.*, 2006). In contrast, other studies have shown little or no age-related changes in activity of enzymes involved in anaerobic ATP generation, such as lactate dehydrogenase, creatine kinase and adenylate kinase (Borges & Essén-Gustavsson, 1989; Coggan *et al.*, 1992).

Aerobic metabolism is the slowest, but most efficient way to regenerate ATP. This oxygen-dependent metabolic pathway is responsible for most of the cellular energy produced. The aerobic system uses blood glucose, glycogen and fat as fuels to resynthesize much more ATP compared to the other pathways. Since this mode of ATP regeneration requires oxygen, and many of the aerobic reactions occur in the mitochondria it is also called “mitochondrial respiration”. As discussed above, when using glucose and glycogen as fuels for aerobic ATP production, the carbohydrate is broken down into pyruvate through glycolysis, and the pyruvate enters TCA cycle within the mitochondria matrix. When fat is used as a substrate, triglycerides (body fat) are first hydrolyzed into free fatty acids and glycerol in a process called lipolysis. Free fatty acids can then be transported into mitochondria and oxidized to generate acetyl-CoA, which enters TCA cycle for further oxidation. The reduction equivalents generated during both the oxidation of fatty acids and carbohydrates are then used to reduce molecules of the mitochondrial electron transport chain. In the process of electron transport along a series of enzyme complexes, an electrochemical gradient is generated across the inner mitochondrial membrane, which is the driving force for the ultimate phosphorylation of

ATP. The aerobic oxidation of carbohydrate and fatty acids necessitate the fast supply of oxygen from blood, particularly during high energy demanding exercise. However, in muscle from old individuals, oxygen is not supplied quickly enough to meet the muscles' needs at least in part due to a lower muscle capillary density. The number of capillaries in contact with muscle fibers decreases by up to 40% with age (Coggan *et al.*, 1992). Moreover, this study (Coggan *et al.*, 1992) also demonstrated that maximal aerobic capacity (measured as VO_2 max) is 35% lower in old compared to young adults. The effects of aging on mitochondrial respiration will be discussed in the next part of this chapter.

A number of different energy substrates can be utilized for muscle contraction, including intramuscular glycogen and triglycerides, as well as blood-borne glucose and fatty acids. The preferred and predominant substrate for energy production used by a muscle cell depends on the type of activity or exercise. During moderate activity, such as walking, energy is generated almost entirely through the aerobic pathway with fat being the predominant energy source. As speed of locomotion increases, in the horse this would be from a walk to a trot or a canter, both aerobic and anaerobic systems are recruited, with fat and glycogen being the main energy source. When horses are performing a fast gallop, as an example of a strenuous, short-term locomotor activity, the energy is mainly generated through the anaerobic pathway, using glycogen/glucose as energy substrates. On the other hand, long-term, endurance exercise relies predominantly on fat as the principle energy source. Limited data have been published regarding the effect of aging on the energetic capacity of equine muscle. Similar to what has been found in older humans, a decline in VO_2 max has been observed in old horses

(McKeever & Malinowski, 1997). Moreover, age appears to be accompanied by an increase in muscle glycolytic capacity, and a concomitant decrease in muscle oxidative capacity in horses (Kim *et al.*, 2005).

Changes in Mitochondrial Function with Aging

Mitochondria are unique organelles in that they contain their own genome (mtDNA). This small genome (16.5 KB in human) encodes 2rRNAs, 22 tRNAs, and 13 protein subunits (Smits *et al.*, 2010). The remainder of the mitochondrial proteins (> 90%) are encoded by the nuclear genome (nDNA) and synthesized in the cytosol before being imported into mitochondria (Johnson *et al.*, 2007; Pagliarini *et al.*, 2008). Most mammalian cells contain hundreds to thousands of mitochondria, and each mitochondrion holds 2-10 copies of mtDNA. Mitochondria vary considerably in shape and size, but they all have the same basic double membrane system, consisting of an inner and an outer mitochondrial membrane. Together they create two separate compartments: internal mitochondrial matrix and the intermembrane space. The mitochondrial matrix contains the enzymes that metabolize pyruvate and fatty acids to generate acetyl CoA, as well as enzymes of the TCA cycle, in which acetyl CoA is further oxidized and the energy carriers, or reduction equivalents, NADH and $FADH_2$ are produced. At the inner mitochondrial membrane, these electron carriers donate electrons to the components of the electron transport system that generates most of the cell's ATP. Since oxidation of NADH and $FADH_2$ is coupled with the phosphorylation of ADP, this process is also named OXPHOS. Besides this principal bioenergetic function, mitochondria also play crucial roles in cell metabolism, apoptotic cell death and intracellular signaling (Finkel & Holbrook, 2000; Ryan & Hoogenraad, 2007). Therefore, proper mitochondrial function is essential for maintenance of cellular homeostasis as

well as general organismal health. Not surprisingly, alterations in mitochondria density and/or function are associated with diverse pathologic states (Wallace, 2005). There is substantial evidence that mitochondrial dysfunction occurs with advancing age in a wide range of species, including human (Cooper *et al.*, 1992; Joseph *et al.*, 2012). The mitochondria theory of aging suggests that accumulated oxidative damage within the mitochondria causes irreversible damage to mitochondrial macromolecules, and eventually leads to cellular aging. The basis for this theory is the fact that mitochondria are both the producer and the target of ROS. The mitochondrial respiratory chain, or electron transport system (ETS), is a major site of ROS production in the cell. Even though the OXPHOS process is efficient, a small percentage of electrons can still prematurely reduce oxygen during normal respiration, resulting in the formation of ROS (Liu *et al.*, 2002). ROS produced within mitochondria represents almost 90% of the total ROS produced in the cell, and it has therefore been suggested that mitochondria are prime targets for oxidative damage. Over the years, substantial evidence has emerged to support that aging is accompanied by changes in mitochondrial integrity and function, including an increase in mtDNA mutations and deletions, reduction in expression of mitochondrial proteins, reduced mitochondrial enzyme activities, and low ATP production.

In general, ROS production is found to increase in aged mitochondria (Chabi *et al.*, 2008). The lack of protective histones, the limited efficiency of mtDNA repair system (Linnane *et al.*, 1989), and close proximity to the ETS make mtDNA extremely vulnerable to oxidative damage. It has been shown that oxidative damage to mtDNA increases in an age-dependent manner in skeletal muscle (Kujith *et al.*, 2005). One

study found that mtDNA deletions occurs in up to 70% of mtDNA molecules in the skeletal muscle of old individuals over the age of 80 (Chabi *et al.*, 2005). Perhaps the strongest evidence suggesting a causative link between mtDNA mutations and aging comes from studies on the mtDNA mutator mice. In those studies, mice with deficiency in the proofreading function of mitochondrial DNA polymerase (POLG) exhibited an accumulation of point mutations and deletions in their mtDNA (Kujoth *et al.*, 2005; Vermulst *et al.*, 2008), which subsequently led to an accelerated aging phenotype. Of note, oxidative damage to proteins and lipids within mitochondria has also been observed (Beal *et al.*, 2002; Muller *et al.*, 2004; Murphy, 2009; Staunton *et al.*, 2011), which undoubtedly will impact mitochondrial function as well. Coupled with the increase in mtDNA damage, the mtDNA content decreases with age in skeletal muscle from humans (Welle *et al.*, 2003a; Short *et al.*, 2005; Menshikova *et al.*, 2006; Lanza *et al.*, 2008) and rodents (Barazzoni *et al.*, 2000). The decline in mtDNA content is believed to be at least in part due to oxidative damage, since the difference in mtDNA content between young and old groups tends to be greater in more oxidative fibers (Barazzoni *et al.*, 2000). If mtDNA content is a valid indicator of mitochondrial content, the mitochondrial content observed by electron microscopy may exhibit a similar decrease with age. In fact, a study using magnetic resonance spectroscopy has shown that the *vastus lateralis* muscle of people over 60 years of age showed lower mitochondrial density compared to their younger counterparts (Conley *et al.*, 2000), and this decline in mitochondrial density was further confirmed by assessment of mitochondrial density using electron microscopy (Peterson *et al.*, 2012). Moreover, activity of citrate synthase (CS), a valid biomarker of mitochondrial density (Larsen *et al.*, 2012), has also reported

to decrease in skeletal muscle from human (Houmard *et al.*, 1998) and horses (Kim *et al.*, 2005), which may explain a decline in muscle oxidative capacity.

Age-related changes in mitochondria oxidative capacity have been well documented in human skeletal muscles (Houmard *et al.*, 1998; Conley *et al.*, 2000; Hunter *et al.*, 2002). However, these studies are not in complete concordance, possibly due to differences in muscle types investigated and physical activity levels of the subjects. The majority of reports, although not all (Houmard *et al.*, 1998; Capel *et al.*, 2005), associated aging with a decline in activity of several mitochondrial enzymes such as 3-OH acyl CoA dehydrogenase activity (3-HADH), CS, complex I-III and cytochrome *c* oxidase (COX; Coggan *et al.*, 1992; Houmard *et al.*, 1998; Barazzoni *et al.*, 2000; Short *et al.*, 2005). These impairments may in turn cause a decline in mitochondria respiratory capacity. Short *et al.* (Short *et al.*, 2005) reported that the maximal capacity of ATP synthesis in skeletal muscle decreased by ~10% per decade, or 5% when normalizing to mitochondrial protein content. Another underlying cause of the reduction in mitochondrial oxidative capacity could be reduction in mitochondrial mRNA or protein. Recent microarray data revealed 957 genes significantly associated with aging, with mRNA levels of complex I, III, IV and V significantly reduced in skeletal muscle from aged subjects (Su *et al.*, 2015). In addition, aged human skeletal muscle appeared to exhibit alteration in mRNA levels of some nDNA-encoded mitochondrial and TCA proteins, including CS (Barazzoni *et al.*, 2000; Welle *et al.*, 2003b; Short *et al.*, 2005). At the protein level, the content of complex I, III, IV and V were decreased in aged skeletal muscle from both humans (Short *et al.*, 2003; Lanza *et al.*, 2008) and rodents (Lombardi *et al.*, 2009, Picard *et al.*, 2010), but increased amounts of complex II

(Lombardi *et al.*, 2009; O'Connell & Ohlendieck, 2009; Picard *et al.*, 2010). The latter is a nuclear DNA encoded protein, and its increase concomitant to the decrease of complexes that contain mtDNA encoded subunits has been suggested as a compensatory mechanism. Furthermore, skeletal muscle mitochondrial protein synthesis declined with age (Guillet *et al.*, 2004), which is likely another contributor to age-related impairment of mitochondrial oxidative capacity and ATP synthesis (Short *et al.*, 2005). Specific mitochondrial enzymes have also been investigated in horses. Kim *et al.* (Kim *et al.*, 2005) investigated the age-associated change in activity of CS and 3-HADH, and found that CS decreased while 3-HADH remained unaltered. In conclusion, reduction in mitochondrial oxidative capacity in older individuals may be due to lower activity of mitochondrial enzymes as well as lower transcript and protein content.

Mitochondrial Quality Control Mechanisms

As discussed above, mitochondria are continuously challenged by ROS, which cause damage to mitochondrial constituents and ultimately mitochondria dysfunction, which in turn leads to increased level of ROS. However, the cell has an intricate surveillance system to maintain mitochondrial integrity and function, a process termed mitochondrial quality control, which includes chaperones and proteases to refold or degrade misfolded mitochondrial proteins; the fission/fusion machinery to repair or facilitate the segregation of damaged areas from the mitochondrial network; and mitochondrial biogenesis and mitophagy to regulate mitochondrial turnover and regeneration. Antioxidant enzymes residing in the mitochondria can also be considered part of the mitochondria quality control system, as they scavenge ROS to reduce oxidative stress and prevent oxidative damage. Moreover, recent research suggests a cross talk between mitochondria and other subcellular compartments like the

endoplasmic reticulum to regulate mitochondrial homeostasis (Nunnari & Suomalainen, 2012; Fu *et al.*, 2013). Of note, the activation and relative contribution of each specific quality control mechanism depends on the overall degree of damage.

Mitochondrial Proteases and Chaperones

Mitochondria contain a series of chaperone proteins and proteases. They are considered to be central to mitochondrial quality control, since they play a crucial role in controlling protein homeostasis. Typically, the major function of chaperones is to recognize non-native, partially misfolded proteins, and to facilitate their refolding into the functional native state. Mitochondria contain several members of the major chaperones, with the most important mitochondrial chaperones belonging to the heat shock protein families Hsp60 and Hsp70 (Luce *et al.*, 2010). However, if mitochondrial damage is excessive and refolding by chaperones fails to occur, proteases distributed in all mitochondrial compartments degrade misfolded or oxidized proteins into small fragments and amino acids. For this reason, protease-mediated mitochondrial quality control is considered to be the first line of defense against mild mitochondrial damage. The two best-known soluble proteases functioning in the mitochondrial matrix are LONP1 (mitochondrial matrix peptidase LONP) and ClpXP (Caseinolitic peptidase XP). Other proteases reside in the inner membrane space and control the protein turnover in certain mitochondrial compartments.

Fission and Fusion

Mitochondria are highly dynamic organelles that undergo constant fission and fusion to regulate the expansion and morphology of the mitochondrial network. This dynamic nature serves as a second line of defense against damage (Westermann *et al.*, 2010; Palmer *et al.*, 2011). The fission process segregates damaged parts of the

mitochondria network from the healthy part and targets them for removal and degradation through the quality control process autophagy. Fusion, on the other hand, facilitates the exchange of mitochondrial proteins and mtDNA between healthy mitochondria (Van der Bliek *et al.*, 2013). Thus, quality control via the fission-fusion machinery is essential for mitochondrial function. Inhibition of fusion induced the accumulation of mtDNA mutations, eventually triggering loss of the mitochondrial genome (Chen *et al.*, 2010). Imbalance between the fission and fusion process causes alterations in mitochondrial structure and function (Shirendeb *et al.*, 2012). For example, loss of fission ability caused a so called hyper-fused mitochondrial network, while excessive fission events resulted in small, round, and fragmented mitochondria (Olichon *et al.*, 2003; Chen *et al.*, 2005). What is more, with age, mitochondria appeared abnormally enlarged and less numerous with age (Terman *et al.*, 2010), indicating that aging may cause a decrease in mitochondrial fission or an increase in fusion events (Yoon *et al.*, 2006).

Autophagy

Selective mitochondrial autophagy, or mitophagy, represents another mitochondrial quality control mechanism. When mitochondrial damage is severe and exceeds the mitochondrial repair capacity, selective autophagic removal of mitochondria is induced (Twig *et al.*, 2008). During mitophagy, damaged or dysfunctional mitochondria are recognized and enveloped by a double-membrane structure called phagophore, which subsequently closes to become an autophagosome. The autophagosome then targets its cargo, the enclosed mitochondria, to a lysosome. Upon fusion of autophagosome and lysosome (autophagolysosome), the lysosomal enzymes catalyze cargo degradation (Kim *et al.*, 2007). Accumulating evidence shows that a

decline in autophagy with age, and that increased autophagy attenuates aging in lab animals (Wu *et al.*, 2013; Schiavi *et al.*, 2015). PINK/Parkin-mediated mitophagy is a well-studied mechanism reported to regulate mitochondria integrity and function in various species (Clark *et al.*, 2006; Gautier *et al.*, 2008; Narendra *et al.*, 2008). Damaged mitochondria are flagged with PTEN-induced kinase (PINK1), followed by recruitment of Parkin to the mitochondria, which initiates the mitophagic process. The accumulation of PINK1 and Parkin on the surface of damaged mitochondria further triggers ubiquitintion of mitochondrial proteins that act as an elimination signal. Ubiquitinated mitochondria are further recognized by an autophagy adapter protein, Sequestosome-1 (p62/SQSTM1). The protein p62/SQSTM1 is tagged to the phagophore membrane by the autophagy protein MAP-LC3-II (Microtubule-associated protein 1A/1B chain 3), and facilitates mitochondrial engulfment by the phagophore. Autophagosome formation is executed by a collection of several autophagy-related proteins (ATG). To date, 35 ATG genes have been identified in yeast (Nakatogawa *et al.*, 2009), and the associated proteins work in concert or sequence to facilitate the formation and engulfment of cytoplasmic cargo. So far, mitophagy has been the only mechanism known to degrade mitochondria, and consequently to turn over the whole mitochondrial genome. Therefore, impairment of mitophagy has been implicated in aging and age-related disorders such as Parkinson's disease (Youle & Narendra, 2011; Green *et al.*, 2011). In humans, an age-related decline in mitophagy was observed (Cavallini *et al.*, 2007) and associated with an accumulation of damaged mitochondria (Masiero & Sandri, 2010). Given that mitochondria are increasingly damaged during the aging process (reviewed by Shigenaga *et al.*, 1994), decreased mitophagic activity

might further exacerbate dysfunction of the mitochondrial population as a whole in older individuals. In contrast, genetically increasing autophagic capacity appears to reduce aging in lab animals (Rana *et al.*, 2013; Wu *et al.*, 2013; Schiavi *et al.*, 2015). Moreover, autophagy can also be stimulated by a number of ways including physical exercise and caloric restriction. For example, caloric restriction leads to an increase in mitophagy and a decrease in levels of senescence markers in rats (Cui *et al.*, 2013). In rodents, exercise, which is known to reduce the aging phenotype, has been shown to induce an increase in levels of mitophagy proteins in skeletal and cardiac muscle (He *et al.*, 2012; Ogura *et al.*, 2011). Hence, decreased mitophagy likely contributes to the decline in mitochondrial quality and function that contributes to the aging phenotype.

Mitochondrial Biogenesis

As one would expect, controlled mitophagy possibly coordinates with mitochondrial biogenesis to sustain a healthy mitochondria pool (Michel *et al.*, 2012). Mitochondrial biogenesis is a complex process, which requires coordinated synthesis and assembly of thousands of proteins encoded by both the nuclear and mitochondrial genomes (Scarpulla, 2008). In addition, mtDNA replication must be coordinated to meet the requirements of the mitochondria extension. The biogenesis process is predominantly regulated by one of the most studied regulators, Peroxisome proliferator-activated receptor-γ coactivator 1α (PGC-1α) (Wu *et al.*, 1999). The transcriptional coactivator regulates various transcription factors involved in mitochondrial biogenesis in mammalian tissues (Wu *et al.*, 1999), including skeletal muscle (Hood *et al.*, 2006). Overexpression of this gene in skeletal muscle increases mitochondrial content (Garnier *et al.*, 2003) and oxidative capacity (Lin *et al.*, 2002), while PGC-1α-deficient mice exhibited a significant decrease in muscle mitochondrial biogenesis (Derbré *et al.*, 2012).

Mitochondrial content in human skeletal muscle declines gradually with advancing age (Crane *et al.*, 2010), and an age-associated impairment of mitochondrial biogenesis has been reported in animal models (Fannin *et al.*, 1999; Sugiyama *et al.*, 1993). Concomitantly, the level of PGC-1α was found to be lower in aged animals when compared to young ones (Viña *et al.*, 2009). Consequently, decreased PGC-1α expression has been suggested an important contributor to impaired mitochondrial biogenesis in old individuals. Mitochondrial biogenesis in muscle can be activated by physical exercise and caloric restriction (López-LIuch *et al.*, 2006; Piantadosi & Suliman, 2012; Wenz *et al.*, 2013). For example, 5-month of endurance exercise induced mitochondrial biogenesis in mice as indicated by increased expression of PGC-1α, as well as its downstream target TFAM (mitochondrial Transcription Factor A) (Safdar *et al.*, 2011). Thus, improving mitochondrial biogenesis may present a potential therapeutic target for age-related muscle wasting and diseases. Both *in vivo* and *in vitro* studies suggest that caloric restriction induced mitochondria biogenesis through activating of PGC-1α (López-LIuch *et al.*, 2006).

Crosstalk between Different Mitochondrial Quality Control Mechanisms

Mitochondria have different defense mechanisms against increasing damage that safeguard mitochondrial integrity. Dysregulation of any these quality control mechanisms is thought to be implicated in skeletal muscle loss and dysfunction observed with aging. In recent years, mounting evidence shows that mitochondrial quality control mechanisms are not acting independently from each other, but instead exert considerable crosstalk. For instance, in the fruit fly, *Drosophila melanogaster*, cellular levels of TFAM vary in concert with LONP1 levels, suggesting that LONP1 may regulate mitochondrial biogenesis by selective degradation of TFAM. More specifically,

knockdown of LONP1 in *D. melanogaster* increased and overexpression of LONP1 reduced TFAM abundance and mtDNA copy number (Matsushima *et al.*, 2010; Matsushima & Kaguni, 2011). Increasing evidence furthermore suggests the existence of crosstalk between the mitochondrial fusion/fission machinery and mitophagy (Tanaka *et al.*, 2010; Westermann, 2010) as malfunctioning mitochondria were segregated from the healthy network by fission, and ultimately eliminated through mitophagy (Youle & Narendra, 2011). Thus, it was hypothesized that fission process is a prerequisite for mitochondria-selective degradation. Support for this hypothesis came recently from studies that observed PINK/Parkin-mediated mitophagy was prevented when fission was inhibited (Tanaka *et al.*, 2010). Similarly, excessive fusion has been shown to inhibit mitophagy (Twig & Shirihai, 2011). The ubiquitination of fusion proteins such as Mfn1 and Mfn2 by the ubiquitin ligase Parkin, which induced mitophagy (Gegg *et al.*, 2010; Tanaka *et al.*, 2010), is yet another example of crosstalk between mitochondria dynamics and mitophagy. Mitochondria-nuclear crosstalk is also known to play a critical role in regulating mitochondrial quality control. Under certain conditions, when the protein degradation system is insufficient to control mitochondrial damage, the mitochondria relay signals to the nucleus, which triggers the expression of mitochondrial chaperones and proteases to improve protein folding or to remove damaged proteins (Jovaisaite & Auwerx, 2015). Moreover, mitochondria signal the expression of transcription factors essential for mitochondrial biogenesis (Pellegrino *et al.*, 2013). Interestingly, it appears that mitochondria also communicate with the endoplasmic reticulum (ER), which is supported by evidence that ER-specific ubiquitin ligase is able to induce a distinct (Parkin-independent) cellular pathway to eliminate damaged

mitochondria (Fu *et al.*, 2013**).** Taken together, different mitochondrial quality control mechanisms communicate and crosstalk with one another to maintain mitochondrial integrity and function. However, if the level of damage exceeds the capacity of these protective mechanisms, or if these protective mechanisms fail to work, damaged mitochondria can induce apoptosis and cell death.

Aging and Muscle Regeneration Capacity

A gradual loss of muscle mass and function, known as sarcopenia, is the most obvious characteristic of aging. The mechanisms responsible for sarcopenia in aged muscle are not completely understood, but the age-related reduction in muscle regenerative capacity is proposed to contribute to the development and exacerbation of sarcopenia. Reduced regeneration capacity of skeletal muscle causes prolonged inflammation (Shadrach & Wagers, 2011), which subsequently leads to loss of muscle mass observed with aging. The regenerative capacity of skeletal muscle is owed to a population of dedicated muscle stem cells, often referred to as satellite cells (Sambasivan *et al.*, 2011).

Satellite Cells and Myogenesis

Satellite cells were first identified in frog striated muscle in 1961 (Mauro, 1961). They are muscle progenitor cells, which reside between the sarcolemma and the basal lamina of muscle fibers and account for 2-5% of sublaminal nuclei in adult muscles (Schultz *et al.*, 1974; Rudnicki *et al.*, 2008). Due to their distinct anatomic position, satellite cells appear as small, wedge-shaped cells under the electron microscope. They exhibit a high nuclear-to-cytoplasmic ratio and few organelles, and condensed nuclear chromatin distinguishes them from myonuclei (Hawke & Garry, 2001). With cell electroporation labeling and lineage tracking technologies, increasing evidence

suggests that satellite cells originate from a dorsal-lateral part of the developing somite, known as dermomyotome (Kassar-Duchossoy *et al.*, 2005; Relaix *et al.*, 2005). During embryonic muscle development, a subset of myogenic progenitor cells that express specific transcription factors (paired box protein 3 and 7, Pax3 and Pax7) arise from the central dermomyotome and remain as an undifferentiated reserve cell population throughout embryogenesis. In the late fetal stage, these cells migrate to the distinct satellite cell niche (Kassar-Duchossoy *et al.*, 2005; Relaix *et al.*, 2005). Satellite cells exist in all vertebrate species, but their density varies between muscles, with that in adult *soleus* muscle was 2-fold higher than that in *tibialis anterior muscle* or *extensor digitorum longus* muscle (Schmalbruch & Hellhammer, 1977; Snow, 1983). Even within the same muscle, more satellite cells are found close to slow type I compared to fast type IIA or IIB myofibers (Gibson & Schultz, 1982; Okada *et al.*, 1984). During the past 5 decades, increasing evidence has greatly supported the notion that satellite cells play a significant role in muscle repair after injury and perhaps in the maintenance of muscle mass (Biressi & Rando, 2010). In adult muscle, satellite cells are typically mitotically quiescent; however, upon stimulation they are driven out of their quiescent state, and start to proliferate, differentiate and fuse to injured myofibers or form new fibers. Importantly, a small proportion of activated satellite cells exit the cell cycle and return to the quiescent state to maintain the satellite cell pool to respond to future muscle injury or growth stimuli. The mechanisms underlying satellite cell activation remains largely unknown. However, the satellite cell microenvironment, also called satellite cell niche, seems to control this transition from quiescence to activation. Some intracellular signals such as nitric oxide cause an increase in hepatocyte growth factor (HGF), which in turn

triggers activation of satellite cells (Wozniak & Anderson, 2007). In addition, fibroblast growth factors (FGFs) are also known to be indispensable for satellite cell activation (Jones *et al.*, 2005). Satellite cell myogenic potential is regulated by the expression of Pax3/7 and myogenic regulatory factors (MRFs). Paired box protein Pax 7 is a canonical biomarker characteristic for satellite cells, as it is specifically expressed in satellite cells, in both quiescent and proliferating stages, while it is abscent in differentiated muscle cells. The crucial role of Pax7 in postnatal maintenance and self-renewal of satellite cells (Seale *et al.*, 2000; Kuang *et al.*, 2006) was supported by a Pax7 mutant study. Shortly after birth, Pax7 mutant mice suffered a progressive loss of satellite cells, which was mainly due to satellite cell death and not exhaustive activation and differentiation; and remnant satellite cells exhibited poor muscle regenerative capacity (Kuang *et al.*, 2006). Pax 3, the paralogue of Pax 7, is also expressed in a subset of quiescent and activated satellite cells (Relaix *et al.*, 2006). Pax3 and Pax 7 play distinct roles in activation of the myogenic differentiation factor MyoD, but do not interfere with the expression of the other myogenic regulatory factors (Relaix *et al.*, 2006). The differentiation factor MyoD induces the differentiation of proliferating satellite cells. Interestingly, Myf5 (myogenic factor 5, which is up-regulated during satellite cell activation) can compensate for the loss of MyoD, and mice lacking *MyoD* exhibit normal muscle morphology but express about 4-fold higher levels of Myf5 (Rudnicki *et al.*, 1992). However, lacking both *Myf5* and *MyoD* leads to a lack of myoblast expansion (Kassar-Duchossoy *et al.*, 2004), indicating that the expression of at least these genes is required for myogenesis. As a downstream target of MyoD, myogenin is involved in differentiation and fusion of myoblasts into a myotube (Megeney and Rudnicki, 1995).

The absence of myogenin expression prevented myoblasts from contributing to postnatal muscle growth. In support of the latter, Knapp *et al.* (Knapp *et al.*, 2006) found that low postnatal myogenin expression resulted in reduced body weight in mice. Taken together, postnatal muscle growth and regeneration depends on satellite cells, whose myogenic capacity is regulated by sequential activation and repression of various myogenic regulatory factors (reviewed by Bentzinger *et al.*, 2012).

Aging Related Decline in Satellite Cell Function

Although skeletal muscle has a remarkable capacity to regenerate after injury thought out most of life and to grow in response to exercise, abnormal muscle regenerative capacity (Bockhold *et al.*, 1998; Chargé *et al.*, 2002) has been observed in aged muscles. In support, autografting experiments with muscle from old rodents indicated that damaged muscle is less frequently replaced, suggesting that aged muscles also have relatively slow muscle repair and regenerative capacity (Kaasik *et al.*, 2007; Fell & Williams, 2008). In line with regenerative impairment, a recent study suggested that regeneration of muscle contractile proteins was much slower in the old rats compared to young rats (Kaasik *et al.*, 2007).

Given the key role of satellite cells in adult muscle regeneration, diminution in their myogenic capacity is considered to contribute directly to the decline in muscle regenerative capacity with age. Indeed, numerous studies have shown the age-associated reduction in both the number and myogenic properties of satellite cells in various species (Roth *et al.*, 2000b; Conboy *et al*, 2003; Chakkalakal *et al.*, 2012; Sousa-Victor *et al.*, 2014). In general, satellite cells account for about 30% of sublaminal nuclei in neonate mice, but this number decreases to only 2-4% in adult mice (Hawke & Garry, 2001). What is more, the progressive decrease in satellite cell number limits

muscle regeneration with aging. For example, Collins *et al*. (Collins *et al.*, 2007) reported that the satellite cell content decreased by 50% in old mice (age 2 yr) when compared to young animals (age 2 mo). Moreover, loss of satellite cells is associated with muscle fiber atrophy, supported by the observation that in elderly humans the type II muscle fiber atrophy was associated with a fiber type-specific decline in satellite cell content in type II fibers (Verdijk *et al.*, 2014). In addition to the decline in satellite cell number, aged satellite cells show functional deterioration, including loss of stemness (Sousa-Victor *et al.*, 2014) and reduced ability to activate, proliferate, and fuse into myotubes (Chargé *et al.*, 2002; Conboy *et al.*, 2003; Baj *et al.*, 2005; Day *et al.*, 2010). However, the mechanisms responsible for either the decline in satellite cell number and function remain unclear. Accumulation of DNA damage (Rossi *et al.*, 2007) and telomere shortening (Sharpless & DePinho, 2007; Flores *et al.*, 2010;) might explain the decline in satellite cell number and regenerative capacity in sarcopenic muscle (Kadi & Ponsot, 2010). In addition to damage to the satellite cell's DNA and reduced expression of differentiation factors, the induction of excessive proliferation might deplete the quiescent pool, as it has been reported for the intestinal stem cell pool in flies (Rera *et al.*, 2011). If this is true for satellite cells, the maintenance of a quiescent satellite cell pool is also crucial for muscle regeneration (Shefer *et al.*, 2006). However, other studies reported no significant decline in the satellite cell pool in aged mice and humans (Roth *et al.*, 2000b; Conboy *et al.*, 2003; Wagers *et al.*, 2005), a discrepancy that could be due to experimental differences such as age or gender of the individuals investigated, or different subpopulations of muscle stem cells examined.

The impact of aging on satellite cell myogenic potential is still debated. There is evidence supporting a decrease of both proliferation and differentiation capacity of satellite cells with age (Schultz & Lipton, 1982; Conboy & Rando, 2005; Conboy *et al.*, 2003; Collins *et al.*, 2007; Buford *et al.*, 2010), while other research found that proliferative capacity remains constant throughout life (Renault *et al.*, 2000; Hawke & Garry, 2001). In the last decade, with the development of molecular and cellular biology techniques, the mechanisms underlying age-related changes in satellite cell function have been extensively investigated. It has become more clear that the age-associated deterioration of satellite cell function arises from both intrinsic changes within the satellite cell itself and influences of extrinsic factors comprising the satellite cell niche. Satellite cells in aged muscle exhibit decreased responsiveness to repair stimuli. More specifically, they fail to respond adequately to endocrine and paracrine signals that would induce their activation and proliferation in younger muscle (Gopinath & Rando, 2008; Kuang *et al.*, 2008). Recent studies have shown that a key activator of satellite cells, Notch ligand Delta-like 1, failed to respond to repair stimuli in aged satellite cells (Conboy *et al.*, 2005), but, in contrast, significantly increased in young muscle to regulate satellite cell activation and proliferation (Conboy *et al.*, 2002). Lower level of Transforming growth factor beta 1 (TGF-β1), an important myogenic regulatory cytokine, has been observed in cells obtained from old individuals compared to that of their young counterparts (Carlson *et al.*, 2009b; Alsharidah *et al.*, 2013). In contrast, FGF2 level in the satellite cell niche appeared to be higher in old muscle, which lead to loss of quiescence and self-renewal capacity, and eventually resulted in diminished regenerative capacity. Suppression of the FGF2 signaling pathway rescued these

defects (Chakkalakal *et al.*, 2012). The strongest evidence supporting the notion that alterations in the satellite cell microenvironment regulate satellite cell function comes from cross-transplantation and parabiotic studies, in which engraftment of satellite cells obtained from young mice into old mice improved muscle regenerative capacity (Conboy *et al.*, 2005; Villeda *et al.*, 2011; Lavasani *et al.*, 2012), while transplantation of satellite cells derived from old into young hosts had the opposite effect (Carlson & Faulkner, 1989). Taken together, these findings suggest that the extracellular environment that defines the satellite cell niche is an important determinant for muscle regeneration through its effect on the satellite cell itself.

As noticed in some transplantation studies, the post-transplantation regenerative capacity of geriatric satellite cells is reduced compared to that of adult satellite cells when transplanted into animals of the same age (Sousa-Victor *et al.*, 2014), suggesting that in addition to extrinsic satellite cell niche conditions, factors intrinsic to the satellite cell might play a role in age-dependent impairment of regenerative capacity. Intrinsic factors such as genomic integrity, mitochondrial dysfunction and epigenetic changes are thought to contribute to the decline in satellite cell myogenic capacity with aging. Epigenetic remodeling or DNA damage to specific genes, such as key cell-cycle regulators, controls cellular fate or turnover of satellite cells, and might therefore impair regenerative capacity of various cell types including muscle and its stem cell populations (Lansdorp & Peter, 2007; Sousa-Victor *et al.*, 2014). Research on mitochondrial function revealed that satellite cell differentiation relies on functional mitochondria, and a decline in their density and/or function may be a potential signal for satellite cell dysfunction. A marked stimulation of mitochondrial biogenesis accompanies

the differentiation of myoblasts into myotubes both *in vivo* (Duguez *et al.*, 2002) and *in vitro* (Moyes *et al.*, 1997; Leary *et al.*, 1998). Myoblasts with either deficiency in respiratory capacity (Herzberg *et al.*, 1993) or in mitochondrial protein synthesis (Korohoda *et al.*, 1993) fail to differentiate into myotubes. Furthermore, in mice and humans, impaired autophagic activity was observed in aged satellite cells (Garcia-Prat *et al.*, 2016). In conclusion, diminished satellite cell function is a consequence of multiple age-related impairments, and each of these intrinsic or extrinsic alterations may affect muscle regenerative capacity, and thereby disturb muscle mass maintenance.

As the population of older horses grows, their owners strive for improved health and management strategies that will enable continued use of their older horses for athletic and/or recreational activities. Many horses are still actively working even at ages greater than 20 years old (Brosnahan & Paradis, 2003a; Brosnahan & Paradis, 2003b). Research involving rodents and humans shows an age-related decrease in skeletal muscle aerobic capacity, regenerative capacity and mitochondrial function as discussed above. Yet, few similar studies have been done in the horse. The overall goal of this dissertation was to examine age-related changes in muscle energy metabolism, regenerative capacity, and mitochondrial function in equine skeletal muscle, and to explore potential mechanisms that contribute to the age-associated alteration in mitochondrial content and quality in equine skeletal muscle.

CHAPTER 2
EFFECTS OF AGING ON MITOCHONDRIAL FUNCTION IN SKELETAL MUSCLE OF AMERICAN QUARTER HORSES*

Background

Aging is a process during which tissue functions progressively decline (Anton *et al.*, 2015; Crescenzo *et al.*, 2015). Age-associated impairment of structure and function of skeletal muscle, one of the body's most metabolically active tissues, has substantial consequences for the well-being of the aging individual. In humans, loss of muscle mass and function, namely sarcopenia, starts to become apparent in the fourth decade of life, progressively worsening in individuals over the age of 70 (Buford *et al.*, 2010). These age-related changes lead to reduced mobility, and consequentially to an impairment of independent living (Anton *et al.*, 2015). While research on skeletal muscle aging in humans, primates, and rodent models has led to numerous publications, equine skeletal muscle aging is less explored. The horse is among the most athletic animals (Taylor *et al.*, 1981), and used as a companion animal in work, competitive and leisure activities. In recent decades the number of horses over the age of 15 years, which is considered aged, has steadily increased in the US (McKeever *et al.*, 2002), in part due to more specialized care and veterinary advances. Several recent surveys have pointed out that horses can still actively work and perform athletically well into their 20s (Brosnahan & Paradis, 2003a; Brosnahan & Paradis, 2003b), an age physiologically analogous to a 65-year-old human. The growing population of aged and geriatric horses in the US and their continued use for work and athletic activities raises

* Reprinted with permission from Li C, White SH, Warren LK, Wohlgemuth SE (2016). Effects of aging on mitochondrial function in skeletal muscle of American American Quarter Horses. *J Appl Physiol (1985)*. **121**, 299-311.

the question whether age-associated changes in skeletal muscle that have been observed in aged humans and laboratory animals also occur in the horse. Moreover, with the willingness of owners to use and work with this older horse population, understanding the physiology of equine aging is warranted. There are some studies that have documented skeletal muscle functional capacity in horses (reviewed by Leisson *et al.*, 2008), and most of these studies used horses younger than 12 years of age (Essén *et al.*, 1980; Lopez-Rivero *et al.*, 1991; Roneus *et al.*, 1991; Roneus, 1993; Barrey *et al.*, 1999), therefore not addressing the problems and phenomena associated with aging into the geriatric stage of life. In the present study, we recruited sedentary horses between the age of 17 and 25 yr to investigate the impact of physiological aging on skeletal muscle function in comparison to a group of young horses.

Skeletal muscle is highly malleable and able to adapt to altered functional demands and stimuli (Flück, 2006). A common adaptation is a change in muscle fiber metabolism through modifying fiber type composition. Skeletal muscle myosin heavy chain, an essential component of the contractile apparatus, exists in different isoforms, which are associated with mode of energy production and muscle fiber function. In large animals, based on the MyHC isoform present, skeletal muscle fibers are classified as type I, associated with predominantly oxidative energy metabolism; type IIX (or historically IIB), associated with predominantly glycolytic energy metabolism; or type IIA, which is an intermediate fiber type, exploiting predominantly oxidative energy production with functional features characteristic of glycolytic fibers. Importantly, hybrid fibers exist, which express more than one isoform, and are more prevalent in muscles undergoing transition, such as aging, or exercise adaptation (reviewed by Pette & Staron, 2000).

Further, muscle groups very rarely express only one fiber type; they are comprised of a combination of the three fiber types. Fiber type distribution in skeletal muscle has been investigated in untrained horses to reflect alterations in muscle function with advancing age. However, the data are contradictory, with some studies reporting an increase in oxidative fibers (Rivero *et al.*, 1993), and others suggesting an age-related shift from oxidative to glycolytic fibers (Lehnhard *et al.*, 2004; Kim *et al.*, 2005). In addition, whether an age-related alteration in fiber type composition is associated with changes in muscle oxidative capacity has not been well investigated in the horse (Rivero *et al.*, 1993; Kim *et al.*, 2005).

Skeletal muscle oxidative metabolism occurs in the mitochondria. Mitochondria are prominent in skeletal muscle and provide ATP for muscle function through the process of OXPHOS, carried out by the complexes ETS. Increasing evidence shows that aging is associated with compromised capacity for OXPHOS in human muscle (Cooper *et al.*, 1992; Joseph *et al.*, 2012), most likely due to a decline in mitochondrial density and/or function (Short *et al.*, 2005). Numerous mitochondrial components have been tested during the past two decades as biomarkers of muscle oxidative capacity in human (Mogensen *et al.*, 2006; Ritov *et al.*, 2006; Boushel *et al.*, 2007) as well as in horses, such as CS, 3-HADH (Kim *et al.*, 2005; Revold *et al.*, 2010), COX (White *et al.*, 2015) and succinate dehydrogenase (Serrano *et al.*, 2000). Among them, activity of CS, COX, and 3-HADH have been used as biomarkers of mitochondrial content and oxidative capacity, respectively (Coggan *et al.*, 1992; Rimbert *et al.*, 2004; Larsen *et al.*, 2012). Moreover, OXPHOS is a complicated process, which requires the coordinated interaction of multiple enzyme complexes. The mere assessment of enzymatic function

of individual components of this system may be insufficient to reveal how well the system functions as a whole, and whether and where age-related defects occur (Saks *et al.*, 1998; Villani *et al.*, 1998; Kunz, 2003). High-resolution respirometry (HRR) with saponin-permeabilized muscle fibers allows the study of OXPHOS in skeletal muscle mitochondria *in situ*. Oxygen consumption of mitochondria still situated within the muscle fiber can be sensitively monitored and evaluated by titrating energy substrates, ADP, complex inhibitors, and uncouplers to the permeabilized fibers. To date only a few groups have applied this technology in horse studies to investigate the effect of training on muscle function (Votion *et al.*, 2010; Votion *et al.*, 2012; White *et al.*, 2015). We are unaware of any studies using HRR with permeabilized muscle fibers to study the impact of aging on integrated mitochondrial respiratory function in horse skeletal muscle.

The objective of this study was to examine the age-associated changes in skeletal muscle fiber type composition and mitochondrial function in the Quarter Horse. We sampled the GLU and TRI, muscles of the extremities with distinct locomotor functions attributed to and associated with different muscle fiber type composition (van den Hoven *et al.*, 1985). To address the question whether alterations in fiber type composition, determined electrophoretically, are associated with changes in muscle oxidative capacity, both the classical spectrophotometric method of enzyme activity assays and the more comprehensive HRR were used to assess mitochondrial OXPHOS capacity. Furthermore, the comparison of mitochondrial function between GLU and TRI muscle allowed us to evaluate muscle-specific responses to aging.

Materials and Methods

Animals

All procedures performed in this study were approved by the University of Florida Institute of Food and Agricultural Sciences Animal Research Committee. A total of 34 Quarter Horses including 24 young (1.8 ± 0.1 years old, 14 fillies and 10 geldings) and 10 aged subjects (17-25 years old, 9 mares and 1 gelding) were utilized in this study. Horse body condition score (BSC) was assessed using the Henneke scoring system with a scale from 1 to 9 (1 = emaciated and 9 = extremely obese) (Henneke *et al.*, 1983). Compared to the young horses, which had a BCS of 5.00, the aged horses had a significantly higher average BCS (5.80 ± 0.25; $P < 0.001$). All horses used in this study were owned by the University of Florida. None of the young horses had undergone any type of conditioning; and none of the aged horses had been athletes in the past, nor been used in competitions, and had been exposed to only low intensity exercise/training in the past, if any. None of the horses used in this study had received forced exercise 6 months prior to the study.

Skeletal Muscle Sampling

Skeletal muscle samples were taken from the right or left GLU (n = 34: 24 young + 10 aged) and from the TRI of a subset of young horses (n = 12) and of all aged horses (n = 10) under local anesthesia using a 14-gauge SuperCore™ biopsy needle (Angiotech, Gainesville, FL, USA). The GLU muscle was located on the croup by tracing approximately one-third down a line from the tuber coxae to the tailhead; and the long head of the TRI muscle was located at the intersection of a line traced between the scapulohumeral and radiohumeral joint and a vertical line extending down from the tricipital crest of the scapula. Briefly, the sample collection site (3 × 3 cm) was shaved,

and the skin was cleaned with 7.5% povidone-iodine and rinsed with 70% ethanol. Horses were sedated with approximately 0.3 mL of detomidine hydrochloride (Dormosedan®, Pfizer Animal Health, Exton, PA) administered i.v. The sampling site was then anesthesized by subcutaneous injection of 0.2-0.3 mL 2% mepivacaine hydrochloride (Carbocaine®-V, Pfizer Animal Health, Exton, PA). The muscle sample (approx. 30 to 40 mg tissue) was taken at a standardized depth of 5 cm within the respective muscle through an initial skin puncture created with a 14-gauge needle and subsequent insertion of the biopsy needle. In order to collect a sufficient quantity of tissue sample, the biopsy needle was reinserted 2-3 times into the same initial puncture at different angles (same depth). Samples were immediately transferred into 1 mL ice-cold biopsy preservation solution (BIOPS; 2.77 mM CaK_2EGTA, 7.23 mM K_2EGTA, 5.77 mM Na_2ATP, 6.56 mM $MgCl_2 \cdot 6H_2O$, 20 mM Taurine, 15 mM Na_2Phosphocreatine, 20 mM Imidazole, 0.5 mM DTT, and 50 mM MES; pH 7.1 (Saks *et al.*, 1998)) for subsequent respiration measurement on fresh tissue sample. The remaining tissue sample was snap-frozen in liquid nitrogen and stored in a dry shipper (MVE SC4/2V, CHART, Inc., Ball Ground, GA, USA) for transport to the laboratory and later stored at -80 °C.

Preparation of Permeabilized Muscle Fibers

The preparation of permeabilized muscle fibers was described previously (Kuznetsov *et al.*, 2008). Briefly, muscle samples were immersed in ice-cold BIOPS solution during transportation to the laboratory. Before further preparation of fibers, fat and connective tissue were removed, and muscle fibers gently separated using two pairs of forceps. Myofiber bundles were transferred to 1 mL fresh BIOPS solution containing 50 µg/mL saponin and the cell membrane was permeabilized for 30 min at 4

°C on a rotator. After the permeabilization, the myofibers were rinsed in ice-cold mitochondrial respiration medium (MiR05; 110 mM sucrose, 60 mM potassium lactobionate, 0.5 mM EGTA, 3 mM $MgCl_2$•$6H_2O$, 20 mM taurine, 10 mM KH_2PO_4, 20 mM HEPES, and 1 g/L BSA; pH 7.1) on a rotator for 10 min at 4 °C. Mitochondrial respiration of these permeabilized myofibers was immediately assessed using HRR.

High-Resolution Respirometry

Mitochondrial respiration (O_2 flux) was determined in duplicate using the high-resolution respirometer Oroboros O2k (OROBOROS INSTRUMENTS, Innsbruck, Austria) at 37°C and in hyperoxic conditions (220-450 µM O_2), according to methods previously described (Kuznetsov *et al.*, 2008). Unless stated otherwise, the concentrations of the following reagents used are final concentrations in the respirometer chamber. Permeabilized fibers (2-3 mg wet weight) were added to the respirometer chamber containing 2 mL of MiR05. The respiration medium was supplemented with 20mM creatine to saturate mitochondrial creatine kinase, which facilitates mitochondrial ADP transport (Saks *et al.*, 1991; Walsh *et al.*, 2001). Oxygen flux was determined with the following titration protocol (Figure 2-1): electron flow through complex I (CI) of the ETS (OXPHOS capacity$_{CI}$, P_{CI}) was supported by the NADH-linked substrates glutamate (10 mM) and malate (2 mM) (LEAK respiration, L), followed by addition of adenosine diphosphate (ADP, 2.5 mM) to stimulate respiration ($OXPHOS_{CI}$, P_{CI}); the addition of succinate (10 mM) supported convergent electron flow through complex I and II (CII) of the ETS (OXPHOS capacity$_{CI+II}$, P_{CI+II}); additional ADP (1.25 mM) and succinate (5 mM) were then titrated to evaluate whether OXPHOS capacity could be increased any further. No further increase was observed, indicating that OXPHOS capacity was measured at a saturating ADP concentration. Subsequent

addition of cytochrome *c* (cyt *c*, 10 μM) tested the integrity of the mitochondrial outer membrane. Only samples with response to cyt *c* below a 15% increase in respiration were included in the analysis. Titration of the uncoupler carbonyl cyanide 4-(trifluoromethoxy) phenylhydrazone (FCCP, 0.5 μM) measured maximum noncoupled respiration (ETS capacity; E). The coupling control ratio L/P was calculated as the ratio of LEAK to OXPHOS capacity (L/P_{CI+II}), and the P_{CI+II}/E coupling control ratio (P/E) was calculated as the ratio of OXPHOS capacity (P_{CI+II}) to ETS capacity.

Sample Preparation and SDS-PAGE for Myosin Heavy Chain Analysis

Frozen muscle was powdered in liquid nitrogen using a BioPulverizer (BioSpec Products, Inc., Bartlesville, OK, USA). Tissue powder was subsequently homogenized with 30 volumes of extraction buffer (50 mM Tris-HCl, pH 8.3, 10 mM EDTA) using a glass tissue grinder (Kontes Dual, size 20, Kimble Chase, Vineland, NJ, USA). The muscle homogenate was transferred to a microcentrifuge tube and diluted with equal volume of protein denaturation buffer (4% SDS, 20% glycerol, and 125 mM Tris-HCl, pH 6.8). The sample was then heated at 50 °C for 20 min and centrifuged at 14,000 x *g* for 20 min (101). Protein content was determined using the Bicinchoninic Acid (BCA) protein assay kit according to the manufacturer's instructions (Thermo Scientific, Inc., Rockford, IL, USA). Samples were stored in equal volume of glycerol at -20 °C until further processing.

MyHC isoforms in muscle homogenates were analyzed using a slightly modified protocol described previously (Talmadge & Roy, 1993). Briefly, the protocol was modified as follows: 1) samples were heated at 95 °C for 3 min; 2) electrophoresis (SDS-PAGE) proceeded at 120V for 18 h; 3) protein load per lane was 2.5 μg. Following electrophoretic protein separation, the gel was stained with Coomassie Brilliant blue

R250 (Bio-Rad Laboratories, Inc., Hercules, CA, USA) for 2 h and the proteins visualized using a cooled CCD camera and acquisition software (G-BOX imaging system, Syngene, Frederick, MD, USA). To verify the nature of the separated bands, a separate gel electrophoresis with a representative subset of muscle sample homogenates was performed. Instead of Coomassie staining, the proteins were transferred to a PVDF membrane using a semi-dry blotter at 20 V for 60 min (Trans-Blot® Bio-Rad Laboratories, Inc., Hercules, CA, USA). The nature of the protein bands were confirmed as MyHC-IIA, MyHC-IIX and MyHC-I isoforms by immunoblotting using primary myosin heavy chain antibodies SC-71 (MyHC-IIA, 1: 150), 6H1 (MyHC-IIX, 1: 100) and BA-D5 (MyHC-I, 1:100) (all from Developmental Studies Hybridoma Bank), and HRP-conjugated goat anti-mouse IgG secondary antibody (1: 80,000, Sigma, St. Louis, MO, USA). Bands were visualized using a HRP substrate (DuoLuX™, VECTOR LABORATORIES, Inc., Burlingame, CA, USA) and the chemiluminescence captured with the G-Box imaging system. The intensity of the Coomassie blue stained protein bands (Figure 2-2) as well as the chemiluminescence intensity was analyzed and quantified by densitometry using the manufacturer's analysis software (GeneTools, Syngene). For each sample, percentages of each MyHC isoforms were calculated as a percentage of the total (100%) MyHC isoforms in each lane.

Spectrophotometric Determination of Enzyme Activities

Enzymatic activities of CS, COX, and 3-HADH in muscle homogenates were measured as previously described (Fong & Schulz, 1978; Spinazzi *et al.*, 2012) using a microplate reader (Synergy HT, BioTek Instruments, Winooski, VT, USA). Briefly, CS activity was assessed at 412 nm by measuring the initial rate of reaction of free CoA-SH with DTNB; COX activity was determined by measuring the maximal, linear rate of

oxidation of fully reduced cytochrome *c* at 550 nm; and 3-HADH was assayed by measuring the oxidation of NADH at 340 nm using acetoacetyl-CoA as substrate.

Statistical Analyses

Data are reported as means ± SE, with the number of samples per group noted in the figure legends. Statistical analyses were performed using SigmaPlot version 12.0 (Systat Software, Inc, San Jose, CA). All data were compared between different age groups and across skeletal muscles using two-way analysis of variance (ANOVA) followed by Student-Newman-Keuls multiple comparison tests. For data that did not express a normal distribution (L/P), a log-transformation was performed prior to statistical analysis, but the original data were presented in the graph. In all comparisons, differences with $P \leq 0.05$ were considered statistically significant, and trends were reported if $0.05 < P < 0.1$.

Results

Aging and Muscle-Fiber Type Composition

The composition of MyHC isoforms was significantly altered in muscles from aged compared to young horses, with increase of MyHC-I and IIA, and decrease of MyHC-IIX, independent of muscle type (Table 2-1; main effect of age; MyHC-I: $P = 0.002$, MyHC-IIA: $P = 0.032$, MyHC-IIX: $P = 0.004$). More specifically, in GLU muscle the percentage of MyHC-I was significantly higher in aged compared to young horses ($P < 0.001$). In addition, there was a trend for a decreased percentage of MyHC-IIX in aged GLU muscle ($P = 0.092$), while the proportion of MyHC-IIA was unaltered ($P = 0.520$). In TRI muscle, no difference in percent MyHC-I was detected between the two age groups ($P = 0.224$). However, aged horses exhibited a higher percentage of MyHC-IIA ($P = 0.023$), and a lower percentage of MyHC-IIX ($P = 0.012$) relative to young animals.

When GLU and TRI muscles were compared, the MyHC composition significantly differed between muscles, and this difference was maintained in both age groups (main effect of muscle type, $P < 0.001$ for all fiber types). More specifically, GLU muscle had a lower percentage of MyHC-I and MyHC-IIA, and a higher percentage of MyHC-IIX compared to TRI.

Effect of Age on Mitochondrial Density and Enzyme Activity

We found a main effect of age on CS activity per mg tissue ($P = 0.014$; Figure 2-3A). Specifically, CS activity did not differ between age groups in GLU ($P = 0.230$), but was lower in TRI muscle from aged horses ($P = 0.023$). When the two muscles were compared, CS activity in the TRI muscle was approximately 2-fold greater compared to the GLU (main effect of muscle type: $P < 0.001$), independent of age, which is consistent with the almost 2-fold difference in percentage of presumably mitochondria-rich (type I and IIA) muscle fibers observed between the two muscles.

There was a main effect of age on COX activity per mg muscle tissue ($P < 0.001$; Figure 2-3B). Specifically, COX activity per mg tissue decreased significantly with age in both muscles ($P < 0.001$). Furthermore, COX activity per mg tissue was significantly lower in GLU compared to TRI muscle (main effect of muscle type: $P < 0.001$). When COX activity was normalized to CS activity to reflect the oxidative capacity on the mitochondrial level (Figure 2-3C), there was a significant effect of age (main effect of age: $P < 0.001$). Specifically, COX activity per mitochondrial unit was 47% lower in aged GLU ($P < 0.001$), and 30% lower in aged TRI muscle ($P = 0.003$). When muscles were compared, COX activity per mitochondrial unit was lower in TRI compared to GLU muscle (main effect of muscle type: $P < 0.001$).

Activity of 3-HADH per mg muscle tissue was not affected by age in either GLU or TRI muscle (main effect of age: $P = 0.125$; Figure 2-3D). Compared to the GLU, the TRI muscle exhibited higher 3-HADH activity per mg muscle tissue (main effect of muscle type: $P < 0.001$). When 3-HADH activity was evaluated per Mt unit by normalizing its activity to CS activity (Figure 2-3E), 3-HADH activity was significantly elevated with age in both muscles (main effect of age: $P < 0.001$; GLU: $P = 0.023$; TRI: $P < 0.001$). When muscles were compared, 3-HADH activity per mitochondrial unit was lower in TRI compared to GLU muscle (main effect of muscle type: $P = 0.044$).

Effects of Age on Mitochondrial Respiration

There were no apparent age-associated changes in mass-specific mitochondrial respiration (O_2 flux; pmol O_2/s/mg wet weight) in either GLU or TRI muscle for any of the assessed respiratory states (LEAK: GLU: $P = 0.487$, TRI: $P = 0.606$; P_{CI}: GLU: $P = 0.820$, TRI: $P = 0.318$; P_{CI+II}: GLU: $P = 0.386$, TRI: $P = 0.422$; ETS capacity: GLU: $P = 0.738$, TRI: $P = 0.918$; Figure 2-4A-D). When muscles were compared, significant differences were detected between GLU and TRI muscle (Figure 2-4A-D). Specifically, the TRI exhibited higher OXPHOS capacity (P_{CI} and P_{CI+II}), and ETS capacity when compared to the GLU muscle (main effect of muscle type: $P < 0.001$ for all).

When O_2 flux was normalized to CS activity (Figure 2-4E-H), we found a significant effect of age for all but OXPHOS capacity supported by glutamate, malate and succinate (P_{CI+II}), independent of muscle type (main effect of age: LEAK: $P = 0.038$; P_{CI}: $P = 0.045$; P_{CI+II}: $P = 0.073$; ETS capacity: $P = 0.007$). In particular, P_{CI} and ETS capacity tended to be higher in aged-GLU muscle ($P = 0.086$ and $P = 0.085$, respectively; Figure 2-4F, H), and ETS capacity was significantly higher in aged-TRI muscle ($P = 0.033$; Figure 2-4H) when compared to the young counterparts. When the

two muscles were compared, OXPHOS capacity supported by glutamate and malate (P_{CI}) (*P* = 0.025), glutamate, malate and succinate (P_{CI+II}) (*P* = 0.027), and ETS capacity (*P* = 0.038) were significantly higher in GLU compared to TRI muscle (*P* values reflect main effects of muscle type; Figure 2-4E-H). These findings are consistent with COX activity per mitochondrial unit, and suggest that the higher oxidative capacity of TRI muscle results from a higher mitochondrial density rather than from oxidative capacity of individual mitochondria.

Effect of Aging on Coupling Control Ratios

We used the O_2 flux in different respiratory states to calculate coupling control ratios. The L/P coupling control ratio ($LEAK/P_{CI+II}$), an indicator for coupling of oxygen consumption and phosphorylation, was between 0.06 and 0.07 for young-TRI and young-GLU muscles, and between 0.08 and 0.11 for aged TRI and GLU muscles, suggesting a tight coupling of mitochondria in permeabilized fibers (Figure 2-5A). There was a main effect of age on the L/P coupling control ratio (*P* = 0.016). Compared to young horses, the L/P ratio was significantly increased by 49 % in GLU (*P* = 0.019), but remained unchanged in TRI muscle (*P* = 0.263). When muscles were compared, the L/P ratio did not differ between GLU and TRI muscle, independent of age (main effect of muscle type: *P* = 0.326).

To examine the extent to which oxidative phosphorylation exploits the full capacity of the ETS, we calculated the P/E coupling control ratio (P_{CI+II}/fully non-coupled ETS capacity; Figure 2-5B). We found that P/E was significantly affected by age (main effect of age: *P* = 0.011), but when the effect in the individual muscles was evaluated, there was only a tendency for the P/E ratio to decrease with age (GLU: *P* = 0.076; TRI:

P = 0.057). No difference in P/E was detected between the two muscles (main effect of muscle type: *P* = 0.854).

Discussion

In the present study, we compared skeletal muscle metabolic phenotype by analyzing muscle fiber type composition and mitochondrial OXPHOS capacity in Quarter Horses of two different age groups. For this comparison, we chose the GLU and the TRI muscle based on their functions. The GLU muscle is located in the hind limb and used for explosive propulsive movement, while the TRI muscle is a postural muscle located in the forelimb, where it supports the body weight during long periods of standing. These different functional demands dictate a different muscle fiber type composition and energy metabolism. Based on differential susceptibility of muscle fiber types to age-related changes that has been reported in humans and rodent models (Houmard *et al.*, 1998; Phillips & Leeuwenburgh, 2005; Joseph *et al.*, 2012), we expected to see different responses to age in fiber type composition and mitochondrial function in these two types of equine muscles.

MyHC isoform appears to be an appropriate marker for muscle fiber type classification, and has been used in numerous studies to characterize skeletal muscle fiber type composition (Rivero *et al.*, 1997; Andersen, 2003; Joseph *et al.*, 2012). Our findings in the Quarter Horse are in agreement with previous findings in horses (van den Hoven *et al.*, 1985). Both GLU and TRI muscles had a relatively high content of MyHC-II isoforms (88-96%), which might partially explain the great capacity for explosive speed of this horse breed. However, GLU muscle had relatively more MyHC-IIX fibers than the TRI muscle, while the TRI muscle contained a greater percentage of MyHC-I fibers. This is consistent with observations in other horse breeds at the same biopsy sampling

depth (van den Hoven *et al.*, 1985), and is in accordance with the muscles' different functional demands for explosive power for propulsion (GLU) or for postural support (TRI), respectively.

In our study, aging was associated with a shift in skeletal muscle fiber type composition toward a MyHC-I or IIA phenotype, but with a differential response in the two muscles investigated. Aging has been shown to affect fiber type distribution in various horse breeds (Essén *et al.*, 1980; Rivero *et al.*, 1993; Lehnhard *et al.*, 2004; Kim *et al.*, 2005) (Table 2-2). For example, Rivero *et al*. and Kim *et al*. (Rivero *et al.*, 1993; Kim *et al.*, 2005) found a decline in percentage of type I fibers with age, but no correlation of age and percentage of type IIA or IIX fibers in the *Semitendinosus* muscle from a group of horses of different breeds, with ages ranging from 2 to over 30 years. Likewise, Lehnhard *et al.* (Lehnhard *et al.*, 2004) reported a decrease in MyHC-I and IIA, and an increase in MyHC-IIX content in GLU from old (20+ years old) compared to young (4-8 years old) Standardbred mares. On the contrary, our results suggest an age-associated increase in MyHC-I fibers in the GLU and MyHC-IIA fibers in the TRI muscle, respectively, concomitant with a relative decrease in MyHC-IIX fibers in both muscles. This is in agreement with findings in humans (Welle *et al.*, 2000), rodents (Sugiura *et al.*, 1992; Sullivan *et al.*, 1995; Pehme *et al.*, 2004), and two reports in horses (Essén *et al.*, 1980; Rivero *et al.*, 1993) (Table 2-2). Indirect support for a fiber type shift to a more oxidative phenotype comes from a study in aging humans by Lanza *et al.* (Lanza *et al.*, 2005). Using phosphorous magnetic resonance spectroscopy of contracting skeletal muscle *in vivo*, the authors demonstrated that older men relied more on oxidative phosphorylation and less on glycolysis for ATP production compared to young men. The

discrepancies between our results and some previously published findings in equine muscle could have resulted from the choice of breed and the age-range investigated. Compared to other breeds, the skeletal muscle of the Quarter Horse is rich in type IIX fibers (Valberg, 2013), which could have accentuated the shift in fiber type distribution compared to breeds with a more balanced distribution. In addition, the age of the young horses investigated in this study was about 2-years, an age at which the skeletal muscle is still developing (Rietbroek *et al.*, 2007), which could have affected the outcome of our measurement in comparison to other studies.

In rodents, fiber type distribution of different muscles was differentially affected by aging. For example, in rats age-related alterations were only observed in slow-twitch *Soleus* muscle but not in fast-twitch *Tibialis anterior* muscle of the same individual (Larsson & Edstrom, 1986). A study in Standardbred trotters (Essén *et al.*, 1980) assessed muscle-specific fiber type adaptions to the aging process and reported that GLU and TRI muscles had the greatest increase in oxidative fiber types among studied muscles.

There are several potential mechanisms that could underlie the age-associated change in relative fiber type composition. A selective age-related susceptibility to atrophy of a specific fiber type could lead to relative increases in the other fiber types (Ciciliot *et al.*, 2013). Selective atrophy of mainly type II(X) fibers and predominantly fast-twitch muscles has been widely accepted and described to occur in rodents (Thompson & Brown, 1999; Lowe *et al.*, 2001) and humans (Joseph *et al.*, 2015). For example, in elderly humans, the elevated relative increase of type I fibers was mainly caused by a selective atrophy of type II fibers (Larsson *et al.*, 1978). Muscle fiber

atrophy observed with age can, at least in part, be driven by several mechanisms, such as a decrease in protein synthesis (reviewed by Yarasheski, 2003), or mitochondria-dependent and -independent apoptosis (Marzetti *et al.*, 2010). To the best of our knowledge apoptosis or protein degradative mechanisms in skeletal muscle have not yet been investigated in the aged horse. Wagner *et al.* (Wagner *et al.*, 2013) reported that whole body protein synthesis was unaffected by age in mixed-breed horses, but that there seems to be a disturbance of skeletal muscle-specific protein synthesis (namely in the mTOR signaling pathway). However, muscle structure, muscle fiber features and other effectors of the mTOR pathway such as atrophy and autophagy proteins were not assessed in this study. A comprehensive assessment of aging equine skeletal muscle will be useful for a deeper understanding of the underlying causes of age-related muscle weakness, especially when development of interventions to attenuate age-related decline in physical performance is desired.

An alternative explanation for the altered fiber type distribution is an age-induced fast-to-slow fiber type transition within a given fiber (reviewed by Larsson & Ansved, 1995). This transition could be caused by denervation of type II fibers followed by either atrophy of the denervated fiber or by subsequent reconstitution of larger motor units with slow motor-neurons, inducing a fiber type switch (Pette & Staron, 2000). Studies in rodents undergoing fast-to-slow conversion indicated that the transition in MyHC isoforms follows a sequential order from MyHC-IIB to MyHC-IIX to MyHC-IIA to MyHC-I (Jaschinski *et al.*, 1998). Based on our data, we speculate that if there was an age-related conversion of fiber types in the muscle of Quarter Horses, it occurred to a differential degree or in a differential time line in the two muscles. With MyHC-IIX

decreasing in both muscles, the GLU displayed an increase in MyHC-I and the TRI in MyHC-IIA portion, which suggest that GLU could have been affected at an earlier time point or to a more severe degree compared to TRI. Similar muscle-specific changes associated with age were suggested by Essén and coworkers (Essén *et al.*, 1980) in a study on racing horses, in which the authors compared age-related responses in fiber type distribution in the GLU muscle with that in other muscles (including TRI muscle). In this study, the GLU muscle was the only muscle that displayed an increased type I/II ratio with age. Further studies need to be conducted to investigate a differential time line or severity of changes in fiber type distribution between different muscles. In addition, in order to distinguish between loss of fibers and fiber type conversion, total fiber number, cross sectional area of fibers, and muscle weight would be ideal parameters to determine. However, the lack of practicality prohibits some of those measures in the study of live animals in which only small muscle biopsies can be acquired.

In summary, our results are in agreement with extensive literature on humans and rodents. However, at this point, we cannot distinguish between selective fiber atrophy or fiber type conversion, nor the development of hybrid fibers. In addition, it needs to be emphasized that the literature is all but consistent in the observation of age-related changes in fiber type composition. Purves-Smith *et al.* (purves-Smith *et al.*, 2014) recently critically reviewed and evaluated the methodology leading to the various and often contradictory findings. The authors concluded that the presence of hybrid fibers, which is rarely assessed, may draw a different picture of age-related changes in fiber type contribution altogether, and that the lack of identification of hybrid fibers could account for the contradictory results on the effect of age on fiber type composition.

Our next aim was to compare the observed shift to a higher percentage of type I or type IIA fibers with the metabolic phenotype on a subcellular level. Specifically, we asked whether the age-induced increase in type I or type IIA fibers was concomitant with altered function and OXPHOS capacity of skeletal muscle mitochondria; and whether muscle oxidative capacity was altered through modifying mitochondrial content, mitochondrial respiratory capacity, or both.

Citrate synthase activity was used as a representative biomarker of mitochondrial density and total cristae area (Larsen *et al.*, 2012). When we compared the two muscles, we found that CS activity was 2-fold higher in TRI muscle compared to GLU muscle, which corresponds with the 2-fold higher proportion of fibers with a presumably predominantly oxidative metabolism (MyHC-IIA + MyHC-I) in TRI muscle compared to GLU muscle. We furthermore found that GLU and TRI muscles were affected differently by age. More specifically, CS activity decreased with age in the TRI muscle but not in the GLU muscle. A decline in CS activity has not often been documented in old sedentary horses (Kim *et al.*, 2005). But findings similar to ours were reported in human studies that revealed an age-associated decline in CS activity in the oxidative portion of the *Gastrocnemius* muscle (Houmard *et al.*, 1998), but not in the relatively more glycolytic *Vastus lateralis* (Grimby *et al.*, 1982; Houmard *et al.*, 1998). The explanation for this divergent change in CS activity between different muscles with aging is not clearly evident, but it may be partially explained by MyHC distribution. In the Quarter Horse, CS activity was unaffected by age in GLU muscle. However, this “preservation” of mitochondrial density did not align with the increase in presumably mitochondria-rich type I fibers, suggesting that the increased proportion of type I fibers

did not cause a proportional increase in mitochondrial density. What is more, CS activity diminished with age in the TRI muscle despite the observed relative increase in MyHC-IIA content. In contrast to our findings, Kim *et al.* (Kim *et al.*, 2005) reported that CS activity in equine *Semimembranosus*, a predominantly glycolytic muscle, was negatively correlated with age, and concomitant with a decreased MyHC-I proportion. However, we cannot deduce from Kim's data whether the decrease in CS activity, and deduced from this mitochondrial density, was proportional to the decline in oxidative fibers. The underlying cause for the age-associated decline in CS activity (Hebert *et al.*, 2015) and mitochondrial density described for human muscle (Conley *et al.*, 2000) might be a decreased rate of mitochondrial protein synthesis (Guillet *et al.*, 2004), or alterations in mitochondrial biogenesis, which is associated with mitochondrial protein synthesis (Joseph *et al.*, 2012). Alternatively, an age-associated imbalance between autophagic removal of mitochondria, namely mitophagy, and mitochondrial biogenesis would diminish mitochondrial density. However, impaired rather than increased mitophagy has been widely observed in aged muscle (reviewed in Hepple, 2014). To the best of our knowledge neither mitochondrial biogenesis nor mitophagy have been assessed in aging equine skeletal muscle, and are the current subject of our laboratory's investigations.

Next, we addressed the question of whether the age-related decrease in mitochondrial density (deduced from CS activity) correlated with decreased oxidative capacity. We assessed muscle mitochondrial function, namely OXPHOS capacity, by both spectrophotometric measurement of COX activity in muscle homogenates, and HRR of skeletal muscle mitochondria *in situ*. In addition to OXPHOS capacity, we also

assessed activity of 3-HADH, an enzyme of the β–oxidation pathway to evaluate the capacity to metabolize fatty acids for energy production. There is some debate on whether differences in muscle tissue OXPHOS are due to mitochondrial content and/or composition of muscle fiber types, or function of the individual mitochondria, or both. Initially, it was suggested that differences in muscle respiration may be attributed solely to the differences in mitochondrial quantity (Hoppeler *et al.*, 1987; Schwerzmann *et al.*, 1989). Recently, a greater number of studies have revealed that differences in muscle oxidative capacity depended on the function of the mitochondria themselves (Jackman & Willis, 1996; Amara *et al.*, 2007). Here, we present COX and 3-HADH activities and O_2 flux relative to muscle weight, as well as per unit mitochondria. The normalization of mitochondrial functional markers to a mitochondrial marker such as CS activity has been recommended by Pesta and Gnaiger (Pesta & Gnaiger, 2012) in order to separate the effects of mitochondrial quality (function) from mitochondrial quantity.

In agreement with studies in humans (Rimbert *et al.*, 2004) and horses (Kim *et al.*, 2005), our data on 3-HADH activity suggest that fatty acid oxidation capacity was not impaired on a muscle level, and even elevated on a mitochondria level in muscles from our aged Quarter Horses. However, others reported an age-related decline of 3-HADH activity in humans (Coggan *et al.*, 1992), and a decreased ability to utilize fatty acids for mitochondrial respiration in mice (Johnson *et al.*, 2015). The preserved ability to metabolize fatty acids suggested by our data in aged horses seems to be concurrent with the structural shift towards a higher percentage of type I and IIA muscle fibers. Gueugneau *et al.* (Gueugneau *et al.*, 2015) reported a higher lipid content in type I and IIA compared to type IIX fibers in human *Vastus lateralis* muscle, and an increase in

intramyocellular lipid content with age, although this was not accompanied with a fiber type shift.

Cytochrome *c* oxidase activity has been validated as a marker of mitochondrial function, specifically of OXPHOS capacity (Larsen *et al.*, 2012). Our data showed that COX activity declined with age in both the GLU and the TRI muscle, whether normalized to wet weight or to mitochondrial unit, suggesting an impairment of OXPHOS capacity in older horses not only through decline in mitochondrial number but also through impaired function of the mitochondria themselves. Joseph *et al.* (Joseph *et al.*, 2012) found that COX activity (per unit muscle weight) in elderly, low functioning humans was lower than in that of young individuals, but the authors did not measure any indicator of mitochondrial density. We observed an over 40% reduction in COX activity with age in both muscles. This decline was more severe in the GLU, especially when the COX activity was normalized to mitochondrial unit. Given that GLU mitochondrial density was not severely affected by age, it appears that the oxidative capacity is primarily impaired on the individual mitochondrial level. On the other hand, in the TRI muscle, which displayed a significant decrease in mitochondrial density, the impairment of COX activity on the mitochondrial level seemed less severe. In the present investigation, we did not measure production of ROS or markers of (oxidative) damage to mitochondrial components, which could potentially underlie the pronounced reduction in COX activity in GLU muscle. Compared to oxidative muscles, muscles of a more glycolytic phenotype have been shown to produce more ROS, to have lower free radical scavenging capacity, and to consequently display higher oxidative damage such as lipid peroxidation (Anderson & Neufer, 2006; Picard *et al.*, 2008; Picard *et al.*,

2011a). Comparing the two muscles, independent of age, an interesting finding was that TRI muscle exhibited higher COX activity than GLU muscle when normalized to muscle weight, but lower COX activity per mitochondrial unit, which suggests that in TRI muscle the higher COX activity on the tissue level was achieved by a higher mitochondrial content. To further explore the muscle-specific impairment of mitochondrial function with aging we measured mitochondrial respiratory function *in situ* using HRR.

Although our results demonstrated that COX activity in skeletal muscle homogenates was dependent on age and muscle type, we cannot deduce whether this alteration reflects a change of muscle mitochondrial OXPHOS. Saponin-permeabilized muscle fibers allow examination of the integrative mitochondrial function in a relatively preserved cytoarchitecture (Kuznetsov *et al.*, 1998; Saks *et al.*, 1998). Our mass-specific respirometry data demonstrated no age-related difference in muscle respiratory capacity across all respiratory states, indicating that the capacity for muscle OXPHOS remained high in both muscles from our aged Quarter Horses. When expressed relative to CS activity, LEAK, OXPHOS (P_{CI}) and ETS capacity were elevated with age (significant main effect of age), independent of muscle type, although only aged-TRI muscle displayed a significant increase in ETS capacity. Products of oxidative stress are known to accumulate with age, and are reported to activate mitochondrial uncoupling proteins (UCPs) and the adenine nucleotide transporter (ANT) (Echtay *et al.*, 2002; Echtay *et al.*, 2005). Both could have caused an increased proton leak, and consequentially increased LEAK respiration. Moreover, the “uncoupling to survive” hypothesis of aging suggests that mild uncoupling, particularly in aged tissue, protects against mitochondrial ROS production and subsequent oxidative damage to

mitochondria and other cellular components (Brand, 2000; Greco *et al.*, 2003; Speakman *et al.*, 2004). The elevated LEAK respiration in aged muscle explains only a minor part of the concurrently increased ETS capacity. It is possible that this increase reflects on a functional level the increasing reliance on oxidative energy production in aged fibers. Jacobs *et al.* (Jacobs *et al.*, 2013a) recently showed in mice that mitochondria-specific ETS capacity was elevated with age in the primarily glycolytic *Gastrocnemius* muscle, but not in the primarily oxidative *Soleus* muscle.

Both mass-specific and mitochondria-specific activated respiration supported by complex I and II substrates (OXPHOS capacity, P_{CI+II}) were not affected by age, which is contrary to the age-related decline in COX activity that we determined in muscle homogenates. A similar case is reported by Chabi *et al.* who assessed state 3 respiration (OXPHOS in the presence of glutamate, malate and ADP) of isolated mitochondria and COX activity in muscle homogenates (Chabi *et al.*, 2008). The control of mitochondrial respiration is shared between all of the complexes and electron carriers in the respiratory electron transport system (Rossignol *et al.*, 2000), suggesting no rate-limiting step *per se*. In addition, it was evident in human mitochondria that maximal complex IV activity is in excess of what is required for OXPHOS (Gnaiger *et al.*, 1998; Villani *et al.*, 1998). This is supported by the observation that inhibition of complex IV activity had to exceed a critical value (40-60%) to cause a detectable decrease in mitochondrial respiration in both isolated mitochondria (Villani & Attardi, 1997; D'Aurelio *et al.*, 2001) and permeabilized muscle fibers (Kunz *et al.*, 2000). These suggestions could explain why we did not detect a decrease in OXPHOS with aging in either muscle as a whole when we assessed mitochondrial respiration with substrates supporting

complex I and II. We did not assess mitochondrial respiration supported by fatty acid oxidation. In rodents, fatty acid-supported respiration was impaired with age (Hey-Mogensen *et al.*, 2012; Johnson *et al.*, 2015), while fat oxidation capacity was similar in muscle from young and old sedentary men (Rimbert *et al.*, 2004). The unaltered 3-HADH activity on a whole muscle level observed here suggests that the capacity to oxidize fatty acids was preserved in skeletal muscle form aged horses. Future studies will have to determine whether capacity for fatty acid β-oxidation is correlated with utilization of this energy by the Mt electron transport chain.

The difference between mass- and mitochondria-specific respiration when comparing GLU and TRI muscles is consistent with our results for COX activity. *Triceps brachii* muscle had higher mass-specific respiratory rates across all states (except LEAK), which could be due to its considerably higher mitochondrial density. However, mitochondria-specific respiration in TRI muscle was lower (with the exception of LEAK). This difference in mass- and mitochondria-specific respiration between different equine muscles is similar to observations in humans and laboratory animals (Jackman & Willis, 1996; Amara *et al.*, 2007). For example, in old mice mass-specific activated respiration was higher and mitochondria-specific activated respiration lower in the oxidative *Soleus* compared to the glycolytic *Gastrocnemius* muscle (Jacobs *et al.*, 2013b), which suggests a mitochondrial specialization with muscle and/or muscle fiber type. Moreover, the finding that mitochondria in glycolytic muscles possessed a higher oxidative capacity than those in oxidative muscles is consistent with observations in other mammals (Jackman *et al.*, 1996; Picard *et al.*, 2008; Jacobs *et al.*, 2013a). Specific mitochondrial phenotypes have been postulated to exist across skeletal muscle types,

with different composition and morphology. For example, others have reported that mitochondrial composition can vary by differential expression of respiratory complex subunit isoforms to sustain the tissue-specific energy demands (Grossman & Lomax, 1997; Huttemann *et al.*, 2001; Kunz, 2003); and Jacobs *et al.* (Jacobs *et al.*, 2013a) determined differential protein expression of all ETS complexes in mouse skeletal muscle homogenates of three different muscles. We thus speculate that mitochondria from GLU muscle might express more COX protein, reflected in the higher mitochondria-specific COX activity and respiratory capacity compared to TRI mitochondria. At this point, we cannot substantiate our speculation, and further analyses will have to quantify mitochondrial components in the different muscles. In addition, mitochondria vary morphometrically between slow and fast fibers. Fast-twitch muscle mitochondria are arranged in a thinner and longer reticular network, while mitochondria in slow-twitch muscle possess a thicker and more truncated network (Ogata & Yamasaki, 1997), which could be related to the lower mitochondria-specific respiratory capacity in TRI muscle.

We found no difference in L/P or P/E ratio between the two muscles. A study with elite athletes pointed out that differences in mitochondrial OXPHOS capacity and mitochondrial coupling control were apparent only when substrates for both complex I and II are provided (Jacobs & Lundby, 2013). We hence calculated L/P and P/E using OXPHOS capacity with a physiological substrate combination that supports electron flow through CI and CII (P_{CI+II}). In the young horses, both muscles exhibited low L/P ratios, indicating a good coupling between respiration and phosphorylation, and the L/P ratios for young horse in our study are similar to those reported by Votion *et al.* (Votion

et al., 2012) for mature horses with the same respiratory substrates (note: these authors determined the respiratory control ratio (RCR); and 1/RCR=L/P). Although there was a main effect of age on L/P, this control ratio increased significantly only in GLU but not in TRI muscle, further confirming that mitochondria from the GLU muscle are more susceptible to age-related damage, which is consistent with the COX activity data. Moreover, a compromised coupling of respiration and phosphorylation is in agreement with the generally elevated LEAK respiration that we observed with age (independent of muscle type). Age affected the P/E phosphorylation control ratio independent of muscle type (main effect of age). In young horses, P/E was around 0.75 in both muscles, consistent with a report on healthy, untrained mature horses with a P/E ratio of 0.8 (Votion *et al.*, 2012). The tendency for an increasing limitation of OXPHOS capacity by the phosphorylation system, indicated by reduced P/E, together with the elevated ETS capacity observed in aged horses, suggests that even though aged horses displayed an elevated maximal ETS capacity, constraints of the phosphorylation system may underlie a lower relative activated respiration, thereby possibly limiting the energy supply in the aging muscle. However, a limited mitochondrial ATP generation might be necessary to reduce the production of ROS (Brand, 2000). ATP production relies on a high proton gradient, which may, in turn, be associated with ROS generation. In this situation, an elevated proton leak, suggested by the higher LEAK respiration in the older muscles, might help to limit oxidative stress and damage.

The data on mitochondrial respiration on the tissue as well as mitochondrial level suggest that despite significant decline in mitochondrial content (CS activity) and COX activity as well as shift in MyHC-isoform composition, integrated mitochondrial function

and intrinsic mitochondrial functionality were not negatively impacted in skeletal muscle from Quarter Horses about 20 years of age. Several interpretations come to mind: 1) In this study, we assessed integrated mitochondrial function *in situ* in permeabilized muscle fibers, a technique that helps to attenuate or even prevent disruptions due to preparative technique (Picard *et al.*, 2011b). But similar to assessment of isolated mitochondria, the mitochondria *in situ* were deprived of their intra- and extracellular milieu, which could have affected mitochondrial function *in vivo* (reviewed in Hepple, 2014). 2) It is possible that the Quarter Horse, which can remain active well beyond the age assessed in this study, does not respond to aging with impaired oxidative capacity like it has been described for rodents and humans. And lastly, 3) the horses investigated in our study might not have reached the age at which integrated and/or intrinsic mitochondrial function becomes overtly impaired, and were instead at a transition age, displaying cellular adaptions rather than impairments, similar to observations made in aging rhesus monkeys (Pugh *et al.*, 2013). Taken together, future studies are needed to test those possibilities, for example by using *in vivo*, non-invasive technologies to assess oxidative capacity within the feasibility of application in large animals, and by expanding the age-range of subjects.

Table 2-1. Fiber-type composition of *gluteus medius* and *triceps brachii* from American Quarter Horses

MyHC Isoforms (%)	*gluteus medius*		*triceps brachii*		Main effect of muscle type, *P* value
	Young (n=24)	Aged (n=9)	Young (n=11)	Aged (n=9)	
MyHC-I	3.39 ± 0.35	6.68 ± 0.87***	10.57 ± 0.99	11.85 ± 0.71	$P < 0.001$
MyHC-IIA	21.35 ± 0.85	23.18 ± 2.65	33.79 ± 1.22	41.42 ± 4.53*	$P < 0.001$
MyHC-IIX	75.26 ± 0.92	70.14 ± 2.82†	55.64 ± 1.59	46.73 ± 4.92*	$P < 0.001$

Values are means ± SE. $^{\dagger}P < 0.1$, ***$P < 0.001$ (Young vs. Aged within GLU); * $P < 0.05$ (Young vs. Aged within TRI).

Table 2-2. Effect of age on fiber-type composition in equine skeletal muscle

Horse breed	Age	Muscle	Methodology	Effect of age	Ref.
SB	2 mo to 28 yr	GLU, TRI	Histochemistry	GLU: type I, IIA↑, type IIB↓; TRI: type I ↔, type IIA↑, type IIB↓	Essén *et al.*, 1980
AL, A	2-3 yr vs. 10-24 yr	GLU	Histochemistry	%type I, IIA↑, %type IIB↓	Rivero *et al.*, 1997
SB	4-8 yr vs. 20^{+} yr	GLU	SDS-PAGE & Coomassie blue staining	%type I, IIA↓, %type IIX↑	Lehnhard *et al*., 2004
TB, SB, QH, CB	2 yr to 30 yr	S	SDS-PAGE & Coomassie blue staining	%type I↓, type IIA, IIB↔	Kim *et al.*, 2005

Horse breeds are as follows: TB, Thoroughbred; SB, Standardbred; QH, American Quarter Horse; CB, crossbred; AL, Andalusian; A, Arabian. Muscles investigated are as follows: GLU, *gluteus medius*; TRI, *triceps brachii*; S, *semimembranosus*. Arrows indicate increased, decreased, or unchanged percentage of fiber type.

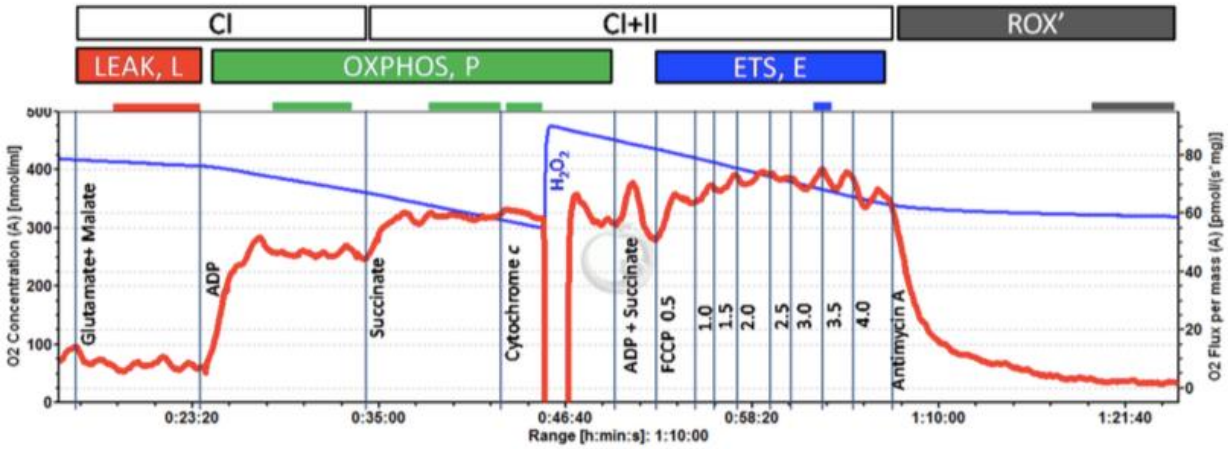

Figure 2-1. Respirometric protocol with permeabilized fibers from American Quarter Horse *gluteus medius* muscle. Shown is a typical trace of oxygen consumption after permeabilized fiber preparation with glutamate/malate and succinate substrate combinations to support electron flow through complex I (CI) and complex II (CII), respectively, of the mitochondrial electron transport system (ETS), and its activation by ADP. Cytochrome *c* was added as a quality control (see text for details), FCCP to induce uncoupling and evaluate ETS capacity, and antimycin A (inhibitor of complex III of the ETS) to evaluate residual oxygen consumption (ROX). The blue line represents the oxygen concentration (nmol/ml), the red line represents the muscle mass-specific O_2 flux (pmol $O_2 \cdot s^{-1} \cdot$mg wet wt^{-1}; negative slope of the blue line normalized to tissue weight). Marked sections correspond to steady-state fluxes at different coupling states (L, P, and E; see text for explanations).

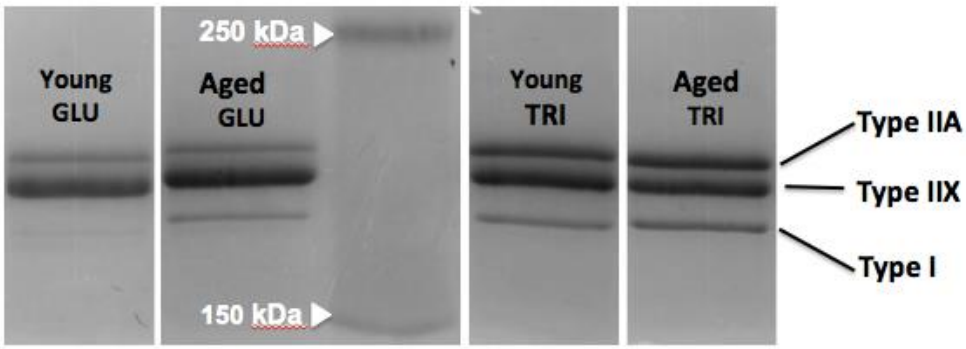

Figure 2-2. Representative SDS polyacrylamide gel stained with Coomassie blue following electrophoretic separation. Bands shown are MyHC isoforms type I, type IIA, and type IIX, in GLU muscle from young (Young-GLU) and aged (Aged-GLU), and TRI muscle from young (Young-TRI) and aged (Aged-TRI) American Quarter Horses. The middle lane shows the molecular mass markers at 250 and 150 kDa.

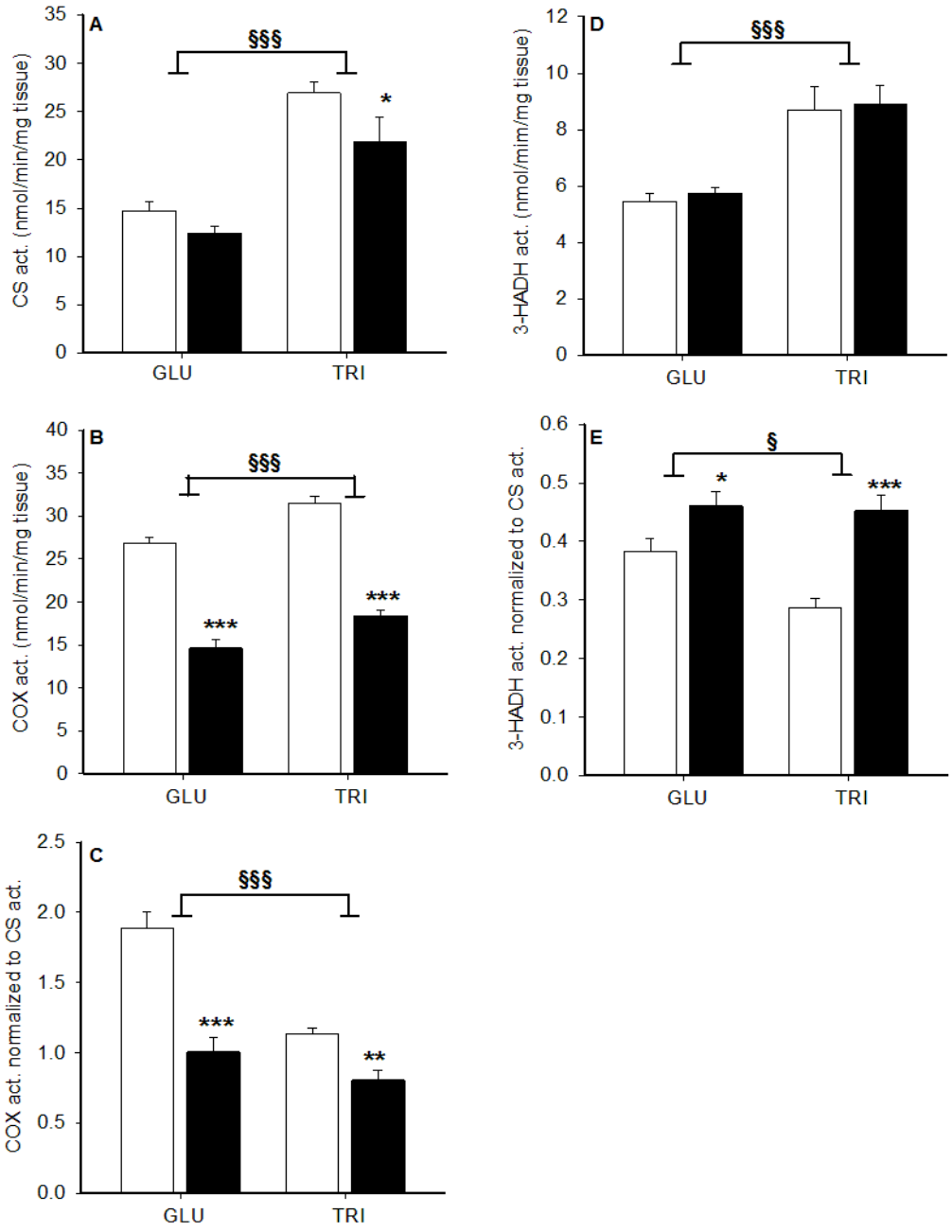

Figure 2-3. Enzyme activities in muscle tissue homogenates from American Quarter Horses. A) activity of CS per milligram tissue of GLU and TRI from young (n = 24 for GLU, n = 11 for TRI) and aged (n = 9 for GLU, n = 10 for TRI) horses. B-E) activity of COX (B and C) and 3-HADH (D and E) normalized to milligram tissue (B and D) and to CS activity (C and E) in GLU and TRI from young (n = 23-24 for GLU, n = 11-12 for TRI) and aged (n = 9-10 for GLU, n= 9-10 for TRI) horses. Values are means ± SE. Open bars represent young horses; solid bars, aged horses. Young vs. aged: *$P < 0.05$, **$P < 0.01$, ***$P < 0.001$. GLU vs. TRI: $^{§}P < 0.05$, $^{§§§}P < 0.001$.

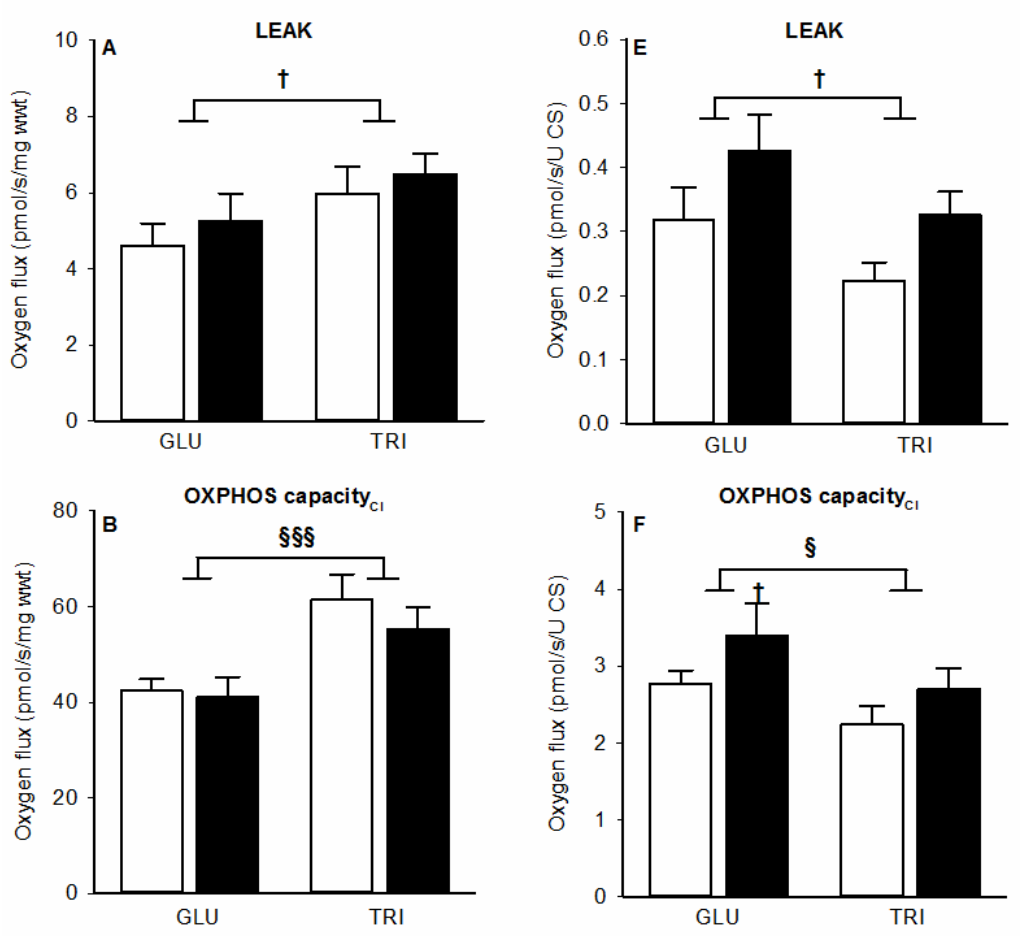

Figure 2-4. Mitochondrial respiration of permeabilized skeletal muscle fibers from American Quarter Horses. Mass-specific O_2 flux (A-D; pmol O_2 s^{-1} mg^{-1} wwt), and O_2 flux normalized to CS activity (E-H; pmol s^{-1} U^{-1} CS), respectively, with LEAK respiration (A and E), OXPHOS capacity$_{CI}$ (B and F), OXPHOS capacity$_{CI+II}$ (C and G), and maximal ETS capacity (D and H) are shown. Values are means ± SE; n =17-18 (Young-GLU), 12(Young-TRI), 9 (Aged-GLU) and 9 (Aged-TRI). Open bars represent young horses; solid bars, aged horses. Young vs. aged: $^{\dagger}P < 0.1$, $^{*}P < 0.05$. GLU vs. TRI: $^{\dagger}P < 0.1$, $^{\S}P < 0.05$, $^{\S\S\S}P < 0.001$.

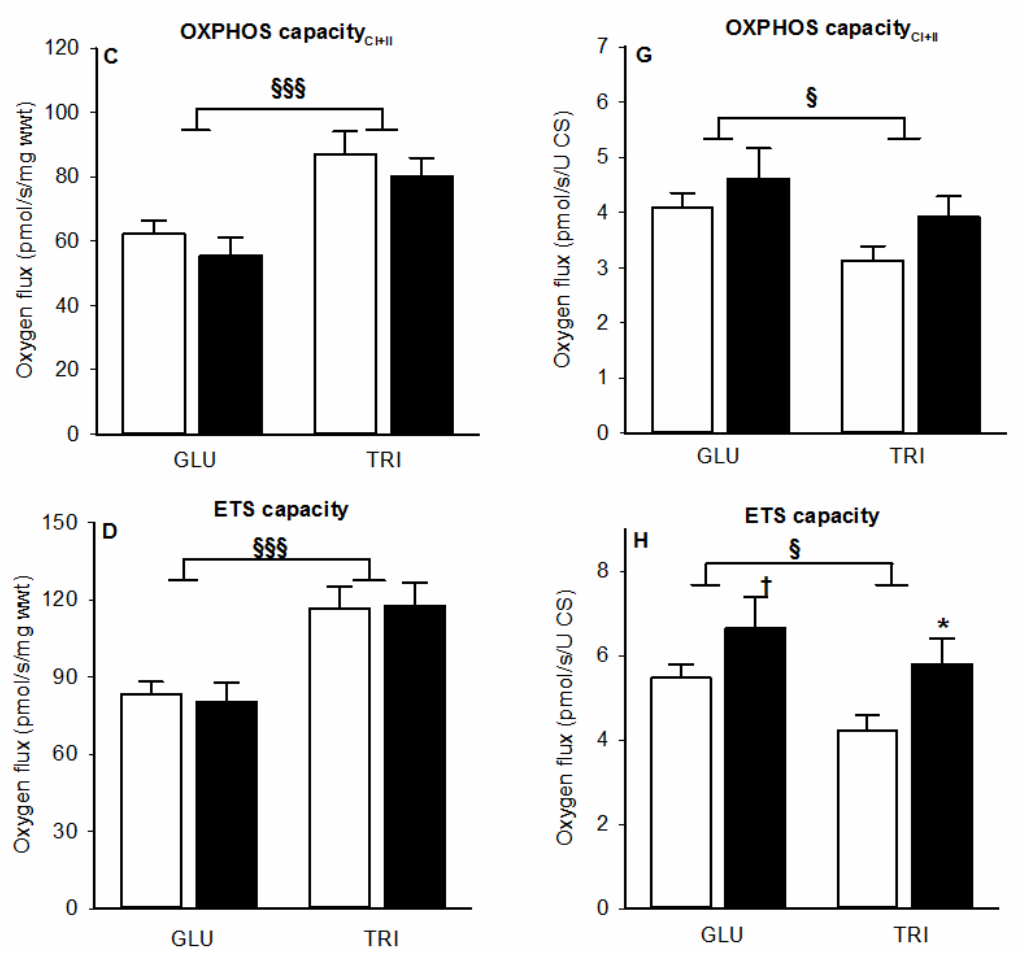

Figure 2-4. Continued

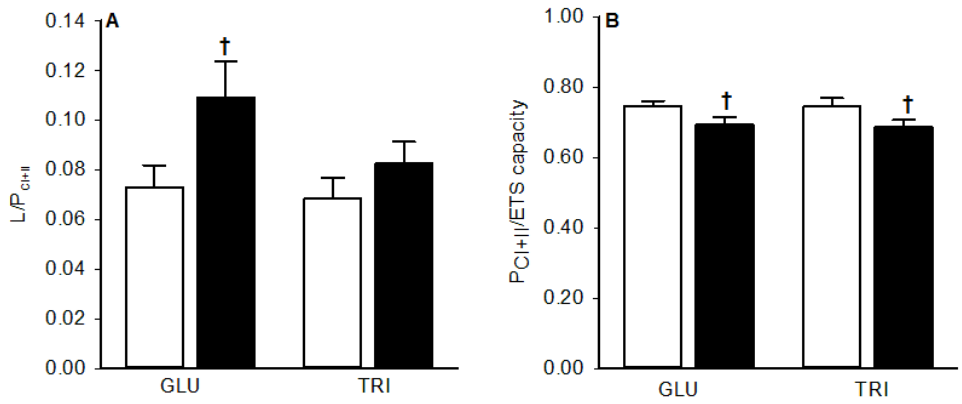

Figure 2-5. Mitochondrial coupling control ratios of permeabilized skeletal muscle fibers from American Quarter Horses. A) L/P coupling control ratio (LEAK/P_{CI+II}) of GLU and TRI from young (n = 18 for GLU, n = 12 for TRI) and aged (n = 8 for GLU, n = 9 for TRI) horses. B) P/E coupling control ratio (P_{CI+II}/ETS capacity) of GLU and TRI from young (n = 18 for GLU, n = 12 for TRI) and aged (n = 9 for GLU, n = 9 for TRI) horses. Values are means ± SE. Open bars represent young horses; solid bars, aged horses. Young vs. aged: $^{\dagger}P < 0.1$.

CHAPTER 3
SKELETAL MUSCLE FROM AGED AMERICAN QUARTER HORSES SHOWS IMPAIRMENTS IN MITOCHONDRIAL BIOGENESIS AND AUTOPHAGY

Background

Mitochondria serve as the combustion engines of life, providing the ATP necessary for skeletal muscle contraction. They do so through OXPHOS, in which ATP and CO_2 are produced at the expense of nutrient substrates and molecular O_2. Given the mitochondria's role in energetic support of locomotion, proper maintenance of a healthy mitochondrial population is critical to ensure efficient energy supply. In human and rodent models, extensive investigation has revealed changes in mitochondrial content and function in a variety of disease models. For example, data collected in old individuals suggest that reduced skeletal muscle mitochondrial content and quality is associated with aging (Short *et al.*, 2005; Picard *et al.*, 2010; Hepple, 2014).

The total mitochondrial content of a cell is tightly regulated by two opposing cellular processes, mitochondrial biogenesis and mitochondria-selective autophagy (mitophagy) (Mishra & Chan, 2016; Wai & Langer, 2016). Mitochondrial biogenesis, the creation of new mitochondria, is responsible for replenishment of new functional mitochondria. On the other hand, mitophagy, one of the key mitochondrial quality control mechanisms, sequesters and degrades dysfunctional or aged mitochondria to maintain a healthy mitochondrial population. Thus, the balance between mitochondrial renewal and elimination of damaged mitochondria is essential for maintaining a certain level of healthy mitochondria to meet energy demands (reviewed by Palikaras *et al.*, 2015). It is not surprising that an impaired balance between these opposing processes can result in numerous pathological conditions, including aging, in diverse organisms ranging from yeast to mammals (Preston *et al.*, 2008; Artal-Sanz & Tavernarakis, 2009;

Kaeherlein, 2010). Mitochondrial biogenesis is a complex process, which requires coordinated synthesis and assembly of thousands of proteins encoded by both the nuclear and mitochondrial genomes (Scarpulla, 2008). In addition, mitochondrial DNA (mtDNA) replication must be coordinated to meet the requirements of the new mitochondrial generation. Growing evidence demonstrates that mitochondrial content in human skeletal muscle declines gradually with advancing age (Crane *et al.*, 2010). Concomitantly, an age-associated impairment of mitochondrial biogenesis capacity has been reported in animal models (Sugiyama *et al.*, 1993; Fannin *et al.*, 1999).

Mitophagy is a specific form of autophagy that selectively degrades dysfunctional mitochondria. The mitochondria are sequestered by a unique double-membrane organelle, called autophagosome, and targeted to be degraded in the lysosomes (Ding & Yin, 2012). Accumulating evidence shows that a decline in autophagy is associated with age, and that increased autophagy delays aging in lab animals (Wu *et al.*, 2013; Schiavi *et al.*, 2015). In humans, an age-related decline in mitophagy was observed (Cavallini *et al.*, 2007) and associated with an accumulation of damaged mitochondria (Masiero & Sandri, 2010). Given that mitochondria are increasingly damaged during the aging process (reviewed by Shigenaga *et al.*, 1994), decreased mitophagic activity might further exacerbate dysfunction of the mitochondrial population as a whole in older individuals. Hence, decreased mitophagy likely contributes to the decline in mitochondrial quality and function that contributes to the aging phenotype.

Previously we have shown that mitochondrial content and function decreased gradually with advanced age in skeletal muscle from American Quarter Horses (Li *et al.*, 2016; Chapter 2 of this dissertation). However, it is not completely understood what

regulates mitochondrial content and function in the equine. One underlying cause for the age-associated decrement of mitochondrial density and function could be an impaired balance between mitochondrial biogenesis and autophagy in muscle from aged horses. Therefore, the purpose of the current study was to explore potential mechanisms that contribute to the age-associated decline in mitochondrial content and quality in equine skeletal muscle by examining the factors involved in mitochondrial biogenesis and autophagy. Because of their distinct locomotor functions and metabolic properties, we compared GLU and TRI muscles from young and aged American Quarter Horses (Li *et al.*, 2016, Chapter 2 of this dissertation). We hypothesized that different muscles respond differently to aging, and that the distinct response is due to differences in the activation of mitochondrial content control mechanisms. A better understanding of the cellular and molecular mechanisms responsible for the maintenance of a healthy mitochondrial population in equine skeletal muscle is a prerequisite to design interventions to prolong health and performance of aging horses.

Materials and Methods

Animals

Healthy young (1.8 ± 0.1 years old, 14 fillies and 10 geldings) and aged (17-25 years old, 11 mares and 1 gelding) American Quarter Horses owned by the University of Florida were enrolled in this study. None of the horses had received forced exercise 6 months prior to the study. The Henneke body condition score (BCS) system (Henneke *et al.*, 2014) with a scale ranging from 1 (emaciated) to 9 (extremely obese) was used to estimate the horse body condition score of the horses enrolled in the study. The BCS was 5.00 for the young group and 5.80 ± 0.25 for the aged group ($P < 0.001$),

respectively. This study was approved by the University of Florida Institute of Food and Agricultural Sciences Animal Research Committee.

Muscle Tissue Sampling

Skeletal muscle microbiopsies were obtained from the GLU (young: n = 24; aged: n = 12) and TRI of a subset of young horses (n = 12) and of all aged horses (n = 12) under local anesthesia following the procedure described previously (Li *et al.*, 2016; Chapter 2 of this dissertation). Muscle samples were collected at a sampling depth of 5 cm, using a 14-gauge SuperCore ™ Biopsy needle (Angiotech, Gainesville, FL, USA), immediately snap-frozen in liquid nitrogen and transported to the laboratory in a dry shipper (MVE SC4/2V, CHART, Inc., Ball Ground, GA, USA), where samples were transferred to a -80 °C freezer.

Analysis of MtDNA Copy Number

To evaluate mitochondrial content in horse skeletal muscle, the relative amount of mtDNA to nuclear DNA (nDNA) was determined using a CFX Connect real-time PCR detection system (Bio-Rad, Laboratories, Inc., Hercules, CA). Total DNA was extracted from muscle samples using Wizard® Genomic DNA purification kit (Promega Corporation, Madison, WI), according to the manufacturer's instructions. One primer pair specific for the mtDNA (NADH dehydrogenase 1, *ND1*) and another specific for the nuclear DNA (β-actin, *ACTB*), were designed using PrimerQuest (Integrated DNA Technologies, Coralville, IA). The primer sequences for the *ND1* gene were: 5'-GGA TGG GCC TCA AAC TCA A-3' (forward) and 5'-GGA GGA CTG AGA GTA GGA TGA T-3' (reverse). The primer sequences used to amplify *ACTB* gene were: 5'-CTC CAT TCT GGC CTC ATT GT-3' (forward) and 5'-AGA AGC ATT TGC GGT GGA-3' (reverse). Another primer pair designed within the *COX1* (*cytochrome c oxidase subunit 1*) region

of the mitochondrial genome was also tested to confirm the result assessed with *ND1*.The primer sequences used for *COX1* gene were: 5'-CAG ACC GTA ACC TGA ACA CTA C-3' (forward) and 5'-GGG TGT CCG AAG AAT CAG AAT AG-3' (reverse). The relative amount of *ND1*, *COX1* and *ACTB* was determined for each sample from a standard curve prepared from a serial dilution of a pool of all the samples. Relative mtDNA copy number was calculated from the ratio *ND1*/*ACTB* and *COX1*/*ACTB*.

RNA Isolation

Total RNA was isolated from ~30 mg of snap-frozen muscle using RNeasy® Plus Universal Mini kit (Qiagen, Valencia, CA) according to the manufacturer's instructions. With the DNA elimination solution included in the kit, genomic DNA was removed from the samples. Immediately following extraction, the RNA concentration and purity were determined using a UV spectrophotometer (Synergy HT, Bio-Tech Instruments, Winooski, VT) by measuring the absorbance at 260 (OD260) and 280 (OD280) nm. All measurements were performed in duplicate.

Analysis of mRNA Expression

First-strand cDNA was synthesized with random primers using the High-Capacity cDNA Reverse Transcription Kit (Applied Biosystems Inc., Foster City, CA) according to the manufacturer's directions. Quantitative real-time PCR (qRT-PCR) analysis was performed using the CFX Connect real-time PCR detection system with a 20 µL reaction volume containing cDNA, primers, and iTaq™ Universal SYBR® Green Supermix (Bio-Rad). All samples were analyzed in duplicate simultaneously with a negative control that contained no cDNA. The data were normalized to GAPDH mRNA in each reaction, and results were expressed as a fold change in mRNA compared with expression in GLU muscle from the young horse group. Forward and reverse primer

sequences are listed in Table 3-1. Melting point dissociation curves generated by the instrument were used to confirm the specificity of the amplified product. The relative quantification was done using the relative standard curve method.

Analysis of Protein Expression by Western Blot

Frozen muscle samples were cryopulverized using a BioPulverizer (BioSpec Products, Inc., Bartlesville, OK, USA) prior to protein extraction. The cryopulverized tissues were immersed 1:50 (w/v) in lysis buffer (25 mM Tris-HCl, pH 7.4, 150 mM NaCl, 5 mM EDTA, 1% Triton X-100, 0.1% SDS, 10% glycerol, 1 mM DTT, 0.5% sodium deoxycholic acid (Wu *et al.*, 2009)) supplemented with 1% Halt™ protease-phosphatase inhibitor cocktail (Fisher Scientific, Pittsburgh, PA). After 10 bouts of 1s-long sonications (Sonic Dismembrator, model F60; Fisher Scientific), the tissue lysate was incubated for 2 h on a rotator at 4 °C, followed by centrifugation at 12,000 x *g* for 20 min at 4 °C. The supernatant was collected and stored at -80°C until further analysis. Protein concentration was determined with the Thermo Scientific™ Pierce™ BCA protein assay kit (Fisher Scientific). Samples were diluted with equal volume of Laemmli buffer (Biorad) and heated for 10 min at 95 °C. Thirty micrograms protein was loaded and resolved by Sodium dodecyl sulfate polyacrylamide gel electrophoresis using precast gels (BioRad), transferred onto a Polyvinylidene fluoride membrane (PVDF; EMD Millipore, Fisher Scientific), and immunoblotted as previously described (Wohlgemuth *et al.*, 2010). Primary antibodies used for immunoblotting recognized p62/SQSTM1 (1:300, Sigma-Aldrich, St. Louis, MO), Atg5 (1:500, Cell Signaling Technology, Danvers, MA), CS (1:100, Santa Cruz, Dallas, TX), LC3 (1:500, Fisher Scientific), and Atg7 (1:1000, Cell Signaling), and secondary antibodies were either horseradish peroxidase- or alkaline phosphatase-conjugated (Sigma-Aldrich). Finally,

DuoLux chemiluminescent/fluorescent substrate for horseradish peroxidase or alkaline phosphatase (Vector Laboratories, Burlingame, CA) was applied, and the chemiluminescent signal captured with the digital imager G:Box Chemi XR5 (Syngene, Frederick, MD), and the intensity was analyzed and quantified using the manufacturer's analysis software (Gene Tools, Syngene). Protein level was expressed relative to total protein loaded, as determined by Ponceau staining.

Statistical Analysis

Statistical analysis was performed using SigmaPlot 13.0 software (Systat Software, Inc, San Jose, CA). The normal distribution of the data was examined using the Shapiro-Wilk test. For data that did not express normal distribution, the $\log_{10}$ transformation was successfully used to normalize the data. Data were analyzed using two-way analysis of variance, with factors of age (Young, Aged) and muscle type (GLU, TRI). Significant main effects and interactions were further tested using Holm-Sidak multiple comparison tests. Data are presented as the means ± SE, with the number of samples per group noted in the figure legends. A P-value ≤ 0.05 was considered statistically significant.

Results

Mitochondrial Content Was Decreased in Aged Skeletal Muscle

We have previously reported that activity of CS, an enzyme of the TCA cycle located in the mitochondria, declined with age in TRI but not GLU muscle from American Quarter Horses (Li *et al.*, 2016; Chapter 2 of this dissertation). We show here that, consistent with enzyme activity, the TRI muscle exhibited higher CS protein content than the GLU muscle (main effect of age: $P = 0.007$). Furthermore, compared to

young muscle relative CS protein content was lower in aged TRI-muscle (P = 0.048), but not in aged-GLU muscle (P = 0.469; Figure 3-1).

Mitochondrial Biogenesis Was Impaired with Age

To elucidate possible mechanisms underlying the age-related decline in TRI mitochondrial content suggested by both CS activity and content, we examined mtDNA copy number, which has been associated with mitochondrial content (Larsen *et al.*, 2012) and biogenesis (Clay *et al.*, 2009). We determined the content of the mitochondrial DNA-encoded gene *ND1*, coding for NADH: ubiquinone oxidoreductase core subunit 1, as a surrogate for mtDNA copy number, and found that, consistent with CS activity and protein expression, mitochondrial DNA content, as indicated by *ND1* gene expression (Figure 3-2A), was ~25% lower in aged-TRI muscle (P = 0.040) but not in aged-GLU muscle (P = 0.395) when compared to the respective muscles in young horses, suggesting an age-related impairment of mitochondrial biogenesis in the TRI muscle. In addition, mitochondrial DNA content in TRI muscle was higher than that of GLU muscle independent of age (main effect of muscle: P = 0.011). We confirmed these results by quantifying content of another mitochondrial DNA-encoded gene, *COX1* (Figure 3-2B), coding for cytochrome *c* oxidase subunit 1 (young-TRI vs. aged-TRI: P = 0.017; young-GLU vs. aged-GLU: P = 0.305; main effect of muscle: P = 0.020). In addition, CS protein content and mtDNA (*COX1*/*ACTB*) correlated significantly (R^2 = 0.3632; P = 0.020; Figure 3-2C) in TRI muscle, with low citrate synthase concurring with low mtDNA copy number.

To further test if any key factors that regulate mitochondrial biogenesis might be altered in aged skeletal muscle, mRNA expression of *Peroxisome proliferator-activated*

receptor gamma coactivator 1-α (*PGC-1α;* Figure 3-2D), *Nuclear Respiratory Factor 1* (*NRF1*; Figure 3-2E) and *mitochondrial Transcription Factor A* (*TFAM*; Figure 3-2F) was measured. Gene expression of a *PGC-1α,* a master regulator of mitochondrial biogenesis in mammals (Ruas *et al.*, 2012), was down-regulated in aged-TRI muscle (~-60%, $P = 0.022$), but unchanged in the GLU ($P = 0.407$). Concordantly, the transcript level of *TFAM*, acting downstream of PGC-1α (Wu *et al.*, 1999) was decreased in aged-TRI muscle ($P = 0.037$), but unchanged in aged-GLU muscle ($P = 0.534$). *Nuclear Respiratory Factor 1* (also acting downstream of PGC-1α (Wu *et al.*, 1999)) mRNA was not altered by age in either muscle (TRI: $P = 0.376$; GLU: $P = 0.513$). When GLU and TRI muscles were compared, the mRNA expression of *PGC-1α*, *NRF1* and *TFAM* was consistently higher in TRI compared to GLU muscle (main effect of muscle: $P < 0.05$ for all).

Transcript Level of MtDNA-Encoded Genes Was Not Affected by Age

As mtDNA content and the expression of mitochondrial biogenesis regulators *PGC-1α* and *TFAM* were decreased with age in TRI muscle, we next sought to measure the expression of mtDNA-encoded genes *ND1*, *COX1* and *COX2*. Surprisingly, no age-associated changes in any of these mtDNA-encoded genes were observed in this study ($P > 0.05$ for all; Fig 3A-C). When muscles were compared, significant differences were detected between GLU and TRI muscle. Specially, the mRNA expression of *ND1*, *COX1* and *COX2* was higher in TRI muscle than that of GLU muscle (main muscle effect: $P < 0.01$ for all), which is consistent with activity and content of CS.

Autophagic Capacity Was Impaired with Age

Along with mitochondrial biogenesis pathways, selective degradation of damaged, dysfunctional mitochondria by (macro)autophagy is considered another

important mechanism to regulate mitochondrial content and homeostasis. To determine whether autophagic flux was impaired with age, we examined the protein expression of nucleoporin 62 (p62, also known as sequestosome 1, SQSTM1; Figure 3-4) in muscle samples. The autophagosome cargo protein p62 binds other proteins and “docks” them to the autophagosome membrane for subsequent engulfment by the organelle (Koltai *et al.*, 2012), and is finally degraded in the autophagolysosome (Pankiv *et al.*, 2007). We found that protein expression of p62 was increased in both aged GLU ($P = 0.012$) and aged TRI ($P = 0.026$) muscle, suggesting an impairment of autophagic clearance in the aged muscles. No difference was observed between muscles within either young or old horses (main effect of muscle: $P = 0.869$).

Autophagosome Formation Was Impacted by Age

Next, we investigated the possible causes of the impaired autophagic clearance by analyzing the expression of autophagy-related proteins 5 (Atg5) and 7 (Atg7), both essential for autophagosome formation (Jin & Van Remmen, 2009). Protein expression of Atg5 was reduced in aged TRI ($P = 0.036$), and unchanged in aged GLU muscle ($P = 0.266$; Figure 3-5D) compared to the respective young counterparts. No age-related changes were observed for Atg7 in either muscle (main age effect: $P = 0.734$; Figure 3-5E). When muscles were compared, TRI exhibited the same protein expression of Atg5, and higher Atg7 protein expression compared to GLU muscle (main muscle effect: $P = 0.383$ for Atg5, and $P < 0.001$ for Atg7). LC3 is a well characterized and commonly used autophagosome marker in mammalian cells (Jin & Klionsky, 2013). Expression of LC3 mRNA (Figure 3-5C) and protein level of the cytosolic form of LC3 (LC3-I, Figure 3-5A) were unchanged in aged compared to young-TRI muscle ($P > 0.05$ for both), while the lipidated form of LC3 (LC3-II, Figure 3-5B), which is integrated in the autophagosomal

membrane and essential for autophagosome formation, was lower ($P = 0.047$), further supporting the notion of impaired autophagosome formation in aged TRI muscle. In the GLU muscle, on the other hand, no aging effects on protein levels of LC3-I or LC3-II were observed despite an age-associated increase in the LC3 transcript level. When GLU and TRI muscles were compared, TRI muscle expressed higher level of LC3 mRNA (main muscle effect: $P < 0.001$) and LC3-I (main muscle effect: $P < 0.05$) compared to GLU muscle. Taken together, these findings suggest that the decreased autophagic clearance indicated by elevated p62 levels was at least partially due to impaired autophagosome formation.

Transcript Level of Lysosomal Degradation Marker LAMP2 Was Not Impacted by Age

To further examine whether impaired autophagic clearance could have been caused by defective lysosomal degradation, we determined the mRNA expression level of lysosomal associated membrane protein 2 (*LAMP2*) using real-time qPCR. The protein LAMP2 is needed for efficient fusion of autophagosome and lysosome (González-Polo *et al.*, 2005), and thereby crucial for completion of the lysosomal–autophagic degradation process. Transcript levels of *LAMP2* (Figure 3-6) did not differ between age groups in either GLU ($P = 0.277$) or TRI ($P = 0.592$) muscle, implying that decreased autophagic clearance was not due to decreased lysosomal degradation. When muscles were compared, *LAMP2* transcript level in TRI muscle was higher compared to GLU muscle (main muscle effect: $P = 0.002$).

Discussion

Mitochondrial damage has been widely discussed for decades as a major contributor to the aging process (reviewed by Sun *et al.*, 2016). The mitochondrial

theory of aging proposes that accumulation of damage to mitochondria and mitochondrial DNA leads to progressive aging in humans and animals (Jang & Van Remmen, 2009). Mitochondrial biogenesis and autophagic removal of damaged mitochondria are two predominate cellular processes whose interplay preserves mitochondrial homeostasis by maintaining mitochondrial quality and content (Mishra & Chan, 2016). Their functional decline and imbalance could be an underlying cause for cellular aging. Here, we investigated how aging affects these two opposing processes, and in conjunction regulate the mitochondrial content in two types of equine skeletal muscle. We have previously described the TRI muscle and the GLU muscle in American Quarter Horses as more oxidative and more glycolytic, respectively, based on fiber type distribution, citrate synthase activity, and capacity for mitochondrial oxidative phosphorylation. We report here that these muscles with different metabolic properties differed in their response to aging with regard to mitochondrial content. More specifically, a decline in mitochondrial content was only observed in the presumably more oxidative TRI muscle, but not in the more glycolytic GLU muscle. In line with decreased mitochondrial content, the decreased gene expression of transcription factors regulating the expression of mitochondrial electron transport system proteins suggests impaired mitochondrial biogenesis in aged-TRI muscle. The combination of age-related accumulation of the autophagy cargo protein p62 in both muscles and decrease of autophagosome-bound LC3 in the TRI muscle suggest compromised autophagy with age that was more pronounced in the TRI muscle. That this decline in autophagic function was more pronounced is supported by a concomitant decrease in abundance of the essential autophagy-related protein Atg5 in the TRI muscle.

Collectively, our results provide the first line of evidence that aging affects mitochondrial biogenesis and autophagy pathways in equine skeletal muscle aging, and that this is likely one of the underlying mechanisms contributing to the observed decrease in mitochondrial content.

The decline in mitochondrial content with age has been reported in both humans and animal models (Barazzoni *et al.*, 2000; Short *et al.*, 2005). We (Li *et al.*, 2016; Chapter 2 of this dissertation) and others (Kim *et al.*, 2005) have previously shown an age-associated decline in mitochondrial content in horse skeletal muscle, indicated by CS activity. In the present study, CS protein content and mtDNA copy number confirmed the changes in mitochondrial content in the TRI muscle we described earlier. Our finding is in agreement with the data reported by others, who showed an age-related decline in mtDNA copy number in skeletal muscle (Welle *et al.*, 2003a; Short *et al.*, 2005) from humans, as well as lab animals (Hartmann *et al.*, 2011; Sczelecki *et al.*, 2014). However, other work reported an increased amount of mtDNA in aged skeletal muscle of human (Pesce *et al.*, 2001) and mice (Masuyama *et al.*, 2005). Larsen *et al.* (Larsen *et al.*, 2012) proposed that in contrast to enzyme activity of CS and Complex I of the mitochondrial electron transport chain, mtDNA copy number is a less reliable determinant of mitochondrial content. These authors based their conclusion on measurements in skeletal muscle samples from young, healthy humans, but it is conceivable that this poor association of mtDNA copy number with mitochondrial content holds true for aged muscle as well. Furthermore, the strength of this association might depend on the muscle type investigated, but comparative data are not available.

Mitochondrial DNA copy number can be indicative of mitochondrial biogenesis (Clay *et al*., 2009). Mitochondrial biogenesis is a complex process which involves replication of the mitochondria's own, circular DNA, transcription and translation of both mitochondrial and nuclear DNA encoded genes, recruitment of newly synthesized proteins and lipids, and import and assembly of mitochondrial and nuclear products (Zhu *et al.*, 2013). We measured mtDNA copy number as surrogate for mtDNA replication in order to evaluate mitochondrial biogenesis in skeletal muscle from aged compared to young horses. Reduced mtDNA copy number observed in TRI muscle from aged horses suggested an impairment of mitochondrial biogenesis. The transcription factor PGC-1α has been suggested as a master regulator of mitochondrial biogenesis. It associates with the transcription factor NRF-1 to subsequently induce expression of a number of metabolic proteins, including TFAM (Austin & St-Pierre, 2012). TFAM translocates to the mitochondria and binds to mtDNA at both the heavy- and light-strand promoters to not only initiate the transcription of mtDNA encoded genes (Fisher *et al.*, 1987), but to induce mtDNA replication (Bonawitz *et al.*, 2006). In accordance with our findings in the TRI muscle from aged horses, recent studies have reported that protein or gene expression of *PGC-1α* expression was decreased in aged murine (Koltai *et al.*, 2012; Sczelecki *et al.*, 2014) and human skeletal muscle (Safdar *et al.*, 2010; Ringholm *et al.*, 2013). The age-related decrease in *PGC-1α* transcript level in the TRI muscle from aged horses was not concurrent with a lower *NRF1* level. However, the mRNA level of *TFAM*, the downstream target of the PGC-1α-NRF1 complex, was lower in aged-TRI muscle compared to young horses, which is consistent with the decline in mitochondrial content in this muscle. In contrast to the TRI muscle,

and consistent with mitochondrial content, the more glycolytic GLU muscle displayed no age-related alterations of any of the markers of mitochondrial biogenesis assessed in this study.

The transcriptional targets of TFAM assessed in this study, which are part of the mitochondrial electron transport system, did not seem to be affected by the apparent age-associated dysregulation of the *PGC-1α-TFAM* axis of mitochondrial biogenesis in the more oxidative TRI muscle. The three mitochondrial genes, *ND1*, *COXI*, and *COXII,* encode subunits of the mitochondrial electron transport chain: NADH dehydrogenase 1, cytochrome *c* oxidase subunit 1, and cytochrome *c* oxidase subunit 2, respectively. The observation that transcription of those genes was not affected by age in either muscle is consistent with findings in aged rat skeletal muscle (Barazzoni *et al.*, 2000), and suggests that there is a compensatory response for decreased template availability. An increased transcription efficiency to maintain transcript level would help to explain the unaltered mitochondrial respiratory capacity observed in a previous study (Li *et al.*, 2016; Chapter 2 of this dissertation). Moreover, we propose that overall ETS activity is more likely to be impaired in individuals older than 80 years (Lezza *et al.*, 1994; Chabi *et al.*, 2005) suffering from severe muscle loss and diseases.

Autophagy, also known as cellular self-digestion, is a crucial quality control process by which cells sequester and degrade dysfunctional, damaged or aged constituents in order to maintain cellular homeostasis. Mitochondrial autophagy, known as mitophagy, is a selective type of autophagy that specifically eliminates damaged or aged mitochondria (Ding & Yin, 2012). During mitophagy, entire mitochondria are sequestered by an expanding cup-shaped double-membrane structure, known as

phagophore (Xie & Klionsky, 2007). The expansion of the phagophore is regulated by autophagy-related, or ATG, proteins, and the phagophore closes and forms a double-membrane limited vesicle, the autophagosome. Furthermore, the regulation of autophagosome size by LC3 is critical to allow sequestration of large mitochondria and protein aggregates. Upon completion, the autophagosome fuses with a lysosome, forming the auto(phago)lysosome in which the sequestered components are ultimately degraded. The impairment of mitophagy was reported to occur in a variety of tissues during normal aging (Cuervo & Dice, 1998; Donati *et al.*, 2001; Cuervo *et al.*, 2005; Joseph *et al.*, 2013). Consequently, an age-related accumulation of damaged mitochondria has been proposed (Terman, 1995) and in fact been observed in various cell types of diverse organisms (Preston *et al.*, 2008; Artal-Sanz & Tavernarakis, 2009; Kaeherlein, 2010). Consistent with these previous reports, we found that aging was associated with a decreased level of autophagy in both GLU and TRI muscles, suggested by p62 protein accumulation. The cargo protein p62 is widely used as a maker of autophagy and involved in mitochondrial aggregation and clearance (Narendra *et al.*, 2010), as it is recruited to mitochondria and targeted for autophagy-mediated degradation (Pankiv *et al.*, 2007). Under normal conditions, p62 is rapidly degraded during autophagy, and an impairment of autophagic degradation leads to accumulation of p62 (Pankiv *et al.*, 2007). Therefore, we propose that the accumulation of p62 in skeletal muscle observed by our group and others (Joseph *et al.*, 2013) indicates a lower autophagic activity in aged muscle cells. Given the aberrant accumulation of p62 protein in aged skeletal muscles, we further confirmed defects in the autophagic process by analyzing the expression of autophagy-related proteins (Atg5, Atg7, LC3

and LAMP2). The protein expression of Atg5, involved in autophagosome formation, significantly declined with age in TRI muscle, but was not significantly affected in GLU muscle. The expression of Atg7, the E1-like enzyme required for autophagosome formation, did not change with age in either muscle, which is in agreement with a previous study in skeletal muscle from old rats (Wohlgemuth *et al.*, 2010). Both, Atg5 and Atg7 are essential in the processing of LC3, a homologue of the yeast autophagy protein Atg8. Upon induction of autophagy, LC3-I, the protein's cytosolic form, is lipidated generating a membrane-bound form, known as LC3-II. This lipidation process depends on an ubiquitin-like conjugation process that involves an Atg12-Atg5 complex, Atg3 and Atg7, which function in concert to facilitate the covalent link of LC3 to autophagosomal precursor membranes. Immunoblot analysis showed an age-associated decrease in LC3-II level in equine TRI muscle, which is consistent with some (McMullen *et al.*, 2009; Carnio *et al.*, 2014; Zhou *et al.*, 2017), but not other (Wohlgemuth *et al.*, 2010; Sebastián *et al.*, 2016) studies conducted in other species. It is noteworthy to mention that the lower level of LC3-II in the aged TRI muscle measured in our study has likely not resulted from reduced content of LC3 precursor, since neither the level of LC3 mRNA nor LC3-I protein were affected by age. Like LC3-II, expression of Atg5 was also reduced in aged TRI muscle, implying impaired regulation of LC3 lipidation and conjugation to the autophagosomal membrane. No age-induced effects were observed in any autophagic markers measured in GLU muscle, suggesting that the formation of autophagosomes, including LC3 lipidation, was not impacted. Overall, these data indicate that upstream autophagy regulators were downregulated in aging equine muscle, and that autophagosome formation was impaired in aged TRI muscle,

while autophagy in the GLU muscle appears to be less affected by age. To investigate whether defects of autophagy in equine skeletal muscle extends to processes downstream of autophagosome formation, we assessed expression of LAMP2. Lysosomes are the terminal compartment for autophagic degradation, and LAMP2 plays a critical role in the fusion of autophagosomes with lysosomes to form the hybrid structure called autophagolysosome. Reduced fusion has been shown in cells depleted of LAMP2, in which autophagic vacuoles accumulated in several tissues (Tanaka *et al.*, 2000). We found that gene expression of *LAMP2* was not altered with aging in either muscle types, implying that the fusion of autophagosomes with lysosomes may not have been impaired at that age. Our findings differ from a previous report in rat skeletal muscle where aging was associated with lower levels of *LAMP2* mRNA (Wohlgemuth *et al.*, 2010). The divergent response in our study could be attributed to factors including the age of animals, as well as different muscle types being studied. We conclude from our data that the compromised autophagic activity did not appear to be a result of defects in lysosomal involvement.

Another noteworthy observation made in our study is the muscle-specific response to aging. More specifically, TRI muscle appears more susceptible to the age-related impact than the GLU muscle, indicated by the decrease in mitochondrial content and the more pronounced effect on autophagy-related markers. We observed here and previously (Li *et al.*, 2016; Chapter 2 of this dissertation) that the more oxidative TRI muscle contains significantly more mitochondria than that of the more glycolytic GLU muscle, independent of age, indicated by CS activity, CS protein content and mtDNA copy number. Similarly, He and coworkers (He *et al.*, 2002) reported that the absolute

mtDNA content in single type I oxidative fibers is double that in single type II glycolytic fibers from human skeletal muscle. In line with the higher mitochondrial content we observed, TRI muscle also displayed a higher expression level of mitochondrial genes (*ND1*, *COXI* and *COX II*), mitochondrial biogenesis markers (*PGC-1α*, *NRF1*, and *TFAM*) and higher proteins levels of autophagy regulators (Atg7, LC3, LC3-I, and LC3-II) when compared to GLU muscle. Interestingly, the more oxidative TRI is also more likely to suffer an age-related decline in mitochondrial content compared to the more glycolytic GLU. Similarly, in rodents CS activity declined with age in the oxidative *soleus* but not in the more glycolytic *extensor digitorum longus* (Picard *et al.*, 2011a), and mtDNA content decreased with age only in *soleus* and *tibialis anterior*, but not in *gastrocnemius* or *extensor digitorum longus* muscles (Pesce *et al.*, 2005). In addition, differential effects of aging on CS activity were observed in human skeletal muscle, with CS activity declining in the *gastrocnemius* but not in the *vastus lateralis*. These results suggest that the age-associated decline in mitochondrial content in skeletal muscle is not uniform. However, it appears to follow a common pattern. The decline in mitochondrial content is larger and begins at an earlier age in muscles with high oxidative capacity (*soleus*, TRI) compared to less oxidative mixed muscles (*gastrocnemius;* GLU); and muscles with high glycolytic capacity (*extensor digitorum longus* and *vastus lateralis*) appear to be less impacted than these other muscle types. The response of the *tibialis anterior* described by Pesce *et al.* (Pesce *et al.*, 2005) seems to represent an exception to this trend, highlighting the lack of uniformity of the age effects in skeletal muscle. It might reflect a differential use of these muscles with aging, affecting the intracellular response, but this context has not yet been illuminated.

The differences in susceptibility to aging between the two muscles observed in our study could be attributed to the differential regulation of mitochondrial biogenesis and autophagy. The imbalance between mitochondrial degradation and biogenesis may underlie the age-associated decline in mitochondrial content. Maintenance of a stable pool of healthy mitochondria requires both autophagy and mitochondrial biogenesis. However, impairment in both biogenesis and autophagy was observed with age in TRI muscle, and decreased mitochondrial content suggests that the effects of declined mitochondrial biogenesis exceeded that of declined autophagy. While we also observed an impairment of autophagic activity in the GLU muscle from aged horses, neither mitochondrial content nor biogenesis were affected in this muscle. It is possible that a more severe imbalance of mitochondrial biogenesis and degradation commences at a later age compared to the TRI muscle.

In summary, we report here, for the first time, the age-associated alterations in mitochondrial biogenesis and autophagy in equine skeletal muscle. We observed a decreased mitochondrial content with age in TRI muscle but not in GLU muscle, implying that the age-related decrease in mitochondrial content is muscle type specific. With age, mitochondrial biogenesis and autophagy were impaired, which might be one underlying cause of the age-associated decline in mitochondrial content. These findings suggest that a targeted approach to balance mitochondrial biogenesis and degradation may prolong health and performance of aged American Quarter Horses.

Table 3-1. Primers used for gene amplification in quantitative reverse transcription-polymerase chain reaction

Gene	GenBank Accession no.	Forward primer sequence (5'-3')	Reverse primer sequence (5'-3')	Product size (bp)
PGC-1α	XM_014738763.1	GAACAGCAGCAGAGACAAATG	GGGTCAGAGGAAGAGACAAAG	104
NRF1	XM_014739148.1	GTGGTCCAGACCTTTAGTAACC	CCATCAGCCACAGCAGAATA	146
TFAM	XM_001503382.3	CTCAGAACCCAGATGCGAAA	CTGCCCTGTAAGCATCTTCATA	108
LC3	XM_005608485.2	CTCAGGAGACATTTGGGATGAA	CGGATCGATCTCAGTTGGTAAC	119
LAMP2	XM_014729146.1	TGAACGTCACTCACGATAAGG	AGCCTAAGTAGAGCAGTTTGAG	100
COX2	NC_001640.1	TCATCCGAAGACGTCCTACA	GCCACGAGAGTTGTCTGATTTA	95
COX1	NC_001640.1	CAGACCGTAACCTGAACACTAC	GGGTGTCCGAAGAATCAGAATAG	91
ND1	NC_001640.1	GGATGGGCCTCAAACTCAA	GGAGGACTGAGAGTAGGATGAT	106
ACTB	NM_001081838.1	CTCCATTCTGGCCTCATTGT	AGAAGCATTTGCGGTGGA	98
GAPDH	NM_001163856.1	GTCATCATCTCTGCTCCTTCTG	GGAGGCATTGCTGACAATCT	99

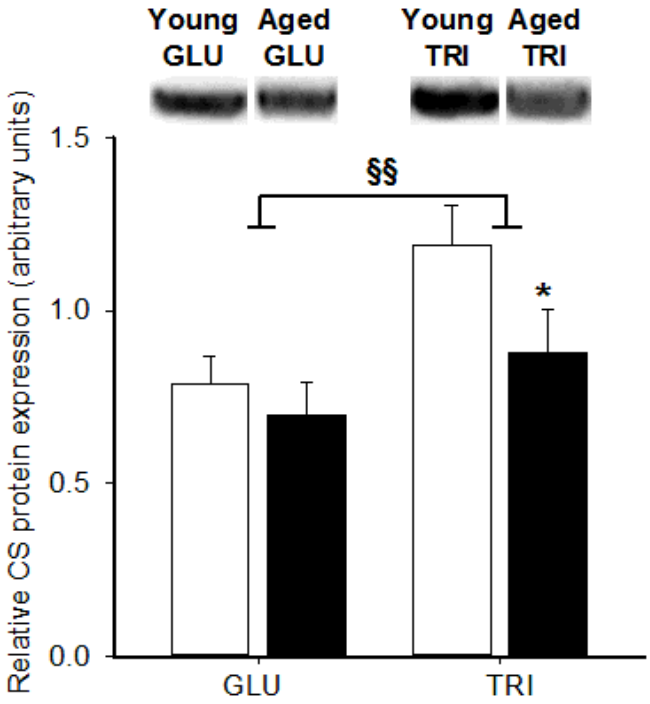

Figure 3-1. Protein expression of citrate synthase in skeletal muscle from American Quarter Horses. Densitometric quantification of citrate synthase (CS) protein expression in GLU and TRI muscle from young (n = 24 for GLU, n = 12 for TRI) and aged (n = 12 for GLU, n = 12 for TRI) horses. Values are means ± SE. Open bars represent young horses; solid bars, aged horses. Young vs. aged: $^{*}P < 0.05$. GLU vs. TRI: $^{\S\S}P < 0.01$. Representative Western blot images are shown above the graph.

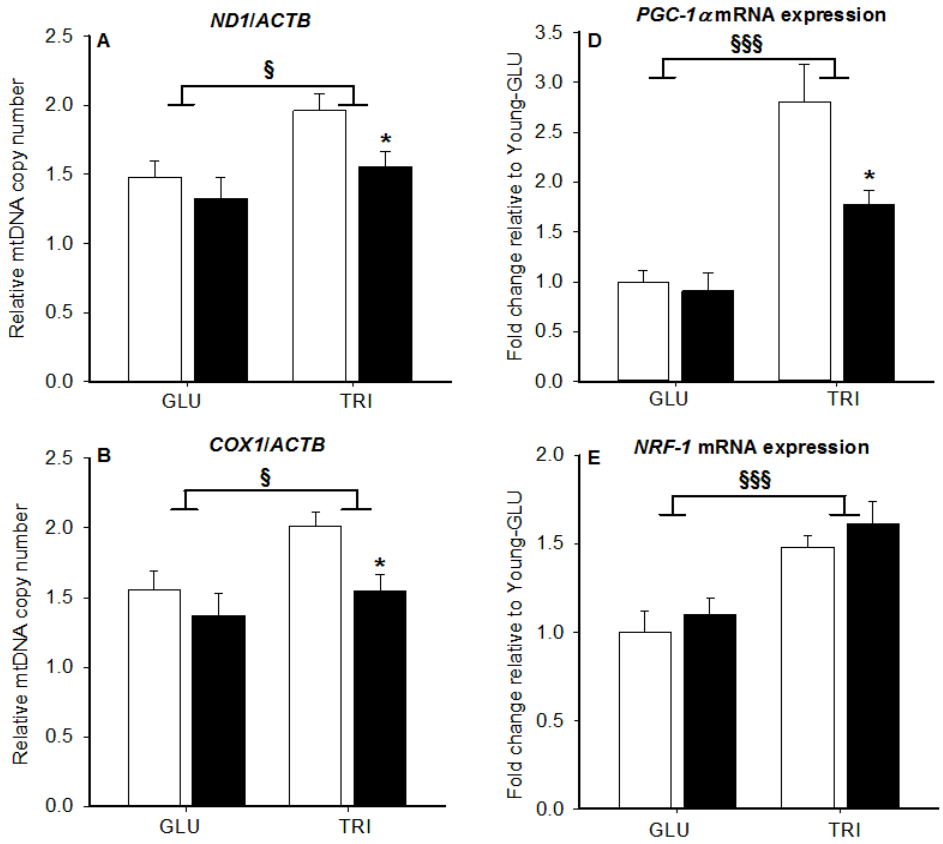

Figure 3-2. Mitochondrial DNA copy number and transcript levels of factors associated with mitochondrial biogenesis in skeletal muscle from American Quarter Horses. Mitochondrial DNA copy number from GLU and TRI muscle of young (n = 7 for GLU, n = 8 for TRI) and aged (n = 6 for GLU, n = 6 for TRI) horses was determined using quantitative real-time PCR of *ND1* (A) and *COX1* (B), normalized to nuclear DNA copy number using the β-actin gene (*ACTB*). C) Correlation between mtDNA copy number (*COX1*/*ACTB*) and citrate synthase protein expression in TRI and GLU muscle (insert: GLU). Each point represents an individual muscle sample from young (open symbols) and aged (closed symbols) subjects. D-F) Real-time PCR analysis of *PGC-1α*, *NRF1* and *TFAM* mRNA levels in GLU and TRI muscle from young (n = 7-8 for GLU, n = 8 for TRI) and aged (n = 7-8 for GLU, n = 8 for TRI) horses. Results are represented as the fold change compared to young-GLU muscle. Values are means ± SE. Open bars represent young horses; solid bars, aged horses. Young vs. aged: **P* < 0.05. GLU vs. TRI: $^{\S}P < 0.05$, $^{\S\S\S}P < 0.001$.

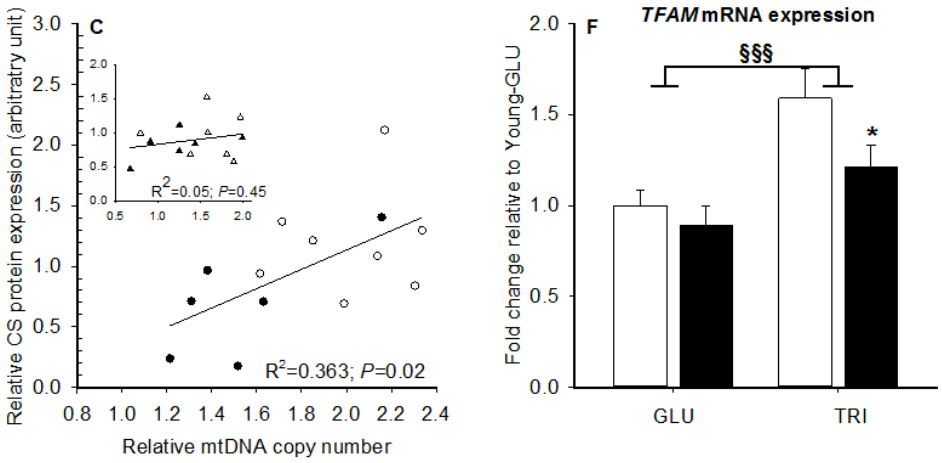

Figure 3-2. Continued

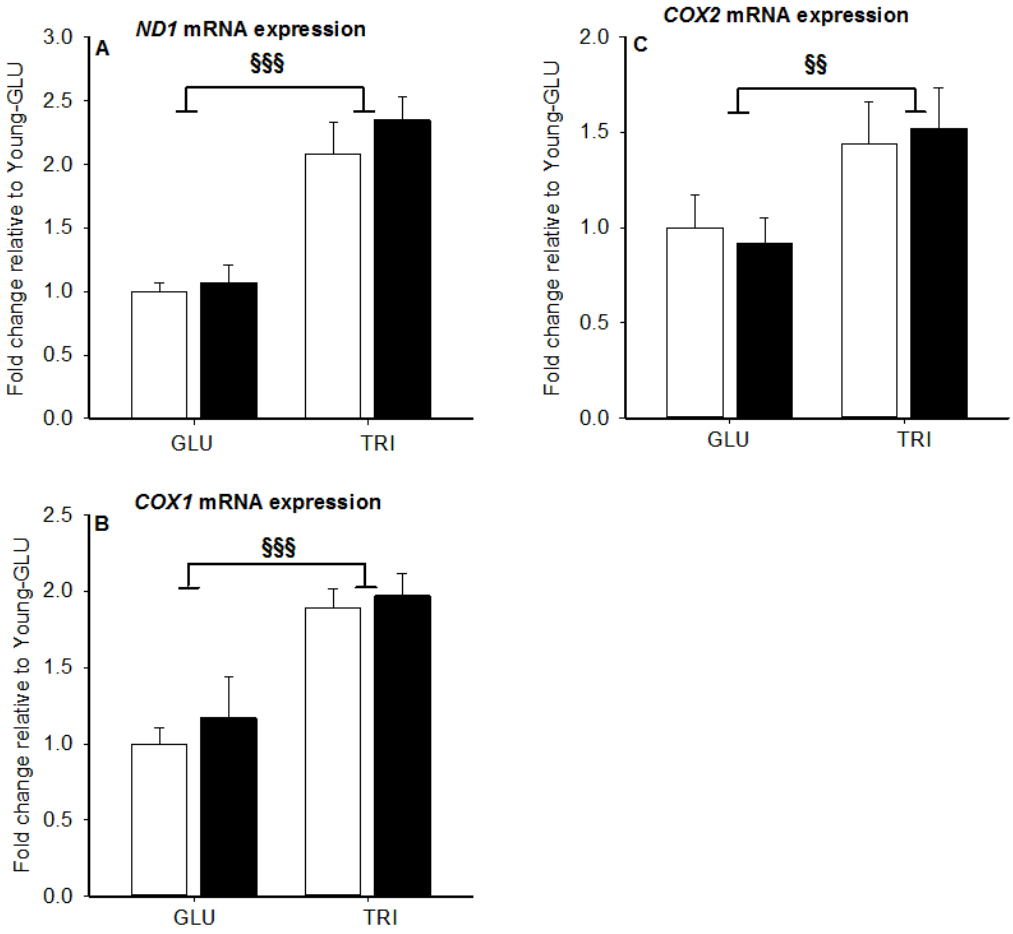

Figure 3-3. Transcript level of mtDNA encoded genes in skeletal muscle from American Quarter Horses. Expression of *ND1* (A), *COX1* (B), and *COX2* (C) mRNA in GLU and TRI muscle from young (n= 7-8 for GLU, n = 8 for TRI) and aged (n = 7-8 for GLU, n = 7-8 for TRI) horses. Results are represented as the fold change compared to young-GLU muscle. Values are means ± SE. Open bars represent young horses; solid bars, aged horses. GLU vs. TRI: $^{§§}P < 0.01$, $^{§§§}P < 0.001$.

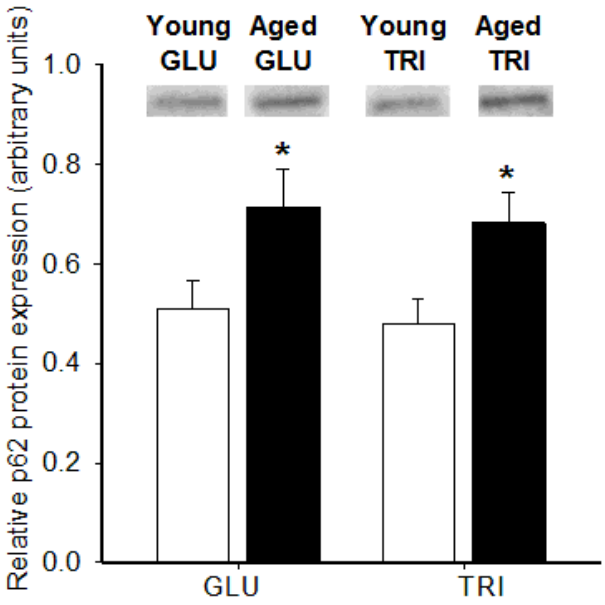

Figure 3-4. Protein expression of p62 in skeletal muscle from American Quarter Horses. Protein level of p62 in GLU and TRI muscle from young (n = 24 for GLU, n = 12 for TRI) and aged (n = 12 for GLU, n = 12 for TRI) horses. Representative Western blot images are shown above the summary graph. Values are means ± SE. Open bars represent young horses; solid bars, aged horses. Young vs. aged: *$P < 0.05$.

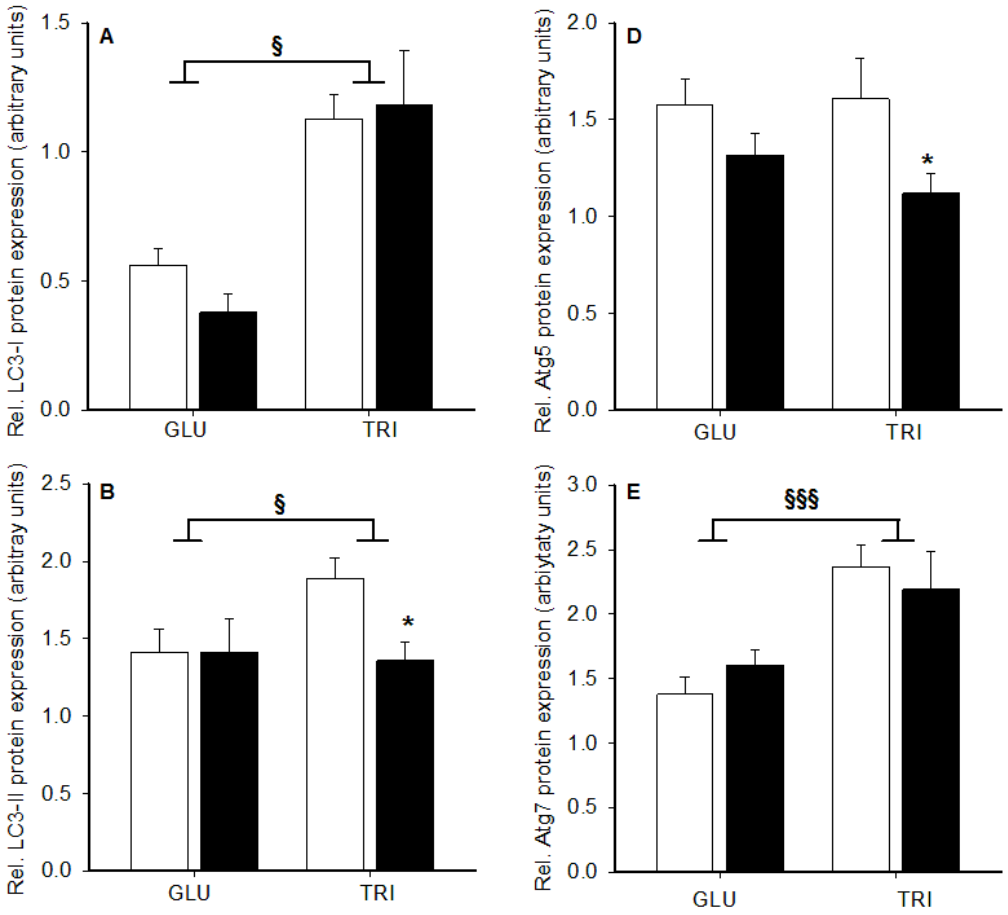

Figure 3-5. Gene and protein expression of autophagy regulatory proteins in skeletal muscle from American Quarter Horses. Protein expression of LC3-I (A) and LC3-II (B), and mRNA expression of *LC3* (C); and protein expression of Atg5 (D) and Atg7 (E) in GLU and TRI muscle from young (mRNA expression: n = 8 for GLU, n = 8 for TRI; protein expression: n = 22-24 for GLU, n = 11-12 for TRI) and aged (mRNA expression: n = 8 for GLU, n = 8 for TRI; protein expression: n = 12 for GLU, n = 11-12 for TRI) horses. F) Representative Western blot images of Atg5, Atg7 and LC3-I and LC3-II in GLU and TRI muscle from young and aged horses. Values are means ± SE. Open bars represent young horses; solid bars, aged horses. Young vs. aged: **P* < 0.05, ****P* < 0.001. GLU vs. TRI: $^{\S}P$ < 0.05, $^{\S\S\S}P$ < 0.001.

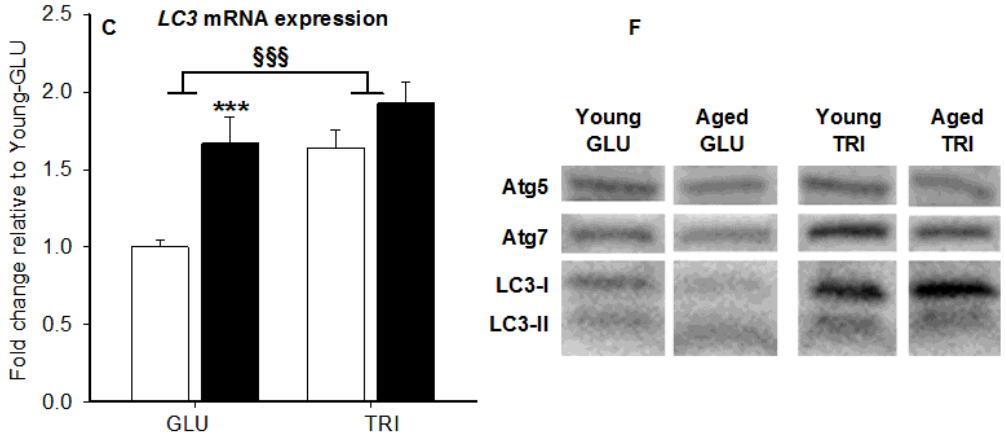

Figure 3-5. Continued

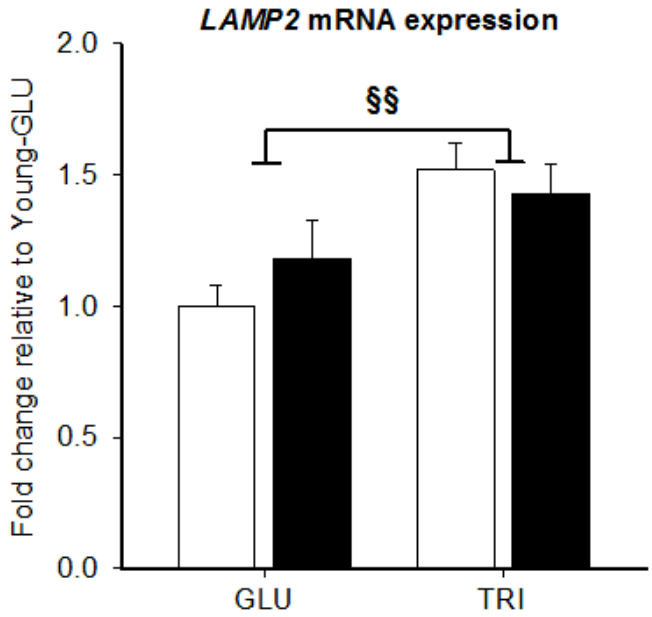

Figure 3-6. Transcript level of the *LAMP2* gene in skeletal muscle from American Quarter Horses. Expression of *LAMP2* mRNA in GLU and TRI muscle from young (n = 8 for GLU; n = 8 for TRI) and aged (n = 8 for GLU; n = 8 for TRI) horses is represented as the fold change compared to young-GLU muscle. Values are means ± SE. Open bars represent young horses; solid bars, aged horses. GLU vs. TRI: $^{§§}P < 0.01$.

CHAPTER 4
AGE-RELATED CHANGES IN MYOGENIC CAPACITY OF SATELLITE CELLS OBTAINED FROM AMERICAN QUARTER HORSES

Background

Healthy skeletal muscle has a remarkable capacity to repair injury via muscle regeneration. In adults, this ability is owed to muscle stem cells, commonly referred to as satellite cells. When those cells were first identified in 1961 (Mauro, 1961), they were described as mononucleated cells “wedged” between the basal lamina and plasma membrane of myofibers. Given the fact that they represent the only source of new myonuclei in postnatal skeletal muscle, satellite cells might be centrally involved in maintenance of healthy muscle mass (Biressi & Rando, 2010). It is hypothesized that a decline in satellite cell function and/or number is a main factor causing the insufficiency of muscle regeneration in elderly humans, which subsequently leads to a loss of myofibers and a decline in muscle cross-sectional area, recognized as sarcopenia (Gopinath & Rando, 2008; García-Prat *et al.*, 2013). Moreover, a number of studies have shown type II muscle fiber atrophy with aging is accompanied by a fibertype-specific decline in satellite cell content (Verdijk *et al.*, 2007; Verney *et al.*, 2008; McKay *et al.*, 2012). In general, satellite cell content and function are suggested to decrease with age (Conboy *et al.*, 2003; McKay *et al.*, 2013; Fry *et al.*, 2015), rendering muscle regeneration insufficient in aged muscle (Brooks & Faulkner, 1990; Ikemoto-Uezumi *et al.*, 2015). However, these findings were based on studies, in which satellite cell regenerative capacity was tested *in vivo* in response to physiological and pathological stimuli, including exercise and injury. The effects of aging on satellite cells themselves were not examined directly.

Although the exact underlying mechanisms contributing to satellite cell dysfunction are not yet fully understood, increasing evidence gathered over the past decade showed that diminished satellite cell function is due to both intrinsic changes in satellite cells themselves and extrinsic alterations in the satellite cell microenvironment, also called the satellite cell niche. Support for the latter mainly comes from transplantation experiments, in which declined regenerative capacity of old satellite cells was rescued by a “young” environment into which the old cells were transplanted (Conboy *et al.*, 2005; Villeda *et al.*, 2011; Lavasani *et al.*, 2012), while young satellite cells lost their regenerative function when transplanted into an “old” niche (Carlson & Faulkner, 1989). Intrinsic changes of satellite cells with age may also regulate satellite cell function. In particular, over the past a few years, the role of mitochondria for satellite cell performance has been increasingly appreciated. As expected given their essential role for energy production, among other vital functions (Finkel & Holbrook, 2000; Ryan & Hoogenraad, 2007), mitochondrial function appears to be a major player in regulating satellite cell myogenic properties (Marzetti *et al.*, 2013; Siegel *et al.*, 2013). Mitochondrial function has been suggested essential for satellite cell maintenance and activation (Cerletti *et al.*, 2012; Stein & Imai *et al.*, 2014; Ryall *et al.*, 2015). In addition, an increase in mitochondrial respiratory function is indispensable during differentiation from myoblasts into myotubes in order to establish the oxidative phenotype that is necessitated by the high energetic demand of muscle contraction. Upon differentiation, myoblasts shift from a previous glycolytic state to predominant reliance mainly on mitochondrial oxidative phosphorylation. This shift is accompanied by a marked increase in mitochondrial biogenesis and mitochondrial oxidative respiration (Remels *et*

al., 2010). However, mitochondrial function is impaired in old satellite cells, indicated by downregulation of the TCA cycle and OXPHOS reactions (Kuilman *et al.*, 2010; López-Otín *et al.*, 2013; Zhang *et al.*, 2016). Mitochondrial quality control mechanisms, including mitochondria-specific proteases and chaperones, fission/fusion processes, mitochondrial biogenesis and autophagy, are responsible for maintenance of mitochondrial homeostasis, and therefore, might also play an important role in regulating mitochondrial function in satellite cells. Indirect support for the role of mitochondria in satellite cell function comes from studies in which satellite cell function was altered in conditions that improved or harmed mitochondrial homeostasis. For example, short-term caloric restriction, which is known to stimulate mitochondrial biogenesis, stimulated satellite cell proliferation in young and old mice (Cerletti *et al.*, 2012), and alterations in mitochondrial biogenesis led to failure of satellite cell-induced muscle regeneration during conditions of muscle wasting (Toledo *et al.*, 2011). Further, impaired autophagy led to increased ROS generation, which in turn drove satellite cell senescence in mice (García-Prat *et al.*, 2016), while autophagy reactivation ameliorated muscle regeneration in mdx mice (Fiacco *et al.*, 2016).

Horses are among the most athletic animals, and they may suffer subtle muscle injuries on a regular basis during their normal daily activities (Taylor *et al.*, 1981). Continuous muscle repair facilitated by a muscle cell's healthy satellite cell population is therefore essential for muscle mass maintenance throughout life. However, not much is known about the effects of aging on satellite cell function in equine muscle. Furthermore, to the best of our knowledge, no studies have so far investigated age-related alterations in mitochondrial quality control, pivotal in maintaining mitochondrial

function, in horse satellite cells; and it is worth noting that those control mechanisms may be negatively affected during the aging process. Therefore, the overall goal of this project was to examine differences in the intrinsic myogenic capacity and mitochondrial quality control mechanisms of satellite cells isolated from young and aged horses, and to compare different muscle types.

Materials and Methods

Animals and Muscle Sample Collection

Clinically healthy young (n = 4, 1 gelding and 3 mares, aged 2-4 years) and aged (n = 4, 1 gelding and 3 mares, aged 20-27 years) American Quarter Horses were used in this study. All horses were owned by the University of Florida and held on pasture at the university's horse teaching unit. None of the horses used had received forced exercise for 6 mo prior to the study. All procedures performed in this study were approved by the University of Florida Institute of Food and Agricultural Sciences Animal Research Committee.

Skeletal muscle microbiopsies were collected in a sterile manner from the GLU and TRI following the procedure described in Li *et al.* (Li *et al.*, 2016; Chapter 2 of this dissertation). Briefly, following administration of local anesthesia, muscle samples were collected at a sampling depth of 5 cm, using a 14-gauge SuperCore ™ Biopsy needle (Angiotech, Gainesville, FL, USA). Muscle samples were placed in ice-cold Dulbecco's phosphate-buffered saline (DPBS, Hyclone™, South Logan, UT, USA) and immediately transported to the lab for satellite cell isolation. As a comparison of cells from young and aged horses was required, muscle was removed from young and aged horse sequentially and processed in parallel throughout all experiments.

Satellite Cell Isolation

Under sterile conditions, muscle samples were washed with PBS to remove any surface blood. After re-suspending in fresh PBS, visible fat and connective tissue were cleaned off, and the remaining tissue minced into a coarse slurry and subsequently digested using pronase (Sigma-Aldrich, St. Louis, MO) for 1 h at 37 °C. The digested tissues were then centrifuged at 1600 × *g* for 10 min, the pellets were re-suspended in PBS and filtered through a 100 µm Steriflip filter (Millipore, Billerica, CA). Following another centrifugation at 1600 × *g* for 10 min, cells were re-suspended in growth medium (GM), Ham's F-10 (Corning, NY) supplemented with 20% horse serum (Gibco®, Thermo Fisher Scientific, Waltham, MA, USA), 1% L-glutamine (Corning), and 1% Antibiotic-Antimycotic (Gibco®, Thermo Fisher Scientific), plated on 100 mm culture dishes coated with gelatin (Sigma-Aldrich), and cultured in an incubator with 5% CO_2 at 37 °C. Media were changed every 48 h. Cells were passaged on day 7 after isolation and subsequently every 2 days (at 60-70% confluence). Cell were passaged three times in total and then cryopreserved until further use. A 30 min pre-plate was performed at each passage step to enrich satellite cells population.

Proliferation and Differentiation Assays

After thawing cryopreserved cells (as passage #4), they were cultured in GM, with medium exchange every 24 h. Cell were trypsinized when they reached 60-70% confluency, washed in PBS once, and this 5^{th} cell passage divided into experimental batches as outlined below. At this 5^{th} passage, cultures contained >90% myogenic cells, based on the expression of the myogenic marker, Pax7, analyzed by immunofluorescent staining using anti-Pax7 (1:2, Developmental Studies Hybridoma

Bank (DSHB), Iowa City, IA, USA) and Alexa fluor 488-conjugated secondary rabbit anti-mouse IgG (1:500) (see also section 2.4).

For differentiation analysis, cells of the 5th passage were allowed to proliferate in GM until they reached 80-90% (submaximal) confluency. At that time, the GM was exchanged for differentiation media (DM), DMEM with low glucose (Corning) supplemented with 1% sodium pyruvate (Lonza, Walkersville, MD), 1% HEPES (Gibco®), 1% L-glutamine (Corning), 1% insulin-transferrin selenium (Gibco®), and 1% Anti-Anti (Gibco®). The differentiation media induces satellite cell differentiation due to the low serum content. Cells were cultured in DM for the indicated time (24 h, 48 h, and 96 h). Because cells from aged horses exhibited a lower proliferation rate in practice experiments, they were prepared and seeded 5 h before cells from young horses in order to reach submaximal confluency at the same time as cells from young horses for simultaneous performance of the differentiation assays.

Measurement of Myoblast Differentiation and Fusion

Cells were seeded at a density of 4 ×10^3/well in 96-well plates in quadruplicate, and the GM exchanged for DM when the cells reached 80-90% confluency (D0-DM, day 0 in DM) as described above. On day 3 in DM (D3-DM), following a quick rinse with PBS, cells were fixed and permeabilized in 100% methanol for 10 min at -20 °C, and subsequently blocked with 5% horse serum in PBS for 45 min at room temperature (RT). Cells were then immunostained with primary antibodies for 1h at RT followed by an overnight incubation in primary antibody at 4°C. Primary antibodies used were as follows: myogenin (2 wells/sample; 1:2, F5D, DSHB) and myosin heavy chain (MyHC) (2 wells/sample; 1:2.4, MF20, DSHB). After incubation with primary antibodies and a quick rinse with PBS supplemented with 0.5% BSA (Sigma-Aldrich) cells were

incubated with Alexa fluor 488-conjugated secondary rabbit anti-mouse IgG (1:500 for MyoG; 1:1000 for MyHC, Thermo Fisher Scientific) for 1h at RT. All immunofluorescently labeled cells were counterstained with Hoechst 33342 (1g/mL, Thermo Fisher Scientific) to label the nuclei. Cells were examined with an EVOS fluorescence microscope (Thermo Fisher Scientific), and labeled cells manually counted and recorded using ImageJ software. Myogenin (a marker of cell differentiation) staining was expressed as a percentage of myogenin-labeled cells relative to the total number of cells (labeled by nuclear stain) in the field of view. The efficiency of fusion (fusion index) was determined by counting the number of nuclei in MyHC positive myofibers as a percentage of the total number of nuclei in the field of view. At least five randomly selected fields of view were imaged per sample. The mean of these measurements was taken as the sample value.

Isolation of Total RNA and Real-Time qPCR

Total RNA was isolated from differentiating cells (D1-DM and D2-DM) using TRIzol (Thermo Fisher Scientific), with genomic DNA removed using a DNA-*free*™ Kit (Thermo Fisher Scientific), according to manufacturer's instructions. Immediately following DNA removal, RNA concentration and purity were determined by measuring the absorbance at 260 and 280 nm with a UV spectrophotometer (Synergy HT, BioTek Instruments). Two micrograms of total RNA was reverse transcribed in a 20 µL reaction system performed with a High-Capacity cDNA Reverse Transcription Kit (Applied Biosystems Inc., Foster City, CA) according to the supplier's guidelines. Subsequently, PCR amplification was carried out using SYBR green fluorescence (iTaq™ Universal SYBR® Green Supermix, Bio-Rad) on a CFX Connect real-time PCR detection system (Bio-Rad), following the manufacturer's recommended protocol. Each assay plate

contained negative controls and a relative standard curve generated with five serial 5-fold dilutions of cDNA pooled from experimental samples. The standard curve was accepted at a R^2 of 0.99 or greater, otherwise the samples were repeated. Melting curve analyses were performed to verify the amplification of a single PCR product. Transcript levels were analyzed using relative standard curve, normalized to *GAPDH* mRNA, and results were expressed as a fold change in mRNA level compared with expression in GLU from the young horse group. All reactions were performed in duplicate. Specific primer sequences are listed in Table 3-1.

MtDNA Copy Number Measurement

Total DNA was extracted from differentiating myoblasts (D1-DM and D2-DM) using Wizard® Genomic DNA purification kit (Promega Corporation, Madison, WI), following the manufacturer's instructions. DNA concentration and purity were determined using a UV spectrophotometer (Synergy HT, BioTek Instruments). Relative quantification of mtDNA copy number was performed by real-time qPCR using primers specific for mitochondrial gene *ND1* (NADH dehydrogenase 1, forward: 5'-GGA TGG GCC TCA AAC TCA A-3'; reverse: 5'-GGA GGA CTG AGA GTA GGA TGA T-3') and normalized against the nuclear gene *ACTB* (*β-actin*, forward: 5'-CTC CAT TCT GGC CTC ATT GT-3'; reverse: 5'-AGA AGC ATT TGC GGT GGA-3'). To confirm the results assessed with *ND1* primers, another pair of primers designed within mitochondria gene *COX1* (*cytochrome c oxidase 1*) region was also tested. Primer sequences for *COX1* were provided below: 5'-CAG ACC GTA ACC TGA ACA CTA C-3' (forward) and 5'-GGG TGT CCG AAG AAT CAG AAT AG-3' (reverse). DNA was amplified using a CFX Connect real-time PCR detection system (Bio-Rad) with conditions listed below: 95 °C for 3 min and 40 cycles of 95 °C for 5 seconds and 60 °C for 30 seconds. Melting curve

analysis was performed from 65 °C to 95 °C. The relative quantification was done using the relative standard method (five serial dilutions of pooled DNA samples) and the R^2 for each standard curve was ≥ 0.99. Data were expressed as a ratio of relative amount of mitochondrial gene to genomic single-copy gene, resulting in a mtDNA/nDNA ratio, a value proportional to the average number of mtDNA copy number in each sample. All samples were amplified in duplicate on the same plates.

Immunoblotting

Whole cell lysates (D1-DM and D2-DM) were obtained by applying Pierce™ RIPA buffer (Thermo Fisher Scientific) containing 1% Halt™ protease-phosphatase inhibitor cocktail (Thermo Fisher Scientific) to adherent cells, followed by scraping the lysed cells off the substrate. Cell lysates were stored at -80 °C until further analysis. Proteins were quantified using Thermo Scientific™ PierceTM BCA protein assay kit (Thermo Fisher Scientific). Equal amounts of the total protein were electrophoretically separated on a Sodium dodecyl sulfate polyacrylamide gel (BioRad) and transferred to a Polyvinylidene fluoride membrane (PVDF; Thermo Fisher Scientific), and immunoblotted under standard conditions as previously described (Wohlgemuth *et al.*, 2010). Primary antibodies used were as follows: anti-p62/SQSTM1 (1:300, Sigma-Aldrich), anti-CS (1:100, Santa Cruz Biotechnology, Dallas, TX), anti-Hsp60 (1:1000, Cell Signaling Technology, Danvers, MA), anti-LC3 (1:500, Thermo Fisher Scientific), and anti-tubulin (1:20,000, Sigma-Aldrich). Secondary antibodies were either horseradish peroxidase- or alkaline phosphatase-conjugated (Sigma-Aldrich). Membranes were then developed with DuoLux chemiluminescent/fluorescent substrate (Vector Laboratories, Burlingame, CA) and the chemiluminescent signals captured with a digital imager (G:Box Chemi XR5, Syngene). Densitometric analysis of band signals was performed using the

manufacturer's analysis software (Gene Tools, Syngene). Protein level was expressed relative to tubulin expression, which served as a loading control.

Statistical Analysis

Data are presented as means ± SE, with the number of samples per group indicated in the figure legends. Statistical analysis was performed using SigmaPlot 13.0 software (Systat Software Inc., San Jose, CA). For data that were not normally distributed as determined by Shapiro-Wilk normality test, a $\log_{10}$ transformation was performed in order to achieve a normal distribution. Data were analyzed for significance by two-way analysis of variance, with factors of age (Young, Aged) and muscle type (GLU, TRI), followed by posthoc Holm-Sidak multiple comparison tests. Data were considered significantly different if the P value ≤ 0.05. Trends were reported if $0.05 < P < 0.1$.

Results

Satellite Cells from Aged Horses Showed Reduced Myogenic Potential

To measure the effect of aging on satellite cell proliferative capacity (Figure 4-1), cells were grown in GM for 6 days until the cells reached confluency. Cells were harvested each day from day 3 (D3) in GM, and the number of cells per well counted. In general, cell number progressively increased from D3 to D6 regardless of age of origin and of muscle type. However, wells with cells obtained from aged TRI tended to have a lower cell number compared to those with cells obtained from young-TRI on D3 (P = 0.086). Similarly, on D4, wells with aged TRI cells tended to have fewer cells compared to those with young-TRI cells (P = 0.062), while significant lower cell numbers were observed in wells with aged GLU cells compared to young-GLU cells on D4 (P = 0.015). After D5, young and aged cells showed similar proliferative capacity, independent of

muscle type. To determine changes in satellite cell differentiation capacity, cells were labeled with myogenin (a key marker of differentiation) and MyHC (a marker for terminal differentiation) on day 3 after induction of differentiation (D3-DM). The number of myogenin$^+$ cells (Figure 4-2) decreased with age (main age effect: $P = 0.007$). More specifically, the percentage of myogenin$^+$ cells (Figure 4-3) was decreased by 33% in cells from aged TRI ($P = 0.017$), and ~30% in cells from aged GLU ($P = 0.079$). Consistent with these findings, the percentage of nuclei in MyHC$^+$ cells was lower in cells from aged compared to young-TRI. However, the fusion capacity (fusion index, number of nuclei in MyHC$^+$ cells/ total number of nuclei in the field of view) was similar between cells derived from young and aged-GLU. These data suggest that satellite cells obtained from aged horses have impairments in proliferation and differentiation, and TRI- derived satellite cells are more susceptible to age-related changes.

Mitochondrial DNA Copy Was Elevated with Age

Differentiation of satellite cells (myoblasts) into myotubes requires a metabolic switch from glycolysis to OXPHOS. In order to meet the energy demands of myotubes, the myoblasts must generate sufficient mitochondria before they fuse into myotubes (day 2 postdifferentiation). To investigate whether mitochondrial density differs between age groups on D1-DM and D2-DM, the protein expression of CS, a key mitochondrial matrix enzyme and commonly used as a marker for mitochondrial content (Larsen *et al.*, 2012), was analyzed (Figure 4-4). No age-related changes in CS content were observed in cells from either muscle type at either time point ($P > 0.1$ for all). Surprisingly, mtDNA copy number analyzed using *ND1* primers was increased in aged cells at D2-DM (Figure 4-5; $P = 0.056$ for GLU, $P = 0.033$ for TRI), but did not differ at D1-DM (Figure 4-5; $P > 0.1$ for all). This was also the case when primers of another

mitochondrial gene, *COX1,* was used, which confirmed that mtDNA copy number was elevated with age in both GLU- and TRI-derived cells at D2-DM (P = 0.028 for GLU; P = 0.021 for TRI). Taken together, our data indicate that the mtDNA copy number is elevated in both GLU- and TRI-derived satellite cells form aged horses.

Mitochondrial Genes Were Downregulated in Differentiated Cells from Aged TRI Muscle

Given the elevated mtDNA copy number in cells from aged muscles, changes in mRNA level of the mtDNA encoded genes *ND1*, *COX1*, and *COX2* was determined using real time qPCR. The increase in mtDNA copy number did not cause a concomitant increase in transcript level of these mtDNA-encoded genes. In fact, gene expression of *ND1* was reduced by 63% in cells from aged TRI at D1-DM (Figure 4-6, P = 0.007), and this reduction was even pronounced, ~80%, at D2-DM (Figure 4-6, P = 0.043). No apparent age-associated changes in *ND1* gene expression were detected in cells derived from aged GLU at either time point. Similarly, *COX1* expression of cells from aged TRI decreased by 43% at D1-DM (P = 0.031), and by 64% at D2-DM (P = 0.017) compared to cells from young-TRI. No age-associated changes in *COX1* gene expression were observed in cells derived from aged GLU at any point during differentiation. Gene expression of *COX2* did not differ between age groups at either D1-DM or D2-DM cells from in either muscle. Collectively, our gene expression data demonstrate that transcript levels of mitochondrial genes are downregulated in differentiated cells derived from aged TRI, which might indicate an impairment of mitochondrial OXPHOS capacity with age.

Satellite Cells Derived from Aged Muscle Exhibited Impaired Mitochondrial Quality Control Mechanism

To investigate possible mechanisms underling the impaired satellite cell regenerative capacity observed in this study, markers relevant to mitochondrial quality control systems were assessed. Protein expression of a mitochondrial specific chaperone, Hsp60, as determined in differentiated satellite cells (Figure 4-7). No significant difference in Hsp60 content was observed between cells derived from young and aged horses in either muscle, suggesting that cells maintain their ability to regulate protein folding and refolding through Hsp60 with age.

Gene expression analysis of mitochondrial biogenesis markers identified a decreased transcription of *PGC-1α* (P = 0.014; Figure 4-8), but unaltered *NRF1* and *TFAM* (Figure 4-8) in satellite cells obtained from aged TRI on D1-DM. On D2-DM, the decrease in *PGC-1α* expression was less pronounced (P = 0.059; Figure 4-8), while gene expression of *NRF1* (P = 0.05; Figure 4-8) and *TFAM* (P = 0.008; Figure 4-8) was lower in satellite cells derived from aged compared to young-TRI at that time point. For cells derived from GLU, expression of all markers relevant to mitochondrial biogenesis investigated here did not change with age on D1-DM (Figure 4-8). However, there was a dramatic decline in *PGC-1α* expression on D2-DM in cells from aged GLU (P = 0.024; Figuire 4-8), which was not accompanied by any change in expression of *NRF1* and *TFAM* (Figure 4-8). Collectively, these findings suggest that mitochondrial biogenesis was impaired with age in differentiated satellite cells.

To investigate autophagic activity during satellite cell differentiation, the autophagy regulators p62, LC3 and LAMP2 were assessed using either western blot or real time qPCR, or both. At D1-DM, accumulation of p62 (P = 0.038) suggests an

impairment of autophagic degradation (Figure 4-9) in cells obtained from aged TRI. Consistent with this finding, an elevated level of the autophagosomal membrane-bound, phosphatidylethanolamine-conjugated form of LC3 (LC3-II; $P = 0.034$; Figure 4-10) was detected in this group. To investigate whether the downstream process of fusion of the autophagosome with the lysosome was affected by age, expression of *LAMP2* was examined (Figure 4-11). Transcript level of *LAMP2* seemed to be numerically lower in cells obtained from aged TRI, but it the variance was high and the difference to cells derived from young TRI did not reach significance. At D2-DM, cells from aged TRI continued to exhibit an accumulation of p62 ($P = 0.048$). Moreover, there was a dramatic reduction in *LC3* gene expression (by 76%, $P = 0.011$) with age in TRI cells. Neither LC3-I or LC3-II protein level differed between cell from young- and aged-TRI. Cells obtained from aged GLU did not show significant changes in expression of either autophagy regulator, but there was a tendency for a decreased LC3-II protein level ($P = 0.076$). Our data indicate poor autophagic degradation activity in differentiated cells obtained from aged TRI.

Discussion

It has been suggested that aged muscle exhibits poor repair and regeneration capacity following exercise-induced damage (Brooks & Faulkner, 1990). However, knowledge on satellite cell biology in healthy aging objectes is still insufficient. Especially in equine, it is largely unknown whether satellite cells of old horses differ in their intrinsic myogenic capacity from those of young individuals. Among the hallmarks of aging, mitochondrial dysfunction has been in the spotlight for a long time. The maintenance of a functional mitochondrial pool is essential for cellular processes, in particular for muscle regeneration where differentiated cells are strictly dependent on

oxidative, mitochondria-supported metabolism (Wagatsuma & Sakuma, 2013). Indeed, given the role of mitochondria in cell differentiation, the question arises whether changes in mitochondrial density and/or function, or alteration in mitochondrial quality control pathways, could subsequently affect satellite cell myogenic capacity.

This work is the first to compare the intrinsic myogenic potential of satellite cells isolated from healthy young and aged horses, and to provide evidence that impaired mitochondrial quality control mechanisms could be a potential cause of the failure of proper satellite cell differentiation. Primary culture of satellite cells isolated from muscle biopsies under standard conditions *in vitro* showed that cells derived from aged horses tended to have a lower cell proliferation rate and significantly reduced differentiation capacity compared to those derived from young horses. Moreover, these age-associated impairments in cell myogenic capacity were more pronounced in cells from the TRI muscle than those from the GLU muscle. Noteworthy, reduced myogenic potential of aged cells was accompanied by an elevation of mtDNA copy number without a concomitant increase in mitochondrial density and function. What is more, the protein content of citrate synthase, a marker of mitochondrial density (Larsen *et al.*, 2012), did not change with age, and the transcript levels of mtDNA-encoded genes were downregulated in aged cells, indicating impaired mitochondrial function. The age-dependent decline in gene expression of mitochondrial biogenesis markers (*PGC-1α*, *NRF1*, and *TFAM*) and the alterations in some of the autophagy markers (p62 and LC3) in aged TRI cells point to insufficient mitochondrial quality control as one of the underlying causes of mitochondrial dysfunction, which in turn may lead to compromised myogenic capacity. At present, our data do not sufficiently explain why the myogenic

potential of cells obtained from aged GLU were slightly impacted, but the significant reduction in *PGC-1α* and a tendency for decreased LC3-II protein could point in the same direction. It is possible, that the more glycolytic GLU experiences the negative impact of aging on satellite cell function at a later age compared to the more oxidative TRI, but this speculation warrants further evaluation.

Skeletal muscle regeneration depends greatly on the interplay between the satellite cell and its local microenvironment, known as the satellite cell niche. In most of the injury-induced muscle regeneration models, the muscle regenerative outcomes seemed to depend more on the age of the niche, rather than on the aged satellite cell itself (Grounds, 1998). Following injury, a dramatic change in levels of growth factors and cytokines has been observed within the satellite cell niche (Edwall *et al.*, 1989; Kurek *et al.*, 1996; Warren *et al.*, 2002). Aged horses, for example, exhibited increased expression of inflammatory cytokines IL-1β, lL-6, and IFNγ mRNA in circulation (McFarlane & Holbrook, 2008), which have been reported to impede cell proliferation and differentiation of C2C12 myoblasts (Al-Shanti & Stewart, 2012), as well as horse satellite cells *in vitro* (LaVigne *et al.*, 2015). In addition, aged satellite cells failed to respond to repair stimuli, such as induced injury (Conboy *et al.*, 2003; Gopinath & Rando, 2008; Kuang *et al.*, 2008), due to a decline in satellite cell activation (Carlson *et al.*, 2008; Conboy *et al.*, 2003). It is important to note that these extrinsic alterations of the niche, such ascytokine levels, and the distinct sensitivities to repair stimulation signals could mask intrinsic changes in the aged satellite cell itself. Furthermore, those experimentally induced or extreme types of injuries are different from physiological attrition and muscle regeneration stimulated by routine physical activities. Our results

point to intrinsic changes with age and thereby can explain, at least in part, why the regenerative capacity is reduced in old compared to adult satellite cells exposed to the same environment (Sousa-Victor *et al.*, 2014), and why old satellite cells can be rejuvenated by specific molecular cues (Carlson *et al.*, 2009a) or by a “youthful” microenvironment (Carlson & Conboy 2007).

One finding of the present study was the difference in satellite cell susceptibility to aging between the two muscles. Satellite cells isolated from TRI were more susceptible to age when compared to cells isolated from GLU. More specifically, TRI-derived aged cells failed to differentiate as well as young cells, which was concomitant to dysregulation of mitochondrial biogenesis and autophagic degradation pathways, and - probably consequential - diminished mitochondrial function. We have previously shown that the fibertype composition of the TRI is more oxidative than that of the GLU (Li *et al.* 2016; Chapter 2 of this dissertation). At the applied sampling depth, TRI contained ~10% MyHC-I and 35% MyHC-IIA, and the GLU ~3% MyHC-I and 21% MyHC- IIA, which is similar to data published by van den Hoven *et al.* (van den Hoven *et al.*, 1985), who reported a higher percentage of type I fibers in TRI compare to GLU in Dutch Saddle Horses at the same sampling depth. Satellite cell number and function differ between muscle types. For example, the percentage of satellite cells in rat *soleus* muscle (predominantly type I fibers) is around 2-fold higher than in more glycolytic muscles, such as the *tibialis anterior* or *extensor digitorum longus* muscle (Gibson & Schultz, 1982; Okada *et al.*, 1984). The different response of intrinsic satellite cell functions to aging could be explained by a different level of oxidative stress the cells might be exposed to. During aging, the production of ROS was elevated within

myofibers (Chabi *et al.*, 2008), which can subsequently cause oxidative damage to surrounding structures, including satellite cells, which are believed to have reduced antioxidant capacity with aging in human (Fulle *et al.*, 2005). The more oxidative TRI is surmised to exert more oxidative stress and damage, due to its higher OXPHOS activity and presumably a concomitantly higher ROS, and to its greater use in routine activities (posture) compared to the GLU (more voluntary and propulsive activities). Consequently, its satellite cells might experience a higher level of oxidative stress and damage, which could underly progressive dysfunction with age. However, this hypothesis needs to be tested further.

Stem cells are known to contain few mitochondria and rely greatly on glycolytic metabolism for energy production, while when differentiated they reportedly rely mostly on OXPHOS for their energy demand (Leary *et al.*, 1998; Wagatsuma & Sakuma, 2013). In support, a dramatic remodeling of the mitochondrial network has been observed during stem cell differentiation (Sin *et al.*, 2016). Interestingly, an impaired mitochondrial network during differentiation is suggested to negatively affect muscle repair (Wagatsuma *et al.*, 2011), implying the importance of mitochondrial biogenesis and dynamics during satellite cell differentiation. In aged satellite cells, especially cells obtained from TRI, we have found an altered expression of genes relevant to mitochondrial biogenesis, which could at least in part explain their diminished differentiation capacity. Surprisingly, mtDNA copy number, as a marker for mitochondria density, was increased in cells obtained from aged GLU and TRI. An increased in mtDNA copy number has been reported in various cells in response to aging or oxidative stress (Gadaleta *et al.*, 1992; Barrientos *et al.*, 1997; Hsin-Chen *et*

al., 2000), and this was explained as a compensatory mechanism for accumulating mtDNA mutations and defects in the OXPHOS system. In our work, lower expression of genes encoding for subunits of OXPHOS complexes in aged cells suggested defects in OXPHOS, which might have induced the increase in mtDNA copy number. However, at present we are not able to distinguish whether the lower transcript level of mitochondrial genes is an inducer or a consequence of the elevated mtDNA copy number, since the aged cells might have poor transcription efficiency even with higher template availability. It is also noteworthy that the age-related elevated mtDNA copy number was not paralleled by increases in CS content, which supports the hypothesized compensatory nature of mtDNA amplification, and speaks against a higher mitochondrial content.

Another finding of this work was the accumulation of p62 in aged satellite cells, indicating an impairment of autophagic degradation. This was further confirmed by elevated LC3II protein level. Involvement of autophagy in cell differentiation has been reported in C2C12 cells (Sin *et al.*, 2016; Call *et al.*, 2017), where the autophagy process was upregulated soon after cell differentiation was initiated. It is believed that in order to develop a healthy and organized mitochondrial network for the higher energetic demands of myotubes, cells must eliminate the pre-existing mitochondria prior to repopulation with newly synthesized ones. Failure of autophagic degradation of existing, possibly impaired, mitochondria during myogenic differentiation may lead to limited energy production for the fusion machinery, and therefore could result in the compromised fusion capacity observed in aged satellite cells obtained from TRI. We hypothesized that the accumulation of p62 and LC3-II was a consequence of decreased expression of LAMP2, which facilitates the fusion of the autophagosome with the

lysosome (Eskenlinen *et al.*, 2004; Köchl *et al.*, 2006). However, we did not detect a significant decrease in *LAMP2* gene expression, and the evaluation of protein expression of markers involved in degradation is needed.

In conclusion, our current work explored the intrinsic changes in mitochondrial function and quality control in normally aged satellite cells obtained from American Quarter Horses. In the early phase of differentiation, the time period before or upon nascent myofibers presented, impaired mitochondrial function was concomitant with, and probably a consequence of, altered mitochondrial quality control. Taken together, these impairments could be a potential cause of compromised myogenic capacity of satellite cell *in vitro*. Aged satellite cells, especially those derived from TRI started to show alterations in mitochondria quality control mechanisms on day 2 post-differentiation. We hypothesize that these alterations might be more pronounced in the late phase of differentiation, which needs to be further studied. Continuing the study of satellite cell biology in healthy aging horses and the pathways that regulate the aging process of the satellite cell itself would help to develop innovative interventions to maintain muscle mass and function in our aging equine companions.

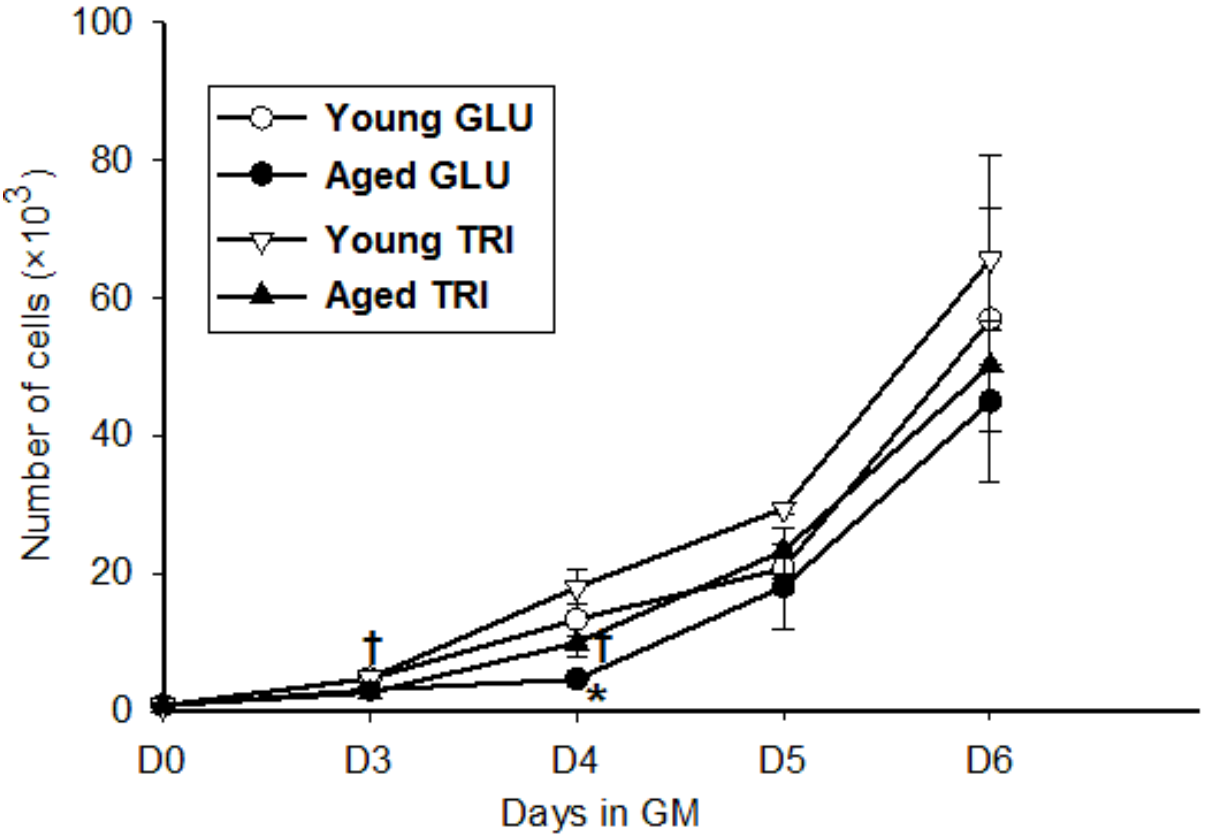

Figure 4-1. Proliferation rate of satellite cells isolated from skelatlal muscle of American Quarter Horses. Cell number measured by direct count of viable cells in a hemocytometer. Satellite cells were grown for 3, 4, 5, or 6 days in growth media. Data for cell count/well are means ± SE (n = 4 for each group; 3 wells per sample at each time point). Young vs. aged: $^{\dagger}P < 0.1$, $^{*}P < 0.05$.

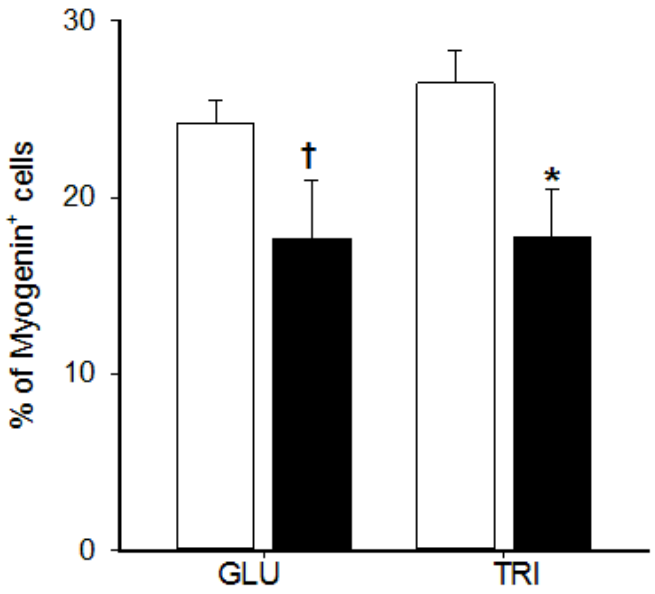

Figure 4-2. Expresion of myogenin in satellite cells isolated from skeletal muscle of American Quarter Horses. Satellite cells isolated from young and aged muscles were differentiated for 3 days, stained for myogenin and counterstained with a nuclear stain (Hoechst). The percentage of myogenin$^+$ cells is shown as means ± SE (n = 4 for each group). Open bars represent young horses; solid bars, aged horses. Young vs. aged: $^{\dagger}P < 0.1$, $^{*}P < 0.05$.

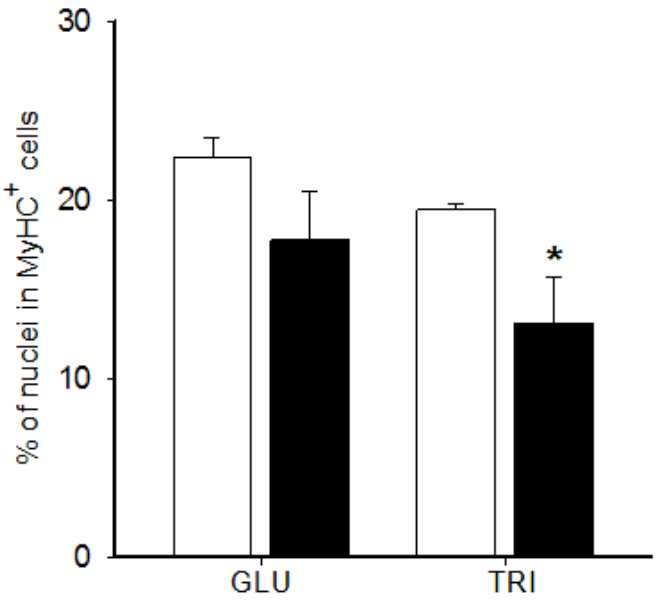

Figure 4-3. Fusion capacity of satellite cells isolated from skeletal muscle of American Quarter Horses. Satellite cells isolated from young and aged muscles were differentiated for 3 days, stained for MyHC and counterstained with a nuclear stain (Hoechst). The fusin capacity is indicated by fusion index that is calculated as the percentage of nuclei present in MyHC$^+$ cells. Values are means ± SE (n = 3-4 for each group). Open bars represent young horses; solid bars, aged horses. Young vs. aged: *P < 0.05.

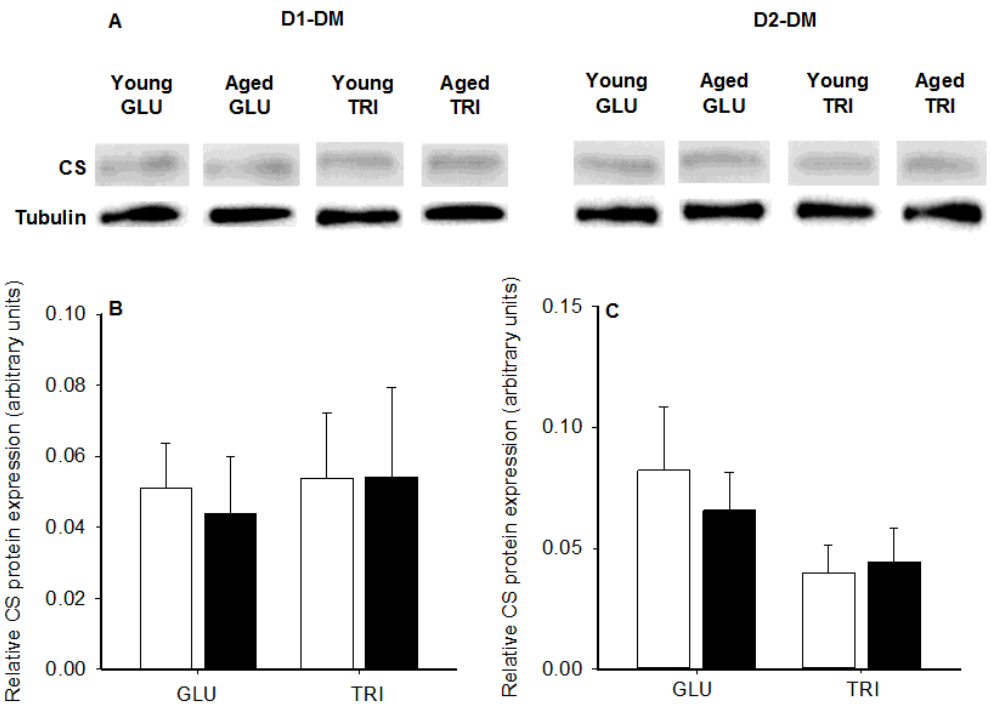

Figure 4-4. The protein expression of citrate synthase in satellite cells isolated from skeletal muscle of American Quarter Horses. A) Representative Western blot image of whole cell lysates at day1 and day 2 postdifferentiation. B-C) Quantification of western blot data normalized to tubulin. Values are means ± SE (n = 3-4 for each group). Open bars represent young horses; solid bars, aged horses.

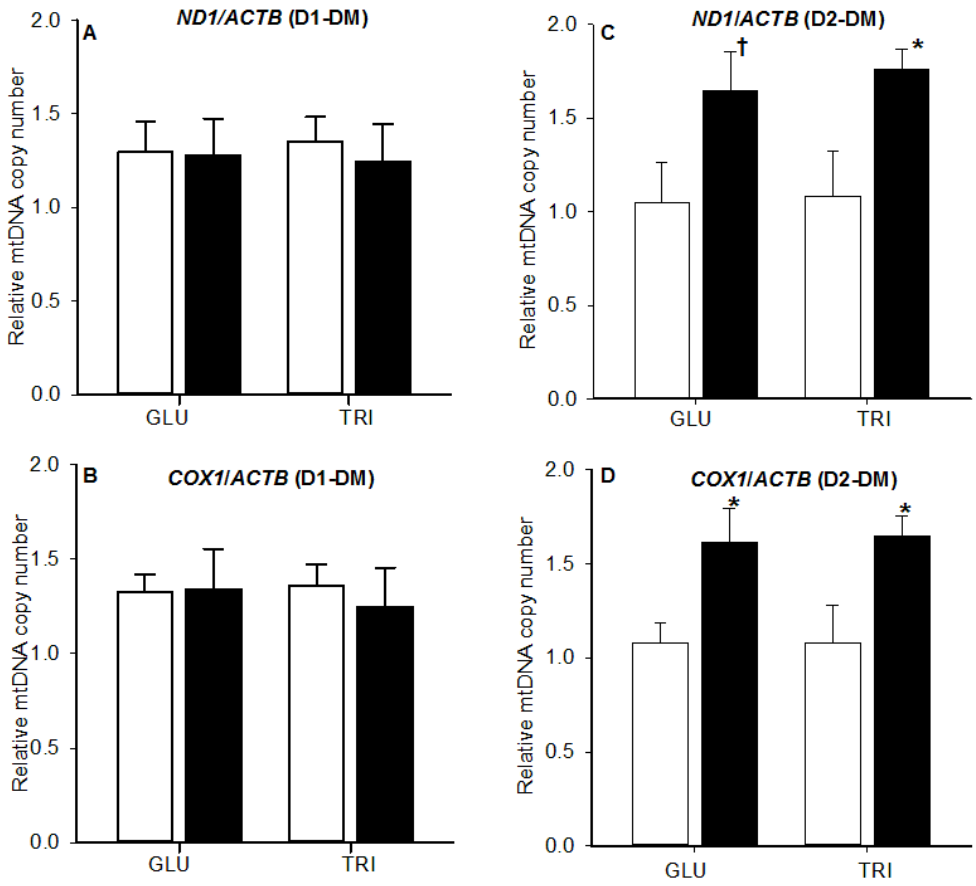

Figure 4-5. Mitochondrial DNA copy number in satellite cells isolated from skeletal muscle of American Quarter Horses. Satellite cells isolated from young and aged muscles were differentiated for 2 days, with a mitochondrial DNA copy number was determined every 24h using quantitative real-time PCR of *ND1* (A and C) and *COX1* (B and D), normalized to nuclear DNA copy number using the β-actin gene (*ACTB*). Values are means ± SE (n = 4 for each group). Open bars represent young horses; solid bars, aged horses. Young vs. aged: $^{\dagger}P < 0.1$, $^{*}P < 0.05$.

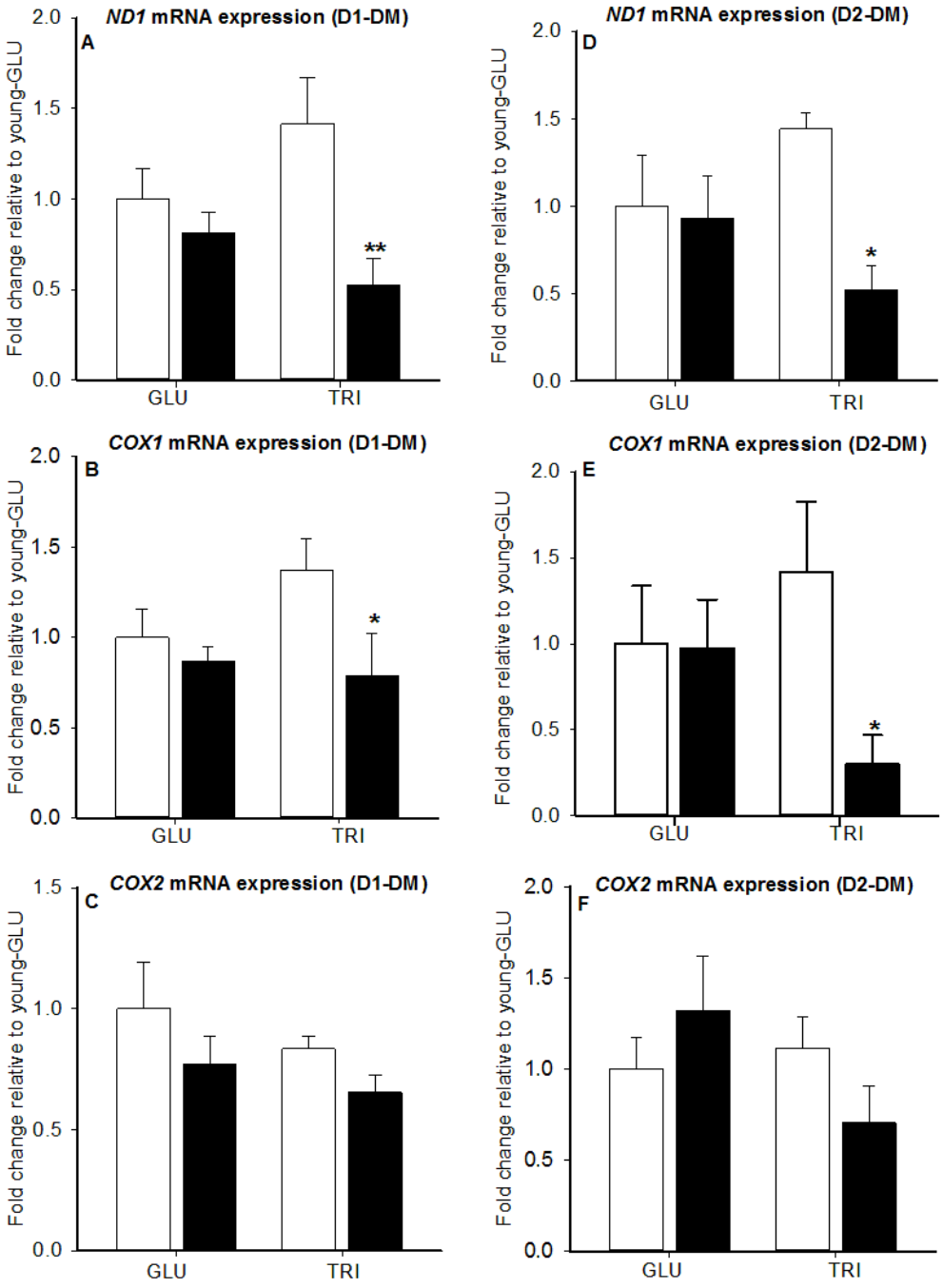

Figure 4-6. Transcript levels of mtDNA encoded genes in differentiated satellite cells. Gene expression of *ND1* (A and D), *COX1* (B and E), *COX2* (C and F) at D1-DM and D2-DM. Values are means ± SE (n = 4 for each group). Open bars represent young horses; solid bars, aged horses. Young vs. aged: **P* < 0.05, ***P* < 0.01.

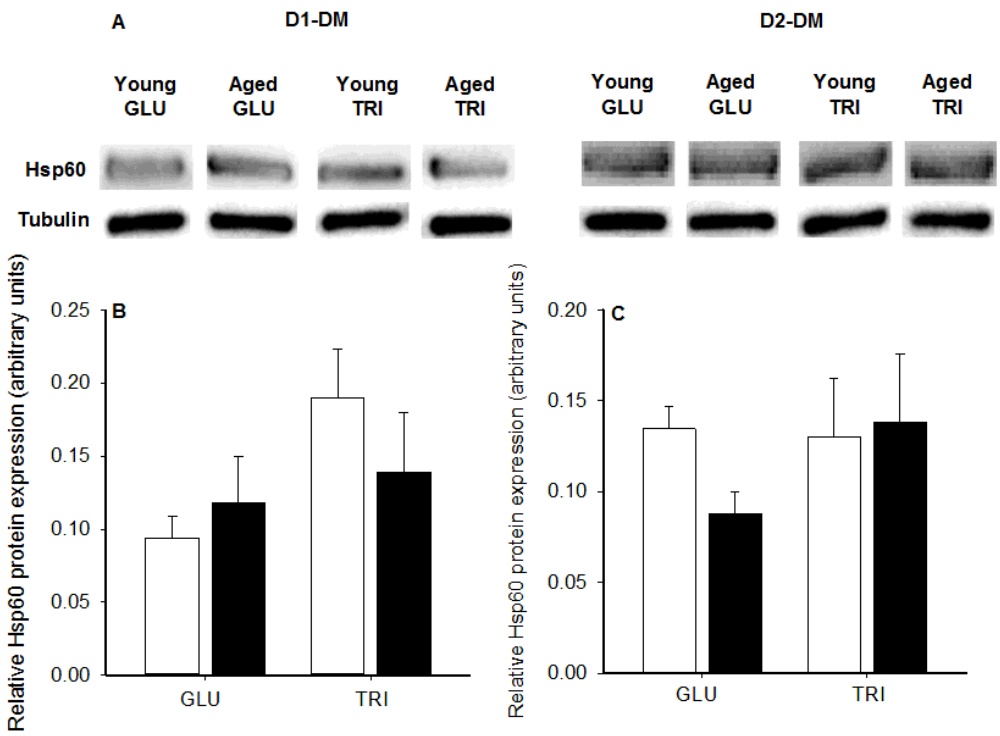

Figure 4-7. Protein expression of Hsp60 in satellite cells during differentiation *in vitro*. Densitometric quantification of Hsp60 protein expression in satellite cells derived from young and aged horses. Representative Western blot images are shown above the graph. Values are means ± SE (n = 3-4 for each group). Open bars represent young horses; solid bars, aged horses.

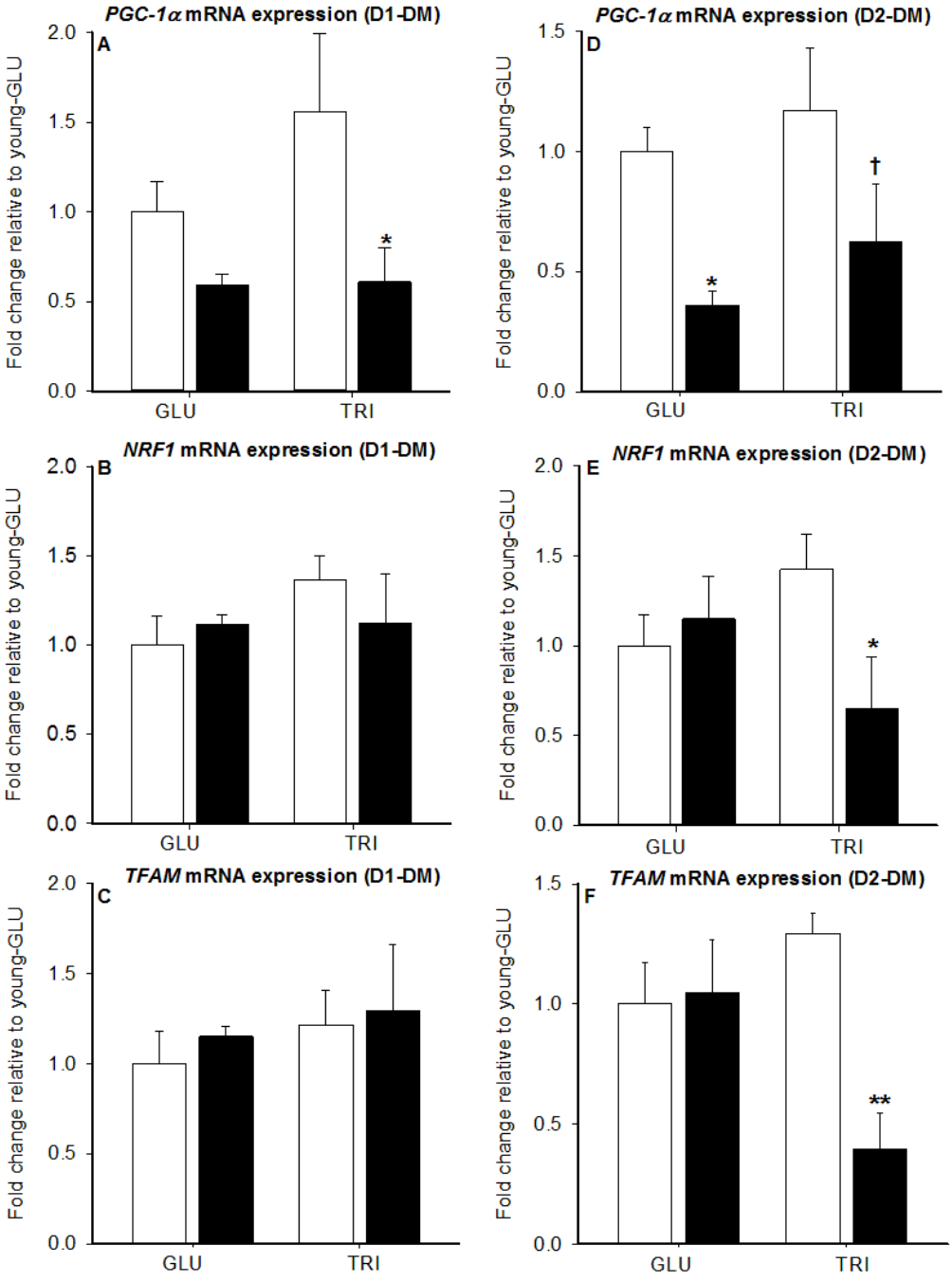

Figure 4-8. Transcript level of genes relevant to mitochondrial biogenesis in satellite cells during differentiation *in vitro*. Gene expression of *PGC-1α*, *NRF1*, and *TFAM* in differentiated satellite cell at D1-DM (A-C) and D2-DM (D-F). Results are represented as the fold change compared to young-GLU muscle. Values are means ± SE (n = 4 for each group). Open bars represent young horses; solid bars, aged horses. Young vs. aged: $^{\dagger}P < 0.1$, $^{*}P < 0.05$, $^{**}P < 0.01$.

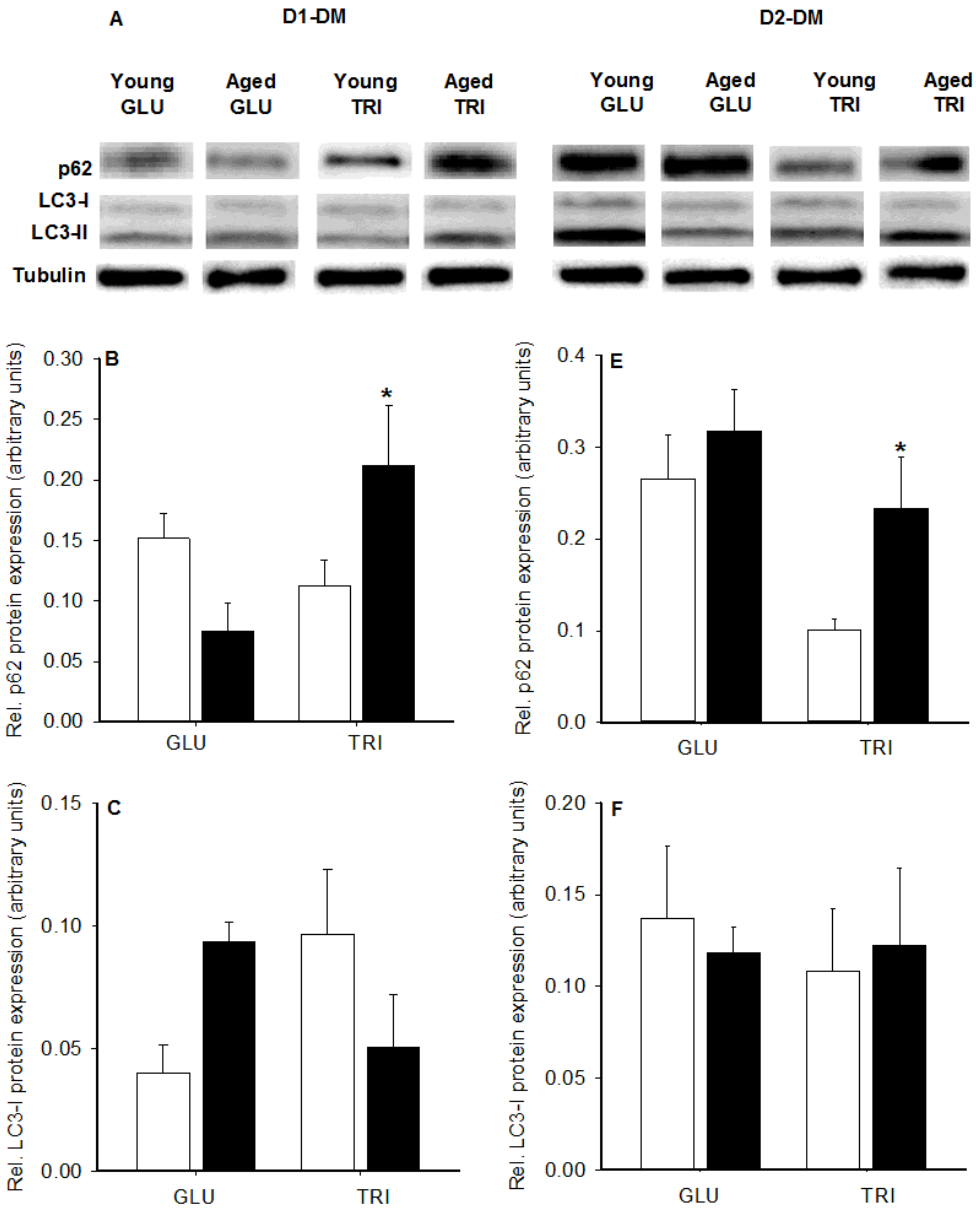

Figure 4-9. Protein expression of autophagy regulators in satellite cells during differentiation *in vitro*. A) Representative Western blot images of autophagy regulators at day1 and day 2 postdifferentiation. Quantification of p62, LC3I, and LC3II in satellite cells derived from young (n = 3-4 for both GLU and TRI) and aged (n = 3-4 for both GLU and TRI) horses at D1-DM (B-D) and D2-DM (E-G). Values are means ± SE. Open bars represent young horses; solid bars, aged horses. Young vs. aged: $^{\dagger}P < 0.1$, $^{*}P < 0.05$

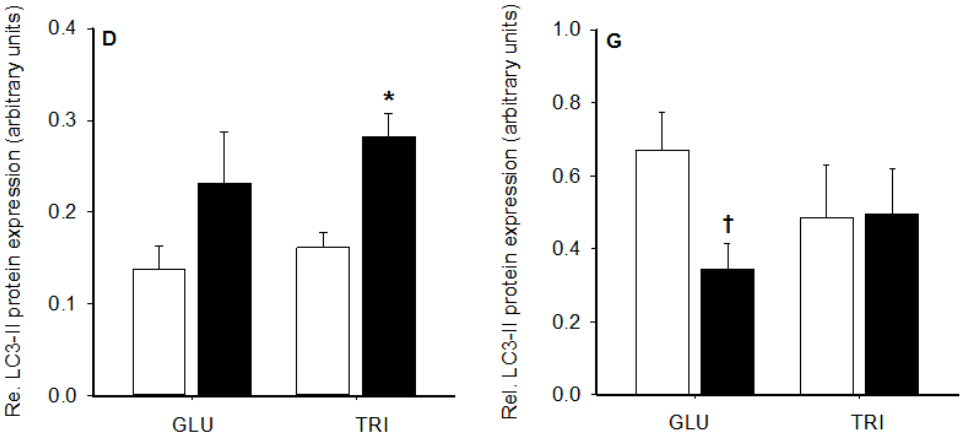

Figure 4-9. Continued

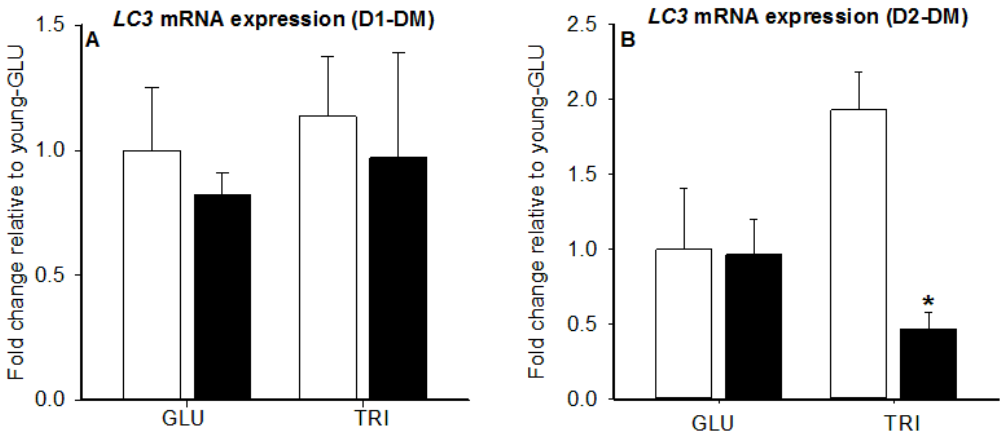

Figure 4-10. Gene expression of *LC3* in satellite cells during differentiation *in vitro*. Expression of *LC3* mRNA in satellite cells isolated from young (n=4 for both GLU and TRI) and aged (n = 4 for both GLU and TRI) horses at D1-DM (A) and D2-DM (B). Data are represented as the fold change compared to young-GLU muscle. Values are means ± SE. Open bars represent young horses; solid bars, aged horses. Young vs. aged: **P* < 0.05.

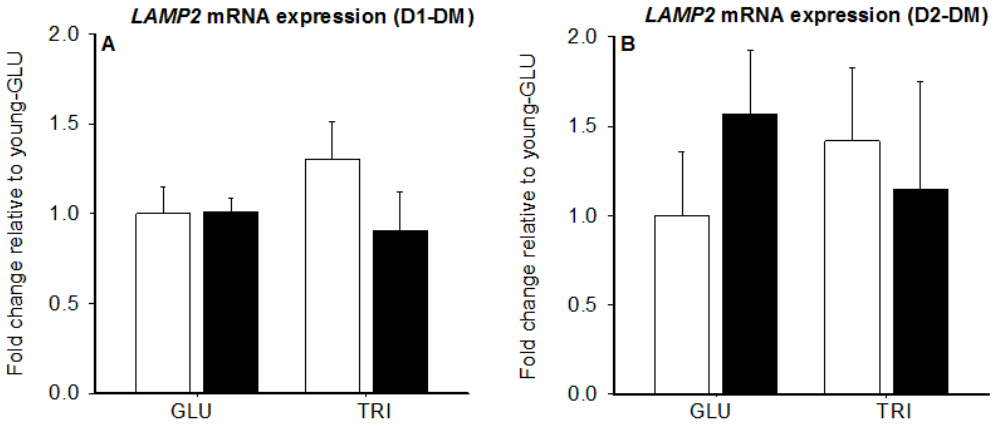

Figure 4-11. Transcript level of the *LAMP2* gene in satellite cell isolated from skeletal muscle from American Quarter Horses. Expression of *LAMP2* mRNA in satellite cells at D1-DM (A) and D2-DM (B) is represented as the fold change compared to young-GLU muscle. Values are means ± SE (n = 3-4 for each group). Open bars represent young horses; solid bars, aged horses.

CHAPTER 5
CONCLUSIONS AND FUTURE DIRECTIONS

As the number of aged horses increases, aged horse population contributes significantly to the whole equine population. With the willingness of owners to use and work with their older horses, understanding the physiology of equine aging and underlying mechanisms is warranted. Yet, few aging studies have been done in the horse. The work in this dissertation has started to evaluate differences in skeletal muscle energy metabolism, especially mitochondrial function, between young and old horses in order to better understand the impacts of aging on equine skeletal muscle.

Effects of aging on skeletal muscle oxidative capacity was first examined in Chapter 2, we conclude that equine skeletal muscle aging was associated with an increase in percentage of type I and IIA fibers, and a decrease in percentage of type IIX fibers. Mitochondrial content and enzymatic activity, as indicated by CS and COX activity, respectively, were decreased with age. Compromised mitochondrial function was observed on the mitochondrial level, but not on the muscle level.

In Chapter 3, aging-related decline in mitochondrial content in equine skeletal muscle was further confirmed and underlying mechanisms responsible for compromised mitochondrial function was explored. Decline in expression level of biogenesis biomarkers in aged-TRI muscle suggests that mitochondrial biogenesis declined with age in equine TRI muscle. In addition, dysregulation of autophagic proteins in TRI muscle indicates that the autophagic flux was impaired in aged-TRI muscle. Taken together, decline in mitochondrial biogenesis activity and autophagic capacity could be the potential cause of impaired mitochondrial function in aged equine skeletal muscle.

After investigating the effects of aging on equine skeletal muscle, we asked how muscle stem cells (namely satellite cells, SCs) were affected by aging in Chapter 4. The ability to regenerate muscle plays a major role in muscle homeostasis after birth and this regenerative capacity is own to muscle SCs. Primary culture of SCs under standard conditions *in vitro* enables us to gain insight into the intrinsic changes of SC function with age. Our data showed that SC derived from aged horses had decreased proliferative and differentiation capacity compared to those from young horses. In line with the decline in SC regenerative capacity, the mitochondrial OXPHOS seemed to decrease with age as indicated by the lower transcript level of mitochondrial genes in SC from aged horses compared to those from young horses. Moreover, impaired mitochondrial biogenesis and autophagic flux were observed in SCs derived from aged horse.

Based on our collective data, we conclude aging was accompanied by compromised mitochondrial function in equine skeletal muscle and satellite cells. However, there was no overt mitochondrial dysfunction on whole muscle level as we found in Chapter 2. If a transition age exists in the horse, defining it might provide insights about a beneficial time point to apply interventions aiming to delay the onset of overt muscle oxidative dysfunction and decline in physical performance. On the other hand, if the horse ages differently from traditional animal models and humans, it will be of interest to characterize the underlying differences. However, it is unlikely that horse ages differently, since we have detected early signs of skeletal muscle aging. Therefore, examining aging effects in even older horses might help to better understand the equine aging process. Moreover, systematically understanding of the underlying mechanisms

responsible for the maintenance of a healthy mitochondrial population in equine skeletal muscle is a prerequisite to design interventions to prolong health and performance of aging horses. An even further step will be if and how interventions that target mitochondrial biology (such as exercise training and resveratrol) affect mitochondrial function in older horses.

APPENDIX A
CITRATE SYNTHASE ACTIVITY PROTOCOL

Adapted from Spinazzi et al. (Spinazzi *et al*., 2012)

To prepare muscle homogenate:

1. Add 10-15 mg powdered (cryopulverized) muscle to each microvial, recording exact tissue weight

2. Add the volume of sucrose homogenization buffer with detergent required to obtain a 40-fold dilution
   a. Sucrose homogenization buffer: 20 mM Tris, 40 mM KCl, 2 mM EGTA, 250 mM sucrose, pH 7.4
   b. Dilute 1 part 5% detergent (n-Dodecyl β-D-maltoside; Sigma D4641) to 100 parts sucrose buffer
   c. Example: 10 mg muscle powder x 40 = 400 µL sucrose homogenization buffer with detergent

3. Sonicate (F60 Sonic Dismembrator, Fisher Scientific, Waltham, MA) each tube by pushing the button on the top of the probe for 1sec, 5-10 times, with the strength between 3-5.
   a. Keep on ice while sonicating
   b. Clean sonicator probe in between samples by rinsing with dH_2O

4. Centrifuge microvials for 3 min at 10,000 x *g* at 4°C

5. Collect supernatant (40-fold dilution)

6. Dilute to 80-fold (1part 40-fold+1part sucrose buffer without detergent (2a))

7. Can store 40-fold and 80-fold homogenates at -80°C until analysis

8. Use 80-fold dilution for assay

To perform assay:

1. Prepare 200 mM Tris (pH 8.0) with Triton-X (0.2% (vol/vol))
   a. Dissolve 1.21 g of Tris in 40 mL distilled H_2O, adjust to pH 8.0 with HCl, add 0.1 mL of Triton-X and adjust the volume to 50 mL
   b. Can be stored at 4°C for up to 2 mo

2. Prepare 10 mM Acetyl CoA
   a. Dissolve 100 mg Acetyl CoA (CHEM-IMPEX INT'L INC #00583) in 11.35 mL distilled H_2O
   b. Can be stored at -80°C in 200 µL aliquots for several months

c. **Once thawed, use same day**

3. Prepare 1 mM DTNB
   a. Dissolve 7.9 mg DTNB (Sigma # D8130) in 20 mL of 100 mM Tris (pH 8.0)
   b. **Prepare fresh daily**

4. Turn on microplate reader, check protocol (CS Spinazzi in Gen5 in Wohlgemuth lab; be sure pathlength correction is INACTIVATED), and preheat to 37°C

5. Prepare 10 mM oxaloacetic acid (OAA)
   a. Dissolve 6.6 mg OAA (Sigma # O4126) in 5 mL distilled H_2O
   b. **Prepare fresh daily**

6. Prepare reaction mix
   a. Per well:
      i. 76 µL distilled H_2O
      ii. 125 µL Tris (200 mM, pH 8.0) with Triton-X (0.2% (vol/vol) from step 1)
      iii. 25 µL DTNB (1 mM from step 3)
      iv. 7.5 µL Acetyl CoA (10 Mm from step 2)

7. Add 4 µL sample to each well

8. Add 233.5 µL reaction mix (from step 6) to each well

9. Read baseline activity at 412 nm for 3 min

10. Start reaction by adding 12.5 µL OAA (10 mM from step 5) to each well using multichannel pipette one column at a time

11. Monitor increase in absorbance at 412 nm for 3 min

To get pathlength:

When the plate is completed, save data and close off the current protocol.

1. Re-open the same protocol you just used (CS Spinazzi in Gen5 in Wohlgemuth lab) but be sure pathlength correction is ACTIVATED

2. Read the plate until you get the pathlength

To calculate activity:

1. Calculate slope (change in absorbance over time) for baseline reading and activity reading for each sample

2. Subtract baseline slope from activity slope

3. CS activity (nmol/min/mg protein) =

$$\frac{(\Delta \text{ Absorbance/min } x1000) \text{ x total volume } (0.250)}{\varepsilon\ (13.6) \text{ x pathlength (cm) x sample volume } (0.004) \text{ x total protein in sample (mg/mL)}}$$

APPENDIX B
CYTOCHROME C OXIDASE ACTIVITY PROTOCOL

Adapted from Spinazzi et al., (Spinazzi *et al*., 2012)

To prepare muscle homogenate:

1. Add 10-15 mg powdered (cryopulverized) muscle to each microvial, recording exact tissue weight

2. Add the volume of sucrose homogenization buffer with detergent required to obtain a 40-fold dilution
   a. Sucrose homogenization buffer: 20 mM Tris, 40 mM KCl, 2 mM EGTA, 250 mM sucrose, pH 7.4
   b. Dilute 1 part 5% detergent (n-Dodecyl β-D-maltoside; Sigma D4641) to 100 parts sucrose buffer
   c. Example: 10 mg muscle powder x 40 = 400 µL sucrose homogenization buffer with detergent

3. Sonicate (F60 Sonic Dismembrator, Fisher Scientific, Waltham, MA) each tube by pushing the button on the top of the probe for 1sec, 5-10 times, with the strength between 3-5.
   a. Keep on ice while sonicating
   b. Clean sonicator probe in between samples by rinsing with dH_2O

4. Centrifuge microvials for 3 min at 10,000 x *g* at 4°C

5. Collect supernatant (40-fold dilution)

6. Dilute to 80-fold (1part 40-fold+1part sucrose buffer without detergent (2a))

7. Can store 40-fold and 80-fold homogenates at -80°C until analysis

8. Use 80-fold dilution for assay

To perform assay:

1. Turn on microplate reader, check protocol (COX Spinazzi in Gen5 in Wohlgemuth lab; be sure pathlength correction is INACTIVATED), and preheat to 37°C

2. Prepare 100 mM potassium phosphate buffer (pH 7.0)
   a. Titrate 100 mM potassium phosphate dibasic with 100 mM potassium phosphate monobasic up to a pH of 7.0
   b. Can be stored at 4°C for up to 2 mo

3. Prepare 1mM reduced cytochrome *c*
    a. To make 1mM oxidized cytochrome *c* by dissolving 12.5 mg oxidized cytochrome *c* (Sigma # C7752) in 1 mL of 20 mM potassium phosphate buffer (20 mM)
    b. Reduce cytochrome *c* solution with a few grains of dithionite (pipette tip) **just before use**
    c. Vortex thoroughly (will change color from brown to orange-pink)

4. Prepare reaction mix
    a. Per well:
        i. 105 µL distilled H2O
        ii. 125 µL potassium phosphate buffer (100 mM, pH 7.0 from step 2)
        iii. 15 µL reduced cytochrome *c* (from step 3)

5. Add 270 µL of reaction mix (from step 4) to each well of a background plate
    a. Read baseline activity of background plate at 550 nm for 10 min
    b. Keep background plate in thermomixer at 37°C after baseline read

6. Add 5 µL sample to each well in separate sample plate
    a. Transfer 245 µL reaction mix from background plate to each well of sample plate using multichannel pipette one column at a time
    b. Monitor decrease in absorbance at 550 nm for 3 min

To get pathlength:

When the plate is completed, save data and close off the current protocol.

1. Re-open the same protocol you just used (COX Spinazzi in Gen5 in Wohlgemuth lab) but be sure pathlength correction is ACTIVATED

2. Read the plate until you get the pathlength

To calculate activity:

1. Calculate slope (change in absorbance over time) for baseline reading and activity reading for each sample

2. Subtract baseline slope from activity slope

3. COX activity (nmol/min/mg protein) =

$$\frac{(\Delta \text{ Absorbance/min} \times 1000) \times \text{total volume (0.250)}}{\varepsilon\ (18.5) \times \text{pathlength (cm)} \times \text{sample volume (0.005)} \times \text{total protein in sample (mg/mL)}}$$

APPENDIX C
3-OH ACYL COA DEHYDROGENASE ACTIVITY PROTOCOL

Adapted from Fong & Schulz (Fong & Schulz, 1978)

To prepare muscle homogenate:

1. Add 10-15 mg powdered (cryopulverized) muscle to each microvial, recording exact tissue weight

2. Add the volume of sucrose homogenization buffer with detergent required to obtain a 40-fold dilution
   a. Sucrose homogenization buffer: 20 mM Tris, 40 mM KCl, 2 mM EGTA, 250 mM sucrose, pH 7.4
   b. Dilute 1 part 5% detergent (n-Dodecyl β-D-maltoside; Sigma D4641) to 100 parts sucrose buffer
   c. Example: 10 mg muscle powder x 40 = 400 µL sucrose homogenization buffer with detergent

3. Sonicate (F60 Sonic Dismembrator, Fisher Scientific, Waltham, MA) each tube by pushing the button on the top of the probe for 1sec, 5-10 times, with the strength between 3-5.
   a. Keep on ice while sonicating
   b. Clean sonicator probe in between samples by rinsing with dH2O

4. Centrifuge microvials for 3 min at 10,000 x *g* at 4°C

5. Collect supernatant (40-fold dilution)

6. Dilute to 80-fold (1part 40-fold+1part sucrose buffer without detergent (2a))

7. Can store 40-fold and 80-fold homogenates at -80°C until analysis

8. Use 80-fold dilution for assay

To perform assay:

1. Turn on microplate reader, check protocol (3-HADH in Gen5 in Wohlgemuth lab; be sure pathlength correction is INACTIVATED), and preheat to 37°C before use

2. Prepare 50 mM potassium phosphate buffer (pH 7.0) with 0.06% (vol/vol) Triton X-100
   a. Titrate 50 mM potassium phosphate dibasic with 50 mM potassium phosphate monobasic up to a pH of 7.0
   b. Add Triton X-100 to a final of 0.06 % in the buffer: (60 µL/100 mL buffer)

c. Can be stored at 4°C for up to 2 mo

3. Prepare 0.9 mM Acetoacetyl coenzyme A sodium salt hydrate (SAAC)
   a. Dissolve 1.533 mg SAAC (Sigma # A1625) in 2 mL of 50 mM potassium phosphate buffer (pH 7.0)
   b. Can be stored at 4°C for up to 2 mo

4. Prepare 7.2 mM β-Nicotinamide Adenine Dinucleotide, reduced disodium salt hydrate (NADH)
   a. Dissolve 5.108 mg NADH (Sigma # N8129) in 1 mL of 50 mM potassium phosphate buffer (pH 7.0)
   b. **Prepare fresh-just before use**

5. Prepare reaction mix
   a. Per well:
      i. 250 µL potassium phosphate buffer (50 mM, pH 7.0) with 0.06% Triton X-100 (from step 2)
      ii. 5 µL NADH (7.2 mM from step 4)

6. Add 10 µL sample to each well

7. Add 255 µL reaction mix (from step 5) to each well

8. Read baseline activity at 340 nm for 2 min

9. Start reaction by adding 10 µL SAAC (0.9 mM from step 3) to each well using multichannel pipette one column at a time

10. Monitor decrease in absorbance at 340 nm for 7 min

To get pathlength:

When the plate is completed, save data and close off the current protocol.

1. Re-open the same protocol you just used (HADH in Gen5 in Wohlgemuth lab) but be sure pathlength correction is ACTIVATED

2. Read the plate until you get the pathlength

To calculate activity:

1. Calculate slope (change in absorbance over time) for baseline reading and activity reading for each sample

2. Subtract baseline slope from activity slope

3. NADH activity (nmol/min/mg protein) =

$$\frac{(\Delta \text{ Absorbance/min } x1000) \text{ x total volume } (0.275)}{\varepsilon\ (6.22) \text{ x pathlength (cm) x sample volume } (0.010) \text{ x total protein in sample (mg/mL)}}$$

APPENDIX D
MYOSIN HEAVY CHAIN ISOFORMS IDENTIFICATION PROTOCOL

** Adapted from Talmadge & Roy (Talmadge & Roy, 1993)**

Part I Gel casting

1. For separating gel, combine all reagents as shown in “TABLE 1 separating gel” column except TEMED and 10% AP, then vortex the solution and degas.

2. Add TEMED and 10% AP to the solution made in step1 and pour to the gel cassette to the mark (a black line drawn 1cm below the comb teeth). **pour the solution smoothly to prevent air bubbles**

3. Immediately overlay the solution with water. **add water slowly and evenly to prevent mixing**

4. Allow the gel to polymerize for 40 min to 1h.

5. When the gel is solid enough, remove the water and rinse the gel surface completely with d-water.

Table D-1. SDS-PAGE gel mixture

Stock solution	Separating gel (mL)	Stacking gel (mL)
100% glycerol	3.0000	1.5000
30% Acrylamide-bis (50:1)	2.6670	0.6650
Tris-HCL 1.5M (pH 8.8)	1.3300	-
Tris-HCL 0.5M (pH 6.8)	-	0.7000
1M glycine	1.0000	-
100 mM EDTA (pH 7.0)	-	0.2000
10% (w/v) SDS	0.4000	0.2000
Distilled H2O	1.4950	1.6810
TEMED	0.0050	0.0025
10% Ammonium persulfate (daily fresh)	0.1000	0.0500

6. For stacking gel, combine all reagents as shown in “Table D-1 stacking gel” column except TEMED and 10% AP, then vortex the solution and degas.

7. Before casting the stacking gel, insert a piece of filter paper to dry the area between the two glass plates above the separating gel. **do not tough the surface of the separating gel**

8. Add TEMED and 10% AP to the solution made in step 6 and pour to the gel cassette until the topof the short glass plate. **pour the solution smoothly to prevent air bubbles**

9. Insert the desired comb, making sure no air bubbles.

10. Allow the stacking gel to polymerize for 45 min.

11. Gently remove the comb and rinse the wells thoroughly with d-water or running buffer.

Part II Electrophoresis

1. Assemble the Mini-Protean 3 (follow the gel-casting manual)

2. Add “upper running buffer (100 mM Tris + 150 mM glycine + 0.1% SDS)” to the inner chamber until merging the wells

3. Take the supernatant from -20°C, and mix with Laemmli buffer

4. Heat the sample mixture for 3 min at 95 °C, then leave at RT until loading

5. Load samples to wells

6. Add “lower running buffer (50 mM Tris + 75 mM glycine + 0.05% SDS)” to the Mini Tank (outer)

7. Run electrophoresis for 18 h at 4°C (run the gel at 120 V for the first 2 h, then at 100 V for the rest 16 h)

8. Remove the gel from electrophoresis chambers and start the Coomassie blue staining

Part III Coomassie blue staining

1. After electrophoresis place gel in a plastic container and overlay with Gel Fix Solution so that gel floats easily. Agitate on an orbital shaker or rocking platform for 0.5 h

2. Remove Gel Fix Solution and verlay gel in at least 100 ml of CBB R-250 Solution and agitate on an orbital shaker or rocking platform 2 h

4. After staining, wash the gels with several changes of water

5. Place gel in at least 100 ml of Detain Solution and agitate on an orbital shaker or rocking platform until resolved blue bands and a clear background appear (~ 2 h). **Destaining must be monitored visually and adjusted accordingly**

6. Place gel in Gel Storage Solution

7. Photograph the gel or analyze the gel spectrophotometrically

8. Buffer recipes for staining
   a. GEL FIX SOLUTION:
      i. 50% Methanol, 40% dH2O, 10% Glacial acetic acid
      ii. Example: Add 250 mL methanol to 200 mL dH_2O. Slowly add 50 mL glacial acetic acid
      iii. Can be stored at RT for several mo
   b. CBB R-250 SOLUTION:
      i. 0.1% CBB R-250, 40% Methanol, 50% dH2O,10% Glacial acetic acid
      ii. Example: Dissolve CBB R-250 in 200 mL Methanol. Add 250 mL dH_2O then 50 mL glacial acetic acid
      iii. Can be stored at RT in a dark bottle for several mo
   c. DESTAIN SOLUTION
      i. 10% Methanol, 83% dH_2O,7% Glacial acetic acid
      ii. Example: Add 50 mL methanol to 415 mL dH_2O. Slowly add 35 mL glacial acetic acid
      iii. Can be stored at RT for several mo
   d. GEL STORAGE SOLUTION
      i. 95% dH_2O, 5% Glacial acetic acid
      ii. Example: Add 25 mL glacial acetic acid to 475 mL dH_2O
      iii. Can be stored at RT for several mo

APPENDIX E
PERMEABILIZED FIBERS PROTOCOL

Adapted from E. Gnaiger/Oroboros

Part I Muscle fiber preparation

1. Prepare BIOPS buffer according to Table E-1

Table E-1. BIOPS buffer, total volume = 1 L

Compounds in BIOPS	Final conc.	Stock solution	Addition to 1 L final	Source and product code
CaK_2EGTA	2.77 mM	100 mM	27.7 mL	
K_2EGTA	7.23 mM	100 mM	72.3 mL	
Na_2ATP	5.77 mM		3.141 g	Sigma A2383
$MgCl_2 \bullet 6H_2O$	6.56 mM		1.334 g	Scharlau MA0036
Taurine	20 mM		2.502 g	Sigma T0625
Na_2Phosphocreatine	15 mM		4.097 g	Sigma P7936
Imidazole	20 mM		1.362 g	Fluka 56750
DTT	0.5 mM		0.077 g	Sigma D0632
MES hydrate	50 mM		9.760 g	Sigma M8250

2. Prepare MiR05 buffer according to Table E-2

Table E-2. MiR05 buffer, total volume = 1 L

Compounds in MiR05 buffer	Final conc.	Addition to 1 L final	Source and product code
EGTA	0.5 mM	0.190 g	Sigma E4378
$MgCl_2 \bullet 6H_2O$	3 mM	0.610 g	Scharlau MA0036
Lactobionic acid	60 mM	120 Ml of 0.5 M K-lactobionate stock	Aldrich 153516
Taurine	20 mM	2.502 g	Sigma T0625
KH_2PO_4	10 mM	1.361 g	Merck 104873
HEPES	20 mM	4.770 g	Sigma H7523
D-Sucrose	110 mM	37.650 g	Sigma 84097
BSA, essenrially fatty acid free	1 g/L	1 g	Sigma A6003

3. Teasing of Muscle Fibers
   The preparation (teasing) of muscle fibers for respiration measurements should not exceed **30 min**, and **should proceed on ice**
   a. Dissect (25 mg of) muscle tissue or receive muscle biopsy specimen and place **immediately** in ice-cold BIOPS Buffer. **Muscle sample CANNOT dry out**! For muscle fiber preparation, place muscle sample in 100 cm culture dish on ice, and

position under dissecting scope

b. Trim muscle of connective tissue and cut muscle longitudinally into smaller layers (ideally there will be fiber monolayers, but this might not be feasible with biopsy samples)
c. Under a dissecting microscope, and using a pair of needle-tipped forceps (Dumont #5), separate fibers from one another to maximize the surface area of the fibers that saponin can access, leaving only small regions of contact. The passive motion of the opening forceps can be used to separate the fibers. **Teasing should not take no longer than 10-15 min**

4. Muscle fiber permeabilization
   a. To permeabilize the prepared muscle fibers, place each fiber bundle in ice-cold **BIOPS buffer containing 50 µg/ml saponin** and incubate on rotator for **30 min at 4°C** (inside fridge). Make sure that the muscle pieces are moving when tube is on the rotator
      i. Add saponin stock solution (5 mg/mL) into vial with BIOPS buffer right before adding the teased muscle fibers: 20 µL saponin stock to 2 mL BIOPS buffer
   b. To **wash** permeabilized fiber bundles, place bundle as best and complete as possible to a new tube containing ice-cold **MiR05 buffer for 10 min on rotator at 4°C** to remove saponin and any extramitochondrial components

Part II Oxygen consumption measurement

1. Adding the tissue into the chamber and getting started
   a. When the O2k is prepared, weigh 2-3 mg of fibers by carefully blotting fiber bundles on Kimwipe and putting on weigh paper in Analytical Balance. Make note of the weight
   b. Transport fibers to O2k by carrying weigh boat or weighing paper with fibers to O2k
   c. Add the weighed fibers to the chamber containing MiR05 containing 20 mM creatine
   d. Add the exact muscle weight to the “Edit Experiment” window in DatLab, choose “mg” as unit; in graph layout choose the layout for specific muscle fiber measurement
   e. As soon as the fibers are in, turn the stirrers back on and insert the stoppers, (semi-open) (using spacer)
   f. Add 10-20 mL pure O_2 gas through the stopper using special syringe and length adapted needle
   g. Watch the O_2 concentration rise (blue line) and insert the stopper completely (closing the chamber) when O_2 concentration reaches ~ 450 µM. The concentration will continue to rise to the desired ~ 500 µM
      i. Make sure that the chamber does not contain any air bubbles since this will disturb and falsify the O_2 flux signal
      ii. Do not let the O_2 concentration fall below 220-200 µM. Semi-open the chamber (use spacer) and, in case of high O2 consumption, reinject O_2 gas until O_2 concentration reaches ~ 450 µM, then close the stopper again.

2. Oxygen Flux measurements - Titration Protocol

a. Some commonly used substrates, inhibitors an uncouplers are listed in Table E-3

Table E-3. Commonly used SUIT chemicals

Substrate	Stock conc. in syringe	Final conc. in 2 mL	Titration (µL)	Storage
Pyruvate	2 M (in H_2O)	5 mM	5	Make fresh
Malate	0.8 M (in H_2O)	2 mM	5	Stored at -20 °C
Glutamate	2 M (in H_2O)	10 mM	10	Stored at -20 °C
Succinate	1 M (in H_2O)	10 mM	20	Stored at -20 °C
Cyt *c*	4 mM (in H_2O)	10 µM	5	Stored at -20 °C
ADP	0.5 M (in H_2O)	1-5 mM (2 mM)	4-20 (8)	Stored at -80 °C
Oligomycin	5 mM (EtOH)	2.5 µM	1	Stored at -20 °C
FCCP	1 mM (EtOH)	0.5 µM steps	0.5µL steps	Stored at -20 °C
Antimycin A	5 mM (EtOH)	2.5 µM	1	Stored at -20 °C

b. Titration protocol (SUIT protocol)

Table E-4. SUIT protocol used in Chapter 2

Titration substrates (final conc. in 2 mL; titration vol)	Response
Glutamate and Malate (10/2 mM; 10/5 µL)	L; LEAK; Small increase and stabilization. Wait for a 5-10 min stable flux
ADP (2.5 mM; 10 µL)	P_{CI}; Rapid increase. Wait 5-10 min after the signal stabilized.
Succinate (10 mM; 20 µL)	P_{CI+II}; Elevation above P_{CI}
Cytochrome *c* (10 µM; 5 µL)	$P_{CI+II\ c}$; No increase or small elevation of flux curve (up to ≤ 10%)
ADP and Succinate (1.25/5 mM; 5/10 µL)	Add 5 µL ADP and 10 µL Succinate to check whether ADP or Succinate was limiting
FCCP (F) (0.5 µM steps; 0.5 ul titrations)	E; ETS; Elevation above P (excess capacity) or just to P_{CI+II}
Antimycin A (2.5 µM; 1 uL)	ROX, residual (non-mitochondrial) respiration. Flux will decrease below LEAK level

Part III Post-measurement device cleaning

1. dH_2O washes (3x)
   a. Take out stoppers and rinse stopper and capillary with water several times (5x)
   b. Siphon off the media from chamber
   c. Fill with water (stirrer on) and siphon off
   d. Repeat 2 more times

2. EtOH washes (3x w/70% EtOH + 1x w/100% EtOH)
   a. Rinse stopper from outside and a capillary with 70% EtOH several times (3x)
   b. Siphon off the water from the chamber and fill with 70% EtOH, insert stopper until receptacle fills with the repeat EtOH; incubate for 5 min while stirring
   c. Repeat 2 more times
   d. Siphon off the 70% EtOH and replace with 100% EtOH, insert stopper until receptacle fills with EtOH; incubate for 15 min while stirring
   e. Proceed to (4) for storage or to (3) for continuation of experiments

3. In preparation of the next experiment: Make sure the stirrer is rotating. Remove the stopper, rinse the surface and cannula of the stopper with dH_2O. Place the stopper clean and securely (in the tube with distilled water). Rinse the chamber with distilled water three times. Then proceed with the next experimental run.

4. For storage: Fill the chamber with 70% EtOH. Insert the stopper loosely and fill 70% EtOH up to the rim of the receptacle. Place the Cover onto the stopper to minimize evaporation and leakage of EtOH. For overnight storage and chemical sterilization keep EtOH in the chamber and switch off the O2k. You can use this method for storage up to several months, with the POS in place, ready for use.

LIST OF REFERENCES

Aksenov MY, Aksenova MV, Payne RM, Smith CD, Markesbery WR, Carney JM (1997). The expression of creatine kinase isoenzymes in neocortex of patients with neurodegenerative disorders: Alzheimer's and Pick's disease. *Exp Neurol*. **146**, 458-465.

Al-Shanti N, Stewart CE (2012). Inhibitory effects of IL-6 on IGF-1 activity in skeletal myoblasts could be mediated by the activation of SOCS-3. *J Cell Biochem*. **113**, 923-933.

Alsharidah M, Lazarus NR, George TE, Agley CC, Velloso CP, Harridge SD (2013). Primary human muscle precursor cells obtained from young and old donors produce similar proliferative, differentiation and senescent profiles in culture. *Aging Cell*. **12**, 333-344.

Amara CE, Shankland EG, Jubrias SA, Marcinek DJ, Kushmerick MJ, Conley KE (2007). Mild mitochondrial uncoupling impacts cellular aging in human muscles in vivo. *Proc Natl Acad Sci U S A*. **104**, 1057-1062.

Andersen JL (2003). Muscle fibre type adaptation in the elderly human muscle. *Scand J Med Sci Sports*. **13**, 40-47.

Andersen JL, Gruschy-Knudsen T, Sandri C, Larsson L, Schiaffino S (1999). Bed rest increases the amount of mismatched fibers in human skeletal muscle. *J Appl Physiol (1985)*. **86**, 455-460.

Anderson EJ, Neufer PD (2006). Type II skeletal myofibers possess unique properties that potentiate mitochondrial H(2)O(2) generation. *Am J Physiol Cell Physiol*. **290**, C844-851.

Anton SD, Woods AJ, Ashizawa T, Barb D, Buford TW, Carter CS, Clark DJ, Cohen RA, Corbett DB, Cruz-Almeida Y, Dotson V, Ebner N, Efron PA, Fillingim RB, Foster TC, Gundermann DM, Joseph AM, Karabetian C, Leeuwenburgh C, Manini TM, Marsiske M, Mankowski RT, Mutchie HL, Perri MG, Ranka S, Rashidi P, Sandesara B, Scarpace PJ, Sibille KT, Solberg LM, Someya S, Uphold C, Wohlgemuth S, Wu SS, Pahor M (2015). Successful aging: Advancing the science of physical independence in older adults. *Ageing Res Rev*. **24**, 304-327.

Artal-Sanz M, Tavernarakis N (2009). Prohibitin couples diapause signalling to mitochondrial metabolism during ageing in C. elegans. *Nature*. **461**, 793-797.

Austin S, St-Pierre J (2012). PGC1α and mitochondrial metabolism--emerging concepts and relevance in ageing and neurodegenerative disorders. *J Cell Sci*. **125**, 4963-4971.

Baj A, Bettaccini AA, Casalone R, Sala A, Cherubino P, Toniolo AQ (2005). Culture of skeletal myoblasts from human donors aged over 40 years: dynamics of cell growth and expression of differentiation markers. *J Transl Med*. **3**, 21.

Baker JS, McCormick MC, Robergs RA (2010). Interaction among Skeletal Muscle Metabolic Energy Systems during Intense Exercise. *J Nutr Metab*. **2010**, 905612.

Balagopal P, Schimke JC, Ades P, Adey D, Nair KS (2001). Age effect on transcript levels and synthesis rate of muscle MHC and response to resistance exercise. *Am J Physiol Endocrinol Metab*. **280**, E203-208.

Barazzoni R, Short KR, Nair KS (2000). Effects of aging on mitochondrial DNA copy number and cytochrome c oxidase gene expression in rat skeletal muscle, liver, and heart. *J Biol Chem*. **275**, 3343-3347.

Barrey E, Valette JP, Jouglin M, Blouin C, Langlois B (1999). Heritability of percentage of fast myosin heavy chains in skeletal muscles and relationship with performance. *Equine Vet J Suppl*, 289-292.

Barrientos A, Casademont J, Cardellach F, Estivill X, Urbano-Marquez A, Nunes V (1997). Reduced steady-state levels of mitochondrial RNA and increased mitochondrial DNA amount in human brain with aging. *Brain Res Mol Brain Res*. **52**, 284-289.

Beal MF (2002). Oxidatively modified proteins in aging and disease. *Free Radic Biol Med*. **32**, 797-803.

Bentzinger CF, Wang YX, Rudnicki MA (2012). Building muscle: molecular regulation of myogenesis. *Cold Spring Harb Perspect Biol*. **4**.

Betros CL, McKeever KH, Kearns CF, Malinowski K (2002). Effects of ageing and training on maximal heart rate and VO2max. *Equine Vet J Suppl*, 100-105.

Biressi S, Rando TA (2010). Heterogeneity in the muscle satellite cell population. *Semin Cell Dev Biol*. **21**, 845-854.

Bockhold KJ, Rosenblatt JD, Partridge TA (1998). Aging normal and dystrophic mouse muscle: analysis of myogenicity in cultures of living single fibers. *Muscle Nerve*. **21**, 173-183.

Boffoli D, Scacco SC, Vergari R, Solarino G, Santacroce G, Papa S (1994). Decline with age of the respiratory chain activity in human skeletal muscle. *Biochim Biophys Acta*. **1226**, 73-82.

Bonawitz ND, Clayton DA, Shadel GS (2006). Initiation and beyond: multiple functions of the human mitochondrial transcription machinery. *Mol Cell*. **24**, 813-825.

Borges O, Essén-Gustavsson B (1989). Enzyme activities in type I and II muscle fibres of human skeletal muscle in relation to age and torque development. *Acta Physiol Scand*. **136**, 29-36.

Boushel R, Gnaiger E, Schjerling P, Skovbro M, Kraunsøe R, Dela F (2007). Patients with type 2 diabetes have normal mitochondrial function in skeletal muscle. *Diabetologia*. **50**, 790-796.

Brand MD (2000). Uncoupling to survive? The role of mitochondrial inefficiency in ageing. *Exp Gerontol*. **35**, 811-820.

Brooks SV, Faulkner JA (1990). Contraction-induced injury: recovery of skeletal muscles in young and old mice. *Am J Physiol*. **258**, C436-442.

Brosnahan MM, Paradis MR (2003a). Assessment of clinical characteristics, management practices, and activities of geriatric horses. *J Am Vet Med Assoc*. **223**, 99-103.

Brosnahan MM, Paradis MR (2003b). Demographic and clinical characteristics of geriatric horses: 467 cases (1989-1999). *J Am Vet Med Assoc*. **223**, 93-98.

Buford TW, Anton SD, Judge AR, Marzetti E, Wohlgemuth SE, Carter CS, Leeuwenburgh C, Pahor M, Manini TM (2010). Models of accelerated sarcopenia: critical pieces for solving the puzzle of age-related muscle atrophy. *Ageing Res Rev*. **9**, 369-383.

Buford TW, Lott DJ, Marzetti E, Wohlgemuth SE, Vandenborne K, Pahor M, Leeuwenburgh C, Manini TM (2012). Age-related differences in lower extremity tissue compartments and associations with physical function in older adults. *Exp Gerontol*. **47**, 38-44.

Call JA, Wilson RJ, Laker RC, Zhang M, Kundu M, Yan Z (2017). Ulk1-mediated autophagy plays an essential role in mitochondrial remodeling and functional regeneration of skeletal muscle. *Am J Physiol Cell Physiol*, ajpcell.00348.02016.

Capel F, Rimbert V, Lioger D, Diot A, Rousset P, Mirand PP, Boirie Y, Morio B, Mosoni L (2005). Due to reverse electron transfer, mitochondrial H2O2 release increases with age in human vastus lateralis muscle although oxidative capacity is preserved. *Mech Ageing Dev*. **126**, 505-511.

Capitanio D, Vasso M, Fania C, Moriggi M, Viganò A, Procacci P, Magnaghi V, Gelfi C (2009). Comparative proteomic profile of rat sciatic nerve and gastrocnemius muscle tissues in ageing by 2-D DIGE. *Proteomics*. **9**, 2004-2020.

Carlson BM, Faulkner JA (1989). Muscle transplantation between young and old rats: age of host determines recovery. *Am J Physiol*. **256**, C1262-1266.

Carlson ME, Conboy IM (2007). Loss of stem cell regenerative capacity within aged niches. *Aging Cell*. **6**, 371-382.

Carlson ME, Conboy MJ, Hsu M, Barchas L, Jeong J, Agrawal A, Mikels AJ, Agrawal S, Schaffer DV, Conboy IM (2009a). Relative roles of TGF-beta1 and Wnt in the systemic regulation and aging of satellite cell responses. *Aging Cell*. **8**, 676-689.

Carlson ME, Hsu M, Conboy IM (2008). Imbalance between pSmad3 and Notch induces CDK inhibitors in old muscle stem cells. *Nature*. **454**, 528-532.

Carlson ME, Suetta C, Conboy MJ, Aagaard P, Mackey A, Kjaer M, Conboy I (2009b). Molecular aging and rejuvenation of human muscle stem cells. *EMBO Mol Med*. **1**, 381-391.

Carnio S, LoVerso F, Baraibar MA, Longa E, Khan MM, Maffei M, Reischl M, Canepari M, Loefler S, Kern H, Blaauw B, Friguet B, Bottinelli R, Rudolf R, Sandri M (2014). Autophagy impairment in muscle induces neuromuscular junction degeneration and precocious aging. *Cell Rep*. **8**, 1509-1521.

Cavallini G, Donati A, Taddei M, Bergamini E (2007). Evidence for selective mitochondrial autophagy and failure in aging. *Autophagy*. **3**, 26-27.

Cerletti M, Jang YC, Finley LW, Haigis MC, Wagers AJ (2012). Short-term calorie restriction enhances skeletal muscle stem cell function. *Cell Stem Cell*. **10**, 515-519.

Chabi B, Ljubicic V, Menzies KJ, Huang JH, Saleem A, Hood DA (2008). Mitochondrial function and apoptotic susceptibility in aging skeletal muscle. *Aging Cell.* **7**, 2-12.

Chabi B, Mousson de Camaret B, Chevrollier A, Boisgard S, Stepien G (2005). Random mtDNA deletions and functional consequence in aged human skeletal muscle. *Biochem Biophys Res Commun*. **332**, 542-549.

Chakkalakal JV, Jones KM, Basson MA, Brack AS (2012). The aged niche disrupts muscle stem cell quiescence. *Nature*. **490**, 355-360.

Chargé SB, Brack AS, Hughes SM (2002). Aging-related satellite cell differentiation defect occurs prematurely after Ski-induced muscle hypertrophy. *Am J Physiol Cell Physiol*. **283**, C1228-1241.

Chen H, Chomyn A, Chan DC (2005). Disruption of fusion results in mitochondrial heterogeneity and dysfunction. *J Biol Chem*. **280**, 26185-26192.

Chen H, Vermulst M, Wang YE, Chomyn A, Prolla TA, McCaffery JM, Chan DC (2010). Mitochondrial fusion is required for mtDNA stability in skeletal muscle and tolerance of mtDNA mutations. *Cell*. **141**, 280-289.

Ciciliot S, Rossi AC, Dyar KA, Blaauw B, Schiaffino S (2013). Muscle type and fiber type specificity in muscle wasting. *Int J Biochem Cell Biol*. **45**, 2191-2199.

Clark IE, Dodson MW, Jiang C, Cao JH, Huh JR, Seol JH, Yoo SJ, Hay BA, Guo M (2006). Drosophila pink1 is required for mitochondrial function and interacts genetically with parkin. *Nature*. **441**, 1162-1166.

Clay Montier LL, Deng JJ, Bai Y (2009). Number matters: control of mammalian mitochondrial DNA copy number. *J Genet Genomics*. **36**, 125-131.

Coggan AR, Spina RJ, King DS, Rogers MA, Brown M, Nemeth PM, Holloszy JO (1992). Histochemical and enzymatic comparison of the gastrocnemius muscle of young and elderly men and women. *J Gerontol*. **47**, B71-76.

Collins CA, Zammit PS, Ruiz AP, Morgan JE, Partridge TA (2007). A population of myogenic stem cells that survives skeletal muscle aging. *Stem Cells*. **25**, 885-894.

Conboy IM, Conboy MJ, Smythe GM, Rando TA (2003). Notch-mediated restoration of regenerative potential to aged muscle. *Science*. **302**, 1575-1577.

Conboy IM, Conboy MJ, Wagers AJ, Girma ER, Weissman IL, Rando TA (2005). Rejuvenation of aged progenitor cells by exposure to a young systemic environment. *Nature*. **433**, 760-764.

Conboy IM, Rando TA (2002). The regulation of Notch signaling controls satellite cell activation and cell fate determination in postnatal myogenesis. *Dev Cell*. **3**, 397-409.

Conboy IM, Rando TA (2005). Aging, stem cells and tissue regeneration: lessons from muscle. *Cell Cycle*. **4**, 407-410.

Conley KE, Esselman PC, Jubrias SA, Cress ME, Inglin B, Mogadam C, Schoene RB (2000). Ageing, muscle properties and maximal O_2 uptake rate in humans. *J Physiol*. **526 Pt 1**, 211-217.

Cooper JM, Mann VM, Schapira AH (1992). Analyses of mitochondrial respiratory chain function and mitochondrial DNA deletion in human skeletal muscle: effect of ageing. *J Neurol Sci*. **113**, 91-98.

Crane JD, Devries MC, Safdar A, Hamadeh MJ, Tarnopolsky MA (2010). The effect of aging on human skeletal muscle mitochondrial and intramyocellular lipid ultrastructure. *J Gerontol A Biol Sci Med Sci*. **65**, 119-128.

Crescenzo R, Bianco F, Mazzoli A, Giacco A, Liverini G, Iossa S (2015). Skeletal muscle mitochondrial energetic efficiency and aging. *Int J Mol Sci*. **16**, 10674-10685.

Cruz-Jentoft AJ, Landi F, Topinková E, Michel JP (2010). Understanding sarcopenia as a geriatric syndrome. *Curr Opin Clin Nutr Metab Care*. **13**, 1-7.

Cuervo AM, Bergamini E, Brunk UT, Dröge W, Ffrench M, Terman A (2005). Autophagy and aging: the importance of maintaining “clean” cells. *Autophagy*. **1**, 131-140.

Cuervo AM, Dice JF (1998). How do intracellular proteolytic systems change with age? *Front Biosci*. **3**, d25-43.

Cui J, Shi S, Sun X, Cai G, Cui S, Hong Q, Chen X, Bai XY (2013). Mitochondrial autophagy involving renal injury and aging is modulated by caloric intake in aged rat kidneys. *PLoS One*. **8**, e69720.

D'Antona G, Pellegrino MA, Adami R, Rossi R, Carlizzi CN, Canepari M, Saltin B, Bottinelli R (2003). The effect of ageing and immobilization on structure and function of human skeletal muscle fibres. *J Physiol*. **552**, 499-511.

D'Aurelio M, Pallotti F, Barrientos A, Gajewski CD, Kwong JQ, Bruno C, Beal MF, Manfredi G (2001). In vivo regulation of oxidative phosphorylation in cells harboring a stop-codon mutation in mitochondrial DNA-encoded cytochrome c oxidase subunit I. *J Biol Chem*. **276**, 46925-46932.

Day K, Shefer G, Shearer A, Yablonka-Reuveni Z (2010). The depletion of skeletal muscle satellite cells with age is concomitant with reduced capacity of single progenitors to produce reserve progeny. *Dev Biol*. **340**, 330-343.

Delmonico MJ, Harris TB, Visser M, Park SW, Conroy MB, Velasquez-Mieyer P, Boudreau R, Manini TM, Nevitt M, Newman AB, Goodpaster BH, Health Ai, and Body (2009). Longitudinal study of muscle strength, quality, and adipose tissue infiltration. *Am J Clin Nutr*. **90**, 1579-1585.

Derbré F, Gomez-Cabrera MC, Nascimento AL, Sanchis-Gomar F, Martinez-Bello VE, Tresguerres JA, Fuentes T, Gratas-Delamarche A, Monsalve M, Viña J (2012). Age associated low mitochondrial biogenesis may be explained by lack of response of PGC-1α to exercise training. *Age (Dordr)*. **34**, 669-679.

Ding WX, Yin XM (2012). Mitophagy: mechanisms, pathophysiological roles, and analysis. *Biol Chem*. **393**, 547-564.

Donati A, Cavallini G, Paradiso C, Vittorini S, Pollera M, Gori Z, Bergamini E (2001). Age-related changes in the regulation of autophagic proteolysis in rat isolated hepatocytes. *J Gerontol A Biol Sci Med Sci*. **56**, B288-293.

Duguez S, Féasson L, Denis C, Freyssenet D (2002). Mitochondrial biogenesis during skeletal muscle regeneration. *Am J Physiol Endocrinol Metab*. **282**, E802-809.

Echtay KS, Pakay JL, Esteves TC, Brand MD (2005). Hydroxynonenal and uncoupling proteins: a model for protection against oxidative damage. *Biofactors*. **24**, 119-130.

Echtay KS, Roussel D, St-Pierre J, Jekabsons MB, Cadenas S, Stuart JA, Harper JA, Roebuck SJ, Morrison A, Pickering S, Clapham JC, Brand MD (2002). Superoxide activates mitochondrial uncoupling proteins. *Nature*. **415**, 96-99.

Edwall D, Schalling M, Jennische E, Norstedt G (1989). Induction of insulin-like growth factor I messenger ribonucleic acid during regeneration of rat skeletal muscle. *Endocrinology*. **124**, 820-825.

Eskelinen EL, Schmidt CK, Neu S, Willenborg M, Fuertes G, Salvador N, Tanaka Y, Lüllmann -Rauch R, Hartmann D, Heeren J, von Figura K, Knecht E, Saftig P (2004). Disturbed cholesterol traffic but normal proteolytic function in LAMP-1/LAMP-2 double-deficient fibroblasts. *Mol Biol Cell*. **15**, 3132-3145.

Essén B, Lindholm A, Thornton J (1980). Histochemical properties of muscle fibres types and enzyme activities in skeletal muscles of Standardbred trotters of different ages. *Equine Vet J*. **12**, 175-180.

Fannin SW, Lesnefsky EJ, Slabe TJ, Hassan MO, Hoppel CL (1999). Aging selectively decreases oxidative capacity in rat heart interfibrillar mitochondria. *Arch Biochem Biophys*. **372**, 399-407.

Fell J, Williams D (2008). The effect of aging on skeletal-muscle recovery from exercise: possible implications for aging athletes. *J Aging Phys Act*. **16**, 97-115.

Fiacco E, Castagnetti F, Bianconi V, Madaro L, De Bardi M, Nazio F, D'Amico A, Bertini E, Cecconi F, Puri PL, Latella L (2016). Autophagy regulates satellite cell ability to regenerate normal and dystrophic muscles. *Cell Death Differ*. **23**, 1839-1849.

Finkel T, Holbrook NJ (2000). Oxidants, oxidative stress and the biology of ageing. *Nature*. **408**, 239-247.

Fisher RP, Topper JN, Clayton DA (1987). Promoter selection in human mitochondria involves binding of a transcription factor to orientation-independent upstream regulatory elements. *Cell*. **50**, 247-258.

Flores I, Blasco MA (2010). The role of telomeres and telomerase in stem cell aging. *FEBS Lett*. **584**, 3826-3830.

Flück M (2006). Functional, structural and molecular plasticity of mammalian skeletal muscle in response to exercise stimuli. *J Exp Biol*. **209**, 2239-2248.

Fong JC, Schulz H (1978). On the rate-determining step of fatty acid oxidation in heart. Inhibition of fatty acid oxidation by 4-pentenoic acid. *J Biol Chem*. **253**, 6917-6922.

Frontera WR, Suh D, Krivickas LS, Hughes VA, Goldstein R, Roubenoff R (2000). Skeletal muscle fiber quality in older men and women. *Am J Physiol Cell Physiol*. **279**, C611-618.

Fry CS, Lee JD, Mula J, Kirby TJ, Jackson JR, Liu F, Yang L, Mendias CL, Dupont-Versteegden EE, McCarthy JJ, Peterson CA (2015). Inducible depletion of satellite cells in adult, sedentary mice impairs muscle regenerative capacity without affecting sarcopenia. *Nat Med*. **21**, 76-80.

Fu M, St-Pierre P, Shankar J, Wang PT, Joshi B, Nabi IR (2013). Regulation of mitophagy by the Gp78 E3 ubiquitin ligase. *Mol Biol Cell*. **24**, 1153-1162.

Fulle S, Di Donna S, Puglielli C, Pietrangelo T, Beccafico S, Bellomo R, Protasi F, Fanò G (2005). Age-dependent imbalance of the antioxidative system in human satellite cells. *Exp Gerontol*. **40**, 189-197.

Gadaleta MN, Rainaldi G, Lezza AM, Milella F, Fracasso F, Cantatore P (1992). Mitochondrial DNA copy number and mitochondrial DNA deletion in adult and senescent rats. *Mutat Res*. **275**, 181-193.

Gannon J, Doran P, Kirwan A, Ohlendieck K (2009). Drastic increase of myosin light chain MLC-2 in senescent skeletal muscle indicates fast-to-slow fibre transition in sarcopenia of old age. *Eur J Cell Biol*. **88**, 685-700.

García-Prat L, Martínez-Vicente M, Perdiguero E, Ortet L, Rodríguez-Ubreva J, Rebollo E, Ruiz-Bonilla V, Gutarra S, Ballestar E, Serrano AL, Sandri M, Muñoz-Cánoves P (2016). Autophagy maintains stemness by preventing senescence. *Nature*. **529**, 37-42.

García-Prat L, Sousa-Victor P, Muñoz-Cánoves P (2013). Functional dysregulation of stem cells during aging: a focus on skeletal muscle stem cells. *FEBS J*. **280**, 4051-4062.

Garnier A, Fortin D, Deloménie C, Momken I, Veksler V, Ventura-Clapier R (2003). Depressed mitochondrial transcription factors and oxidative capacity in rat failing cardiac and skeletal muscles. *J Physiol*. 551, 491-501.

Gautier CA, Kitada T, Shen J (2008). Loss of PINK1 causes mitochondrial functional defects and increased sensitivity to oxidative stress. *Proc Natl Acad Sci U S A*. **105**, 11364-11369.

Gegg ME, Cooper JM, Chau KY, Rojo M, Schapira AH, Taanman JW (2010). Mitofusin 1 and mitofusin 2 are ubiquitinated in a PINK1/parkin-dependent manner upon induction of mitophagy. *Hum Mol Genet*. **19**, 4861-4870.

Gelfi C, Vasso M, Cerretelli P (2011). Diversity of human skeletal muscle in health and disease: contribution of proteomics. *J Proteomics*. **74**, 774-795.

Gelfi C, Vigano A, Ripamonti M, Pontoglio A, Begum S, Pellegrino MA, Grassi B, Bottinelli R, Wait R, Cerretelli P (2006). The human muscle proteome in aging. *J Proteome Res*. **5**, 1344-1353.

Gibson MC, Schultz E (1982). The distribution of satellite cells and their relationship to specific fiber types in soleus and extensor digitorum longus muscles. *Anat Rec*. **202**, 329-337.

Gnaiger E, Lassnig B, Kuznetsov A, Rieger G, Margreiter R (1998). Mitochondrial oxygen affinity, respiratory flux control and excess capacity of cytochrome c oxidase. *J Exp Biol*. **201**, 1129-1139.

Gollnick PD, Armstrong RB, Saubert CW, Piehl K, Saltin B (1972). Enzyme activity and fiber composition in skeletal muscle of untrained and trained men. *J Appl Physiol*. **33**, 312-319.

Goodpaster BH, Park SW, Harris TB, Kritchevsky SB, Nevitt M, Schwartz AV, Simonsick EM, Tylavsky FA, Visser M, Newman AB (2006). The loss of skeletal muscle strength, mass, and quality in older adults: the health, aging and body composition study. *J Gerontol A Biol Sci Med Sci*. **61**, 1059-1064.

Gopinath SD, Rando TA (2008). Stem cell review series: aging of the skeletal muscle stem cell niche. *Aging Cell*. **7**, 590-598.

Greco M, Villani G, Mazzucchelli F, Bresolin N, Papa S, Attardi G (2003). Marked aging-related decline in efficiency of oxidative phosphorylation in human skin fibroblasts. *FASEB J*. **17**, 1706-1708.

Green DR, Galluzzi L, Kroemer G (2011). Mitochondria and the autophagy-inflammation-cell death axis in organismal aging. *Science*. **333**, 1109-1112.

Grimby G, Danneskiold-Samsøe B, Hvid K, Saltin B (1982). Morphology and enzymatic capacity in arm and leg muscles in 78-81year old men and women. *Acta Physiol Scand*. **115**, 125-134.

Grossman LI, Lomax MI (1997). Nuclear genes for cytochrome c oxidase. *Biochim Biophys Acta*. **1352**, 174-192.

Grounds MD (1998). Age-associated changes in the response of skeletal muscle cells to exercise and regeneration. *Ann N Y Acad Sci*. **854**, 78-91.

Gueugneau M, Coudy-Gandilhon C, Théron L, Meunier B, Barboiron C, Combaret L, Taillandier D, Polge C, Attaix D, Picard B, Verney J, Roche F, Féasson L, Barthélémy JC, Béchet D (2015). Skeletal muscle lipid content and oxidative activity in relation to muscle fiber type in aging and metabolic syndrome. *J Gerontol A Biol Sci Med Sci*. **70**, 566-576.

Guillet C, Prod'homme M, Balage M, Gachon P, Giraudet C, Morin L, Grizard J, Boirie Y (2004). Impaired anabolic response of muscle protein synthesis is associated with S6K1 dysregulation in elderly humans. *FASEB J*. **18**, 1586-1587.

Gutmann E, Hanzlíková V (1966). Motor unit in old age. *Nature*. **209**, 921-922.

Hartmann N, Reichwald K, Wittig I, Dröse S, Schmeisser S, Lück C, Hahn C, Graf M, Gausmann U, Terzibasi E, Cellerino A, Ristow M, Brandt U, Platzer M, Englert C (2011). Mitochondrial DNA copy number and function decrease with age in the short-lived fish Nothobranchius furzeri. *Aging Cell*. **10**, 824-831.

Hasten DL, Pak-Loduca J, Obert KA, Yarasheski KE (2000). Resistance exercise acutely increases MHC and mixed muscle protein synthesis rates in 78-84 and 23-32 yr olds. *Am J Physiol Endocrinol Metab*. **278**, E620-626.

Hawke TJ, Garry DJ (2001). Myogenic satellite cells: physiology to molecular biology. *J Appl Physiol (1985)*. **91**, 534-551.

He C, Bassik MC, Moresi V, Sun K, Wei Y, Zou Z, An Z, Loh J, Fisher J, Sun Q, Korsmeyer S, Packer M, May HI, Hill JA, Virgin HW, Gilpin C, Xiao G, Bassel-Duby R, Scherer PE, Levine B (2012). Exercise-induced BCL2-regulated autophagy is required for muscle glucose homeostasis. *Nature*. **481**, 511-515.

He L, Chinnery PF, Durham SE, Blakely EL, Wardell TM, Borthwick GM, Taylor RW, Turnbull DM (2002). Detection and quantification of mitochondrial DNA deletions in individual cells by real-time PCR. *Nucleic Acids Res*. **30**, e68.

Hebert SL, Marquet-de Rougé P, Lanza IR, McCrady-Spitzer SK, Levine JA, Middha S, Carter RE, Klaus KA, Therneau TM, Highsmith EW, Nair KS (2015). Mitochondrial Aging and Physical Decline: Insights From Three Generations of Women. *J Gerontol A Biol Sci Med Sci*. **70**, 1409-1417.

Henneke DR, Potter GD, Kreider JL, Yeates BF (1983). Relationship between condition score, physical measurements and body fat percentage in mares. *Equine Vet J*. **15**, 371-372.

Hepple RT (2014). Mitochondrial involvement and impact in aging skeletal muscle. *Front Aging Neurosci*. **6**, 211.

Herndon LA, Schmeissner PJ, Dudaronek JM, Brown PA, Listner KM, Sakano Y, Paupard MC, Hall DH, Driscoll M (2002). Stochastic and genetic factors influence tissue-specific decline in ageing C. elegans. *Nature*. **419**, 808-814.

Herzberg NH, Zwart R, Wolterman RA, Ruiter JP, Wanders RJ, Bolhuis PA, van den Bogert C (1993). Differentiation and proliferation of respiration-deficient human myoblasts. *Biochim Biophys Acta*. **1181**, 63-67.

Hey-Mogensen M, Jeppesen J, Madsen K, Kiens B, Franch J (2012). Obesity augments the age-induced increase in mitochondrial capacity for H2O2 release in Zucker fatty rats. *Acta Physiol (Oxf)*. **204**, 354-361.

Hood DA, Irrcher I, Ljubicic V, Joseph AM (2006). Coordination of metabolic plasticity in skeletal muscle. *J Exp Biol*. **209**, 2265-2275.

Hoppeler H, Hudlicka O, Uhlmann E (1987). Relationship between mitochondria and oxygen consumption in isolated cat muscles. *J Physiol*. **385**, 661-675.

Houmard JA, Weidner ML, Gavigan KE, Tyndall GL, Hickey MS, Alshami A (1998). Fiber type and citrate synthase activity in the human gastrocnemius and vastus lateralis with aging. *J Appl Physiol (1985)*. **85**, 1337-1341.

Hunter GR, Newcomer BR, Weinsier RL, Karapondo DL, Larson-Meyer DE, Joanisse DR, Bamman MM (2002). Age is independently related to muscle metabolic capacity in premenopausal women. *J Appl Physiol (1985)*. **93**, 70-76.

Hüttemann M, Kadenbach B, Grossman LI (2001). Mammalian subunit IV isoforms of cytochrome c oxidase. *Gene*. **267**, 111-123.

Ikemoto-Uezumi M, Uezumi A, Tsuchida K, Fukada S, Yamamoto H, Yamamoto N, Shiomi K, Hashimoto N (2015). Pro-Insulin-Like Growth Factor-II Ameliorates Age-Related Inefficient Regenerative Response by Orchestrating Self-Reinforcement Mechanism of Muscle Regeneration. *Stem Cells*. **33**, 2456-2468.

Jackman MR, Willis WT (1996). Characteristics of mitochondria isolated from type I and type IIb skeletal muscle. *Am J Physiol*. **270**, C673-678.

Jacobs RA, Díaz V, Meinild AK, Gassmann M, Lundby C (2013a). The C57Bl/6 mouse serves as a suitable model of human skeletal muscle mitochondrial function. *Exp Physiol*. **98**, 908-921.

Jacobs RA, Díaz V, Soldini L, Haider T, Thomassen M, Nordsborg NB, Gassmann M, Lundby C (2013b). Fast-twitch glycolytic skeletal muscle is predisposed to age-induced impairments in mitochondrial function. *J Gerontol A Biol Sci Med Sci*. **68**, 1010-1022.

Jacobs RA, Lundby C (2013). Mitochondria express enhanced quality as well as quantity in association with aerobic fitness across recreationally active individuals up to elite athletes. *J Appl Physiol (1985)*. **114**, 344-350.

Jang YC, Sinha M, Cerletti M, Dall'Osso C, Wagers AJ (2011). Skeletal muscle stem cells: effects of aging and metabolism on muscle regenerative function. *Cold Spring Harb Symp Quant Biol*. **76**, 101-111.

Jang YC, Van Remmen H (2009). The mitochondrial theory of aging: insight from transgenic and knockout mouse models. *Exp Gerontol*. **44**, 256-260.

Janssen I, Heymsfield SB, Wang ZM, Ross R (2000). Skeletal muscle mass and distribution in 468 men and women aged 18-88 yr. *J Appl Physiol (1985)*. **89**, 81-88.

Jaschinski F, Schuler M, Peuker H, Pette D (1998). Changes in myosin heavy chain mRNA and protein isoforms of rat muscle during forced contractile activity. *Am J Physiol*. **274**, C365-370.

Johnson DT, Harris RA, French S, Blair PV, You J, Bemis KG, Wang M, Balaban RS (2007). Tissue heterogeneity of the mammalian mitochondrial proteome. *Am J Physiol Cell Physiol*. **292**, C689-697.

Johnson ML, Lalia AZ, Dasari S, Pallauf M, Fitch M, Hellerstein MK, Lanza IR (2015). Eicosapentaenoic acid but not docosahexaenoic acid restores skeletal muscle mitochondrial oxidative capacity in old mice. *Aging Cell*. **14**, 734-743.

Johnson ML, Robinson MM, Nair KS (2013). Skeletal muscle aging and the mitochondrion. *Trends Endocrinol Metab*. **24**, 247-256.

Jones NC, Tyner KJ, Nibarger L, Stanley HM, Cornelison DD, Fedorov YV, Olwin BB (2005). The p38alpha/beta MAPK functions as a molecular switch to activate the quiescent satellite cell. *J Cell Biol*. **169**, 105-116.

Joseph AM, Adhihetty PJ, Buford TW, Wohlgemuth SE, Lees HA, Nguyen LM, Aranda JM, Sandesara BD, Pahor M, Manini TM, Marzetti E, Leeuwenburgh C (2012). The impact of aging on mitochondrial function and biogenesis pathways in skeletal muscle of sedentary high- and low-functioning elderly individuals. *Aging Cell*. **11**, 801-809.

Joseph AM, Adhihetty PJ, Wawrzyniak NR, Wohlgemuth SE, Picca A, Kujoth GC, Prolla TA, Leeuwenburgh C (2013). Dysregulation of mitochondrial quality control processes contribute to sarcopenia in a mouse model of premature aging. *PLoS One*. **8**, e69327.

Jovaisaite V, Auwerx J (2015). The mitochondrial unfolded protein response—synchronizing genomes. *Curr Opin Cell Biol*. **33**, 74-81.

Kaasik P, Umnova M, Pehme A, Alev K, Aru M, Selart A, Seene T (2007). Ageing and dexamethasone associated sarcopenia: peculiarities of regeneration. *J Steroid Biochem Mol Biol*. **105**, 85-90.

Kaczor JJ, Ziolkowski W, Antosiewicz J, Hac S, Tarnopolsky MA, Popinigis J (2006). The effect of aging on anaerobic and aerobic enzyme activities in human skeletal muscle. *J Gerontol A Biol Sci Med Sci*. **61**, 339-344.

Kadi F, Ponsot E (2010). The biology of satellite cells and telomeres in human skeletal muscle: effects of aging and physical activity. *Scand J Med Sci Sports*. **20**, 39-48.

Kaeberlein M (2010). Lessons on longevity from budding yeast. *Nature*. **464**, 513-519.

Kassar-Duchossoy L, Gayraud-Morel B, Gomès D, Rocancourt D, Buckingham M, Shinin V, Tajbakhsh S (2004). Mrf4 determines skeletal muscle identity in Myf5: Myod double-mutant mice. *Nature*. **431**, 466-471.

Kassar-Duchossoy L, Giacone E, Gayraud-Morel B, Jory A, Gomès D, Tajbakhsh S (2005). Pax3/Pax7 mark a novel population of primitive myogenic cells during development. *Genes Dev*. **19**, 1426-1431.

Kim I, Rodriguez-Enriquez S, Lemasters JJ (2007). Selective degradation of mitochondria by mitophagy. *Arch Biochem Biophys*. **462**, 245-253.

Kim JS, Hinchcliff KW, Yamaguchi M, Beard LA, Markert CD, Devor ST (2005). Age-related changes in metabolic properties of equine skeletal muscle associated with muscle plasticity. *Vet J*. **169**, 397-403.

Klitgaard H, Mantoni M, Schiaffino S, Ausoni S, Gorza L, Laurent-Winter C, Schnohr P, Saltin B (1990). Function, morphology and protein expression of ageing skeletal muscle: a cross-sectional study of elderly men with different training backgrounds. *Acta Physiol Scand*. **140**, 41-54.

Knapp JR, Davie JK, Myer A, Meadows E, Olson EN, Klein WH (2006). Loss of myogenin in postnatal life leads to normal skeletal muscle but reduced body size. *Development*. **133**, 601-610.

Köchl R, Hu XW, Chan EY, Tooze SA (2006). Microtubules facilitate autophagosome formation and fusion of autophagosomes with endosomes. *Traffic*. **7**, 129-145.

Koltai E, Hart N, Taylor AW, Goto S, Ngo JK, Davies KJ, Radak Z (2012). Age-associated declines in mitochondrial biogenesis and protein quality control factors are minimized by exercise training. *Am J Physiol Regul Integr Comp Physiol*. **303**, R127-134.

Komatsu M, Waguri S, Koike M, Sou YS, Ueno T, Hara T, Mizushima N, Iwata J, Ezaki J, Murata S, Hamazaki J, Nishito Y, Iemura S, Natsume T, Yanagawa T, Uwayama J, Warabi E, Yoshida H, Ishii T, Kobayashi A, Yamamoto M, Yue Z, Uchiyama Y, Kominami E, Tanaka K (2007). Homeostatic levels of p62 control cytoplasmic inclusion body formation in autophagy-deficient mice. *Cell*. **131**, 1149-1163.

Korohoda W, Pietrzkowski Z, Reiss K (1993). Chloramphenicol, an inhibitor of mitochondrial protein synthesis, inhibits myoblast fusion and myotube differentiation. *Folia Histochem Cytobiol*. **31**, 9-13.

Kostek MC, Delmonico MJ (2011). Age-related changes in adult muscle morphology. *Curr Aging Sci*. **4**, 221-233.

Kuang S, Chargé SB, Seale P, Huh M, Rudnicki MA (2006). Distinct roles for Pax7 and Pax3 in adult regenerative myogenesis. *J Cell Biol*. **172**, 103-113.

Kuang S, Gillespie MA, Rudnicki MA (2008). Niche regulation of muscle satellite cell self-renewal and differentiation. *Cell Stem Cell*. **2**, 22-31.

Kuilman T, Michaloglou C, Mooi WJ, Peeper DS (2010). The essence of senescence. *Genes Dev*. **24**, 2463-2479.

Kujoth GC, Hiona A, Pugh TD, Someya S, Panzer K, Wohlgemuth SE, Hofer T, Seo AY, Sullivan R, Jobling WA, Morrow JD, Van Remmen H, Sedivy JM, Yamasoba T, Tanokura M, Weindruch R, Leeuwenburgh C, Prolla TA (2005). Mitochondrial DNA mutations, oxidative stress, and apoptosis in mammalian aging. *Science*. **309**, 481-484.

Kumar V, Selby A, Rankin D, Patel R, Atherton P, Hildebrandt W, Williams J, Smith K, Seynnes O, Hiscock N, Rennie MJ (2009). Age-related differences in the dose-response relationship of muscle protein synthesis to resistance exercise in young and old men. *J Physiol*. **587**, 211-217.

Kunz WS (2003). Different metabolic properties of mitochondrial oxidative phosphorylation in different cell types--important implications for mitochondrial cytopathies. *Exp Physiol*. **88**, 149-154.

Kunz WS, Kudin A, Vielhaber S, Elger CE, Attardi G, Villani G (2000). Flux control of cytochrome c oxidase in human skeletal muscle. *J Biol Chem*. **275**, 27741-27745.

Kurek JB, Nouri S, Kannourakis G, Murphy M, Austin L (1996). Leukemia inhibitory factor and interleukin-6 are produced by diseased and regenerating skeletal muscle. *Muscle Nerve*. **19**, 1291-1301.

Kuznetsov AV, Mayboroda O, Kunz D, Winkler K, Schubert W, Kunz WS (1998). Functional imaging of mitochondria in saponin-permeabilized mice muscle fibers. *J Cell Biol*. **140**, 1091-1099.

Kuznetsov AV, Veksler V, Gellerich FN, Saks V, Margreiter R, Kunz WS (2008). Analysis of mitochondrial function in situ in permeabilized muscle fibers, tissues and cells. *Nat Protoc*. **3**, 965-976.

Kwong LK, Sohal RS (2000). Age-related changes in activities of mitochondrial electron transport complexes in various tissues of the mouse. *Arch Biochem Biophys*. **373**, 16-22.

Lansdorp PM (2007). Immortal strands? Give me a break. *Cell*. **129**, 1244-1247.

Lanza IR, Befroy DE, Kent-Braun JA (2005). Age-related changes in ATP-producing pathways in human skeletal muscle in vivo. *J Appl Physiol (1985)*. **99**, 1736-1744.

Lanza IR, Short DK, Short KR, Raghavakaimal S, Basu R, Joyner MJ, McConnell JP, Nair KS (2008). Endurance exercise as a countermeasure for aging. *Diabetes*. **57**, 2933-2942.

Larsen S, Nielsen J, Hansen CN, Nielsen LB, Wibrand F, Stride N, Schroder HD, Boushel R, Helge JW, Dela F, Hey-Mogensen M (2012). Biomarkers of mitochondrial content in skeletal muscle of healthy young human subjects. *J Physiol*. **590**, 3349-3360.

Larsson L, Ansved T (1995). Effects of ageing on the motor unit. *Prog Neurobiol*. **45**, 397-458.

Larsson L, Edström L (1986). Effects of age on enzyme-histochemical fibre spectra and contractile properties of fast- and slow-twitch skeletal muscles in the rat. *J Neurol Sci*. **76**, 69-89.

Larsson L, Karlsson J (1978). Isometric and dynamic endurance as a function of age and skeletal muscle characteristics. *Acta Physiol Scand*. **104**, 129-136.

Larsson L, Sjödin B, Karlsson J (1978). Histochemical and biochemical changes in human skeletal muscle with age in sedentary males, age 22--65 years. *Acta Physiol Scand*. **103**, 31-39.

Lavasani M, Robinson AR, Lu A, Song M, Feduska JM, Ahani B, Tilstra JS, Feldman CH, Robbins PD, Niedernhofer LJ, Huard J (2012). Muscle-derived stem/progenitor cell dysfunction limits healthspan and lifespan in a murine progeria model. *Nat Commun*. **3**, 608.

LaVigne EK, Jones AK, Londoño AS, Schauer AS, Patterson DF, Nadeau JA, Reed SA (2015). Muscle growth in young horses: Effects of age, cytokines, and growth factors. *J Anim Sci*. **93**, 5672-5680.

Leary SC, Battersby BJ, Hansford RG, Moyes CD (1998). Interactions between bioenergetics and mitochondrial biogenesis. *Biochim Biophys Acta*. **1365**, 522-530.

Lee CK, Klopp RG, Weindruch R, Prolla TA (1999). Gene expression profile of aging and its retardation by caloric restriction. *Science*. **285**, 1390-1393.

Lehnhard RA, McKeever KH, Kearns CF, Beekley MD (2004). Myosin heavy chain profiles and body composition are different in old versus young Standardbred mares. *Vet J*. **167**, 59-66.

Leisson K, Jaakma U, Seene T (2008). Adaptation of equine locomotor muscle fiber types to endurance and intensive high speed training. *J Equine Vet Sci*. **28**, 395-401.

Lexell J, Downham D, Sjöström M (1986). Distribution of different fibre types in human skeletal muscles. Fibre type arrangement in m. vastus lateralis from three groups of healthy men between 15 and 83 years. *J Neurol Sci*. **72**, 211-222.

Lexell J, Taylor CC, Sjöström M (1988). What is the cause of the ageing atrophy? Total number, size and proportion of different fiber types studied in whole vastus lateralis muscle from 15- to 83-year-old men. *J Neurol Sci*. **84**, 275-294.

Lezza AM, Boffoli D, Scacco S, Cantatore P, Gadaleta MN (1994). Correlation between mitochondrial DNA 4977-bp deletion and respiratory chain enzyme activities in aging human skeletal muscles. *Biochem Biophys Res Commun*. **205**, 772-779.

Li C, White SH, Warren LK, Wohlgemuth SE (2016). Effects of aging on mitochondrial function in skeletal muscle of American American Quarter Horses. *J Appl Physiol (1985)*. **121**, 299-311.

Lin J, Wu H, Tarr PT, Zhang CY, Wu Z, Boss O, Michael F, Puigserver P, Isotani E, Olson EN, Lowell BB, Bassel-Duby R, Spiegelman BM (2002).Transcriptional co-activator PGC-1 alpha drives the formation of slow-twitch muscle fibres. *Nature*, 418, 797-801.

Linnane AW, Marzuki S, Ozawa T, Tanaka M (1989). Mitochondrial DNA mutations as an important contributor to ageing and degenerative diseases. *Lancet*. **1**, 642-645.

Liu Y, Fiskum G, Schubert D (2002). Generation of reactive oxygen species by the mitochondrial electron transport chain. *J Neurochem*. **80**, 780-787.

Lombardi A, Silvestri E, Cioffi F, Senese R, Lanni A, Goglia F, de Lange P, Moreno M (2009). Defining the transcriptomic and proteomic profiles of rat ageing skeletal muscle by the use of a cDNA array, 2D- and Blue native-PAGE approach. *J Proteomics*. **72**, 708-721.

Lopez-Rivero JL, Morales-Lopez JL, Galisteo AM, Aguera E (1991). Muscle fibre type composition in untrained and endurance-trained Andalusian and Arab horses. *Equine Vet J*. **23**, 91-93.

Lowe DA, Surek JT, Thomas DD, Thompson LV (2001). Electron paramagnetic resonance reveals age-related myosin structural changes in rat skeletal muscle fibers. *Am J Physiol Cell Physiol*. **280**, C540-547.

Luce K, Weil AC, Osiewacz HD (2010). Mitochondrial protein quality control systems in aging and disease. *Adv Exp Med Biol*. **694**, 108-125.

López-Lluch G, Hunt N, Jones B, Zhu M, Jamieson H, Hilmer S, Cascajo MV, Allard J, Ingram DK, Navas P, de Cabo R (2006). Calorie restriction induces mitochondrial biogenesis and bioenergetic efficiency. *Proc Natl Acad Sci U S A*. **103**, 1768-1773.

López-Otín C, Blasco MA, Partridge L, Serrano M, Kroemer G (2013). The hallmarks of aging. *Cell*. **153**, 1194-1217.

Marzetti E, Calvani R, Cesari M, Buford TW, Lorenzi M, Behnke BJ, Leeuwenburgh C (2013). Mitochondrial dysfunction and sarcopenia of aging: from signaling pathways to clinical trials. *Int J Biochem Cell Biol*. **45**, 2288-2301.

Marzetti E, Calvani R, Tosato M, Cesari M, Di Bari M, Cherubini A, Collamati A, D'Angelo E, Pahor M, Bernabei R, Landi F, Consortium S (2017). Sarcopenia: an overview. *Aging Clin Exp Res*. **29**, 11-17.

Marzetti E, Hwang JC, Lees HA, Wohlgemuth SE, Dupont-Versteegden EE, Carter CS, Bernabei R, Leeuwenburgh C (2010). Mitochondrial death effectors: relevance to sarcopenia and disuse muscle atrophy. *Biochim Biophys Acta*. **1800**, 235-244.

Masiero E, Sandri M (2010). Autophagy inhibition induces atrophy and myopathy in adult skeletal muscles. *Autophagy*. **6**, 307-309.

Masuyama M, Iida R, Takatsuka H, Yasuda T, Matsuki T (2005). Quantitative change in mitochondrial DNA content in various mouse tissues during aging. *Biochim Biophys Acta*. **1723**, 302-308.

Matsushima Y, Goto Y, Kaguni LS (2010). Mitochondrial Lon protease regulates mitochondrial DNA copy number and transcription by selective degradation of mitochondrial transcription factor A (TFAM). *Proc Natl Acad Sci U S A*. **107**, 18410-18415.

Matsushima Y, Kaguni LS (2012). Matrix proteases in mitochondrial DNA function. *Biochim Biophys Acta*. **1819**, 1080-1087.

MAURO A (1961). Satellite cell of skeletal muscle fibers. *J Biophys Biochem Cytol*. **9**, 493-495.

McFarlane D, Holbrook TC (2008). Cytokine dysregulation in aged horses and horses with pituitary pars intermedia dysfunction. *J Vet Intern Med*. **22**, 436-442.

McKay BR, Ogborn DI, Baker JM, Toth KG, Tarnopolsky MA, Parise G (2013). Elevated SOCS3 and altered IL-6 signaling is associated with age-related human muscle stem cell dysfunction. *Am J Physiol Cell Physiol*. **304**, C717-728.

McKay BR, Ogborn DI, Bellamy LM, Tarnopolsky MA, Parise G (2012). Myostatin is associated with age-related human muscle stem cell dysfunction. *FASEB J*. **26**, 2509-2521.

McKeever KH (2002). Exercise physiology of the older horse. *Vet Clin North Am Equine Pract*. **18**, 469-490.

McKeever KH, Malinowski K (1997). Exercise capacity in young and old mares. *Am J Vet Res*. **58**, 1468-1472.

McMullen CA, Ferry AL, Gamboa JL, Andrade FH, Dupont-Versteegden EE (2009). Age-related changes of cell death pathways in rat extraocular muscle. *Exp Gerontol*. **44**, 420-425.

Megeney LA, Rudnicki MA (1995). Determination versus differentiation and the MyoD family of transcription factors. *Biochem Cell Biol*. **73**, 723-732.

Menshikova EV, Ritov VB, Fairfull L, Ferrell RE, Kelley DE, Goodpaster BH (2006). Effects of exercise on mitochondrial content and function in aging human skeletal muscle. *J Gerontol A Biol Sci Med Sci*. **61**, 534-540.

Michel S, Wanet A, De Pauw A, Rommelaere G, Arnould T, Renard P (2012). Crosstalk between mitochondrial (dys)function and mitochondrial abundance. *J Cell Physiol*. **227**, 2297-2310.

Miller MS, Lekkas P, Braddock JM, Farman GP, Ballif BA, Irving TC, Maughan DW, Vigoreaux JO (2008). Aging enhances indirect flight muscle fiber performance yet decreases flight ability in Drosophila. *Biophys J*. **95**, 2391-2401.

Mishra P, Chan DC (2016). Metabolic regulation of mitochondrial dynamics. *J Cell Biol*. **212**, 379-387.

Mogensen M, Bagger M, Pedersen PK, Fernström M, Sahlin K (2006). Cycling efficiency in humans is related to low UCP3 content and to type I fibres but not to mitochondrial efficiency. *J Physiol*. **571**, 669-681.

Moore DR, Robinson MJ, Fry JL, Tang JE, Glover EI, Wilkinson SB, Prior T, Tarnopolsky MA, Phillips SM (2009). Ingested protein dose response of muscle and albumin protein synthesis after resistance exercise in young men. *Am J Clin Nutr*. **89**, 161-168.

Moyes CD, Mathieu-Costello OA, Tsuchiya N, Filburn C, Hansford RG (1997). Mitochondrial biogenesis during cellular differentiation. *Am J Physiol*. **272**, C1345-1351.

Muller FL, Liu Y, Van Remmen H (2004). Complex III releases superoxide to both sides of the inner mitochondrial membrane. *J Biol Chem*. **279**, 49064-49073.

Murphy MP (2009). How mitochondria produce reactive oxygen species. *Biochem J*. **417**, 1-13.

Möller P, Bergström J, Fürst P, Hellström K (1980). Effect of aging on energy-rich phosphagens in human skeletal muscles. *Clin Sci (Lond)*. **58**, 553-555.

Nair KS (2005). Aging muscle. *Am J Clin Nutr*. **81**, 953-963.

Nakatogawa H, Suzuki K, Kamada Y, Ohsumi Y (2009). Dynamics and diversity in autophagy mechanisms: lessons from yeast. *Nat Rev Mol Cell Biol*. **10**, 458-467.

Narendra D, Kane LA, Hauser DN, Fearnley IM, Youle RJ (2010). p62/SQSTM1 is required for Parkin-induced mitochondrial clustering but not mitophagy; VDAC1 is dispensable for both. *Autophagy*. **6**, 1090-1106.

Narendra D, Tanaka A, Suen DF, Youle RJ (2008). Parkin is recruited selectively to impaired mitochondria and promotes their autophagy. *J Cell Biol*. **183**, 795-803.

Nilwik R, Snijders T, Leenders M, Groen BB, van Kranenburg J, Verdijk LB, van Loon LJ (2013). The decline in skeletal muscle mass with aging is mainly attributed to a reduction in type II muscle fiber size. *Exp Gerontol*. **48**, 492-498.

Nunnari J, Suomalainen A (2012). Mitochondria: in sickness and in health. *Cell*. **148**, 1145-1159.

O'Connell K, Ohlendieck K (2009). Proteomic DIGE analysis of the mitochondria-enriched fraction from aged rat skeletal muscle. *Proteomics*. **9**, 5509-5524.

Ogata T, Yamasaki Y (1997). Ultra-high-resolution scanning electron microscopy of mitochondria and sarcoplasmic reticulum arrangement in human red, white, and intermediate muscle fibers. *Anat Rec*. **248**, 214-223.

Ogura Y, Iemitsu M, Naito H, Kakigi R, Kakehashi C, Maeda S, Akema T (2011). Single bout of running exercise changes LC3-II expression in rat cardiac muscle. *Biochem Biophys Res Commun*. **414**, 756-760.

Okada S, Nonaka I, Chou SM (1984). Muscle fiber type differentiation and satellite cell populations in normally grown and neonatally denervated muscles in the rat. *Acta Neuropathol*. **65**, 90-98.

Olichon A, Baricault L, Gas N, Guillou E, Valette A, Belenguer P, Lenaers G (2003). Loss of OPA1 perturbates the mitochondrial inner membrane structure and integrity, leading to cytochrome c release and apoptosis. *J Biol Chem*. **278**, 7743-7746.

Pagliarini DJ, Calvo SE, Chang B, Sheth SA, Vafai SB, Ong SE, Walford GA, Sugiana C, Boneh A, Chen WK, Hill DE, Vidal M, Evans JG, Thorburn DR, Carr SA, Mootha VK (2008). A mitochondrial protein compendium elucidates complex I disease biology. *Cell*. **134**, 112-123.

Palikaras K, Lionaki E, Tavernarakis N (2015). Balancing mitochondrial biogenesis and mitophagy to maintain energy metabolism homeostasis. *Cell Death Differ*. **22**, 1399-1401.

Palmer CS, Osellame LD, Stojanovski D, Ryan MT (2011). The regulation of mitochondrial morphology: intricate mechanisms and dynamic machinery. *Cell Signal*. **23**, 1534-1545.

Pankiv S, Clausen TH, Lamark T, Brech A, Bruun JA, Outzen H, Øvervatn A, Bjørkøy G, Johansen T (2007). p62/SQSTM1 binds directly to Atg8/LC3 to facilitate degradation of ubiquitinated protein aggregates by autophagy. *J Biol Chem*. **282**, 24131-24145.

Pastoris O, Boschi F, Verri M, Baiardi P, Felzani G, Vecchiet J, Dossena M, Catapano M (2000). The effects of aging on enzyme activities and metabolite concentrations in skeletal muscle from sedentary male and female subjects. *Exp Gerontol*. **35**, 95-104.

Pehme A, Alev K, Kaasik P, Seene T (2004). Age-related changes in skeletal-muscle myosin heavy-chain composition: effect of mechanical loading. *J Aging Phys Act*. **12**, 29-44.

Pellegrino MW, Nargund AM, Haynes CM (2013). Signaling the mitochondrial unfolded protein response. *Biochim Biophys Acta*. **1833**, 410-416.

Pesce V, Cormio A, Fracasso F, Lezza AM, Cantatore P, Gadaleta MN (2005). Age-related changes of mitochondrial DNA content and mitochondrial genotypic and phenotypic alterations in rat hind-limb skeletal muscles. *J Gerontol A Biol Sci Med Sci*. **60**, 715-723.

Pesce V, Cormio A, Fracasso F, Vecchiet J, Felzani G, Lezza AM, Cantatore P, Gadaleta MN (2001). Age-related mitochondrial genotypic and phenotypic alterations in human skeletal muscle. *Free Radic Biol Med*. **30**, 1223-1233.

Pesta D, Gnaiger E (2012). High-resolution respirometry: OXPHOS protocols for human cells and permeabilized fibers from small biopsies of human muscle. *Methods Mol Biol*. **810**, 25-58.

Peterson CM, Johannsen DL, Ravussin E (2012). Skeletal muscle mitochondria and aging: a review. *J Aging Res*. **2012**, 194821.

Pette D (2002). The adaptive potential of skeletal muscle fibers. *Can J Appl Physiol*. **27**, 423-448.

Pette D, Staron RS (2000). Myosin isoforms, muscle fiber types, and transitions. *Microsc Res Tech*. **50**, 500-509.

Phillips T, Leeuwenburgh C (2005). Muscle fiber specific apoptosis and TNF-alpha signaling in sarcopenia are attenuated by life-long calorie restriction. *FASEB J*. **19**, 668-670.

Piantadosi CA, Suliman HB (2012). Redox regulation of mitochondrial biogenesis. *Free Radic Biol Med*. **53**, 2043-2053.

Picard M, Csukly K, Robillard ME, Godin R, Ascah A, Bourcier-Lucas C, Burelle Y (2008). Resistance to Ca2+-induced opening of the permeability transition pore differs in mitochondria from glycolytic and oxidative muscles. *Am J Physiol Regul Integr Comp Physiol*. **295**, R659-668.

Picard M, Ritchie D, Thomas MM, Wright KJ, Hepple RT (2011a). Alterations in intrinsic mitochondrial function with aging are fiber type-specific and do not explain differential atrophy between muscles. *Aging Cell*. **10**, 1047-1055.

Picard M, Ritchie D, Wright KJ, Romestaing C, Thomas MM, Rowan SL, Taivassalo T, Hepple RT (2010). Mitochondrial functional impairment with aging is exaggerated in isolated mitochondria compared to permeabilized myofibers. *Aging Cell*. **9**, 1032-1046.

Picard M, Taivassalo T, Ritchie D, Wright KJ, Thomas MM, Romestaing C, Hepple RT (2011b). Mitochondrial structure and function are disrupted by standard isolation methods. *PLoS One*. **6**, e18317.

Preston CC, Oberlin AS, Holmuhamedov EL, Gupta A, Sagar S, Syed RH, Siddiqui SA, Raghavakaimal S, Terzic A, Jahangir A (2008). Aging-induced alterations in gene transcripts and functional activity of mitochondrial oxidative phosphorylation complexes in the heart. *Mech Ageing Dev*. **129**, 304-312.

Pugh TD, Conklin MW, Evans TD, Polewski MA, Barbian HJ, Pass R, Anderson BD, Colman RJ, Eliceiri KW, Keely PJ, Weindruch R, Beasley TM, Anderson RM (2013). A shift in energy metabolism anticipates the onset of sarcopenia in rhesus monkeys. *Aging Cell*. **12**, 672-681.

Purves-Smith FM, Sgarioto N, Hepple RT (2014). Fiber typing in aging muscle. *Exerc Sport Sci Rev*. **42**, 45-52.

Rana A, Rera M, Walker DW (2013). Parkin overexpression during aging reduces proteotoxicity, alters mitochondrial dynamics, and extends lifespan. *Proc Natl Acad Sci U S A*. **110**, 8638-8643.

Reed SA, LaVigne EK, Jones AK, Patterson DF, Schauer AL (2015). HORSE SPECIES SYMPOSIUM: The aging horse: Effects of inflammation on muscle satellite cells. *J Anim Sci*. **93**, 862-870.

Relaix F, Montarras D, Zaffran S, Gayraud-Morel B, Rocancourt D, Tajbakhsh S, Mansouri A, Cumano A, Buckingham M (2006). Pax3 and Pax7 have distinct and overlapping functions in adult muscle progenitor cells. *J Cell Biol*. **172**, 91-102.

Relaix F, Rocancourt D, Mansouri A, Buckingham M (2005). A Pax3/Pax7-dependent population of skeletal muscle progenitor cells. *Nature*. **435**, 948-953.

Remels AH, Langen RC, Schrauwen P, Schaart G, Schols AM, Gosker HR (2010). Regulation of mitochondrial biogenesis during myogenesis. *Mol Cell Endocrinol*. **315**, 113-120.

Renault V, Piron-Hamelin G, Forestier C, DiDonna S, Decary S, Hentati F, Saillant G, Butler-Browne GS, Mouly V (2000). Skeletal muscle regeneration and the mitotic clock. *Exp Gerontol*. **35**, 711-719.

Rera M, Bahadorani S, Cho J, Koehler CL, Ulgherait M, Hur JH, Ansari WS, Lo T, Jones DL, Walker DW (2011). Modulation of longevity and tissue homeostasis by the Drosophila PGC-1 homolog. *Cell Metab*. **14**, 623-634.

Revold T, Mykkänen AK, Karlström K, Ihler CF, Pösö AR, Essén-Gustavsson B (2010). Effects of training on equine muscle fibres and monocarboxylate transporters in young Coldblooded Trotters. *Equine Vet J Suppl*, 289-295.

Rietbroek NJ, Dingboom EG, Joosten BJ, Eizema K, Everts ME (2007). Effect of show jumping training on the development of locomotory muscle in young horses. *Am J Vet Res*. **68**, 1232-1238.

Rimbert V, Boirie Y, Bedu M, Hocquette JF, Ritz P, Morio B (2004). Muscle fat oxidative capacity is not impaired by age but by physical inactivity: association with insulin sensitivity. *FASEB J*. **18**, 737-739.

Ringholm S, Olesen J, Pedersen JT, Brandt CT, Halling JF, Hellsten Y, Prats C, Pilegaard H (2013). Effect of lifelong resveratrol supplementation and exercise training on skeletal muscle oxidative capacity in aging mice; impact of PGC-1α. *Exp Gerontol*. **48**, 1311-1318.

Ritov VB, Menshikova EV, Kelley DE (2006). Analysis of cardiolipin in human muscle biopsy. *J Chromatogr B Analyt Technol Biomed Life Sci*. **831**, 63-71.

Rivero JL, Galisteo AM, Agüera E, Miró F (1993). Skeletal muscle histochemistry in male and female Andalusian and Arabian horses of different ages. *Res Vet Sci*. **54**, 160-169.

Rivero JL, Talmadge RJ, Edgerton VR (1997). A sensitive electrophoretic method for the quantification of myosin heavy chain isoforms in horse skeletal muscle: histochemical and immunocytochemical verifications. *Electrophoresis*. **18**, 1967-1972.

Rogers MA, Hagberg JM, Martin WH, Ehsani AA, Holloszy JO (1990). Decline in VO2max with aging in master athletes and sedentary men. *J Appl Physiol (1985)*. **68**, 2195-2199.

Romanello V, Sandri M (2015). Mitochondrial Quality Control and Muscle Mass Maintenance. *Front Physiol*. **6**, 422.

Ronéus M (1993). Muscle characteristics in standardbreds of different ages and sexes. *Equine Vet J*. **25**, 143-146.

Ronéus M, Lindholm A, Asheim A (1991). Muscle characteristics in Thoroughbreds of different ages and sexes. *Equine Vet J*. **23**, 207-210.

Rooyackers OE, Adey DB, Ades PA, Nair KS (1996). Effect of age on in vivo rates of mitochondrial protein synthesis in human skeletal muscle. *Proc Natl Acad Sci U S A*. **93**, 15364-15369.

Rossi DJ, Bryder D, Seita J, Nussenzweig A, Hoeijmakers J, Weissman IL (2007). Deficiencies in DNA damage repair limit the function of haematopoietic stem cells with age. *Nature*. **447**, 725-729.

Rossignol R, Letellier T, Malgat M, Rocher C, Mazat JP (2000). Tissue variation in the control of oxidative phosphorylation: implication for mitochondrial diseases. *Biochem J*. **347 Pt 1**, 45-53.

Roth SM, Ferrell RF, Hurley BF (2000a). Strength training for the prevention and treatment of sarcopenia. *J Nutr Health Aging*. **4**, 143-155.

Roth SM, Martel GF, Ivey FM, Lemmer JT, Metter EJ, Hurley BF, Rogers MA (2000b). Skeletal muscle satellite cell populations in healthy young and older men and women. *Anat Rec*. **260**, 351-358.

Roubenoff R (2001). Origins and clinical relevance of sarcopenia. *Can J Appl Physiol*. **26**, 78-89.

Ruas JL, White JP, Rao RR, Kleiner S, Brannan KT, Harrison BC, Greene NP, Wu J, Estall JL, Irving BA, Lanza IR, Rasbach KA, Okutsu M, Nair KS, Yan Z, Leinwand LA, Spiegelman BM (2012). A PGC-1α isoform induced by resistance training regulates skeletal muscle hypertrophy. *Cell*. **151**, 1319-1331.

Rudnicki MA, Braun T, Hinuma S, Jaenisch R (1992). Inactivation of MyoD in mice leads to up-regulation of the myogenic HLH gene Myf-5 and results in apparently normal muscle development. *Cell*. **71**, 383-390.

Rudnicki MA, Le Grand F, McKinnell I, Kuang S (2008). The molecular regulation of muscle stem cell function. *Cold Spring Harb Symp Quant Biol*. **73**, 323-331.

Ryall JG, Dell'Orso S, Derfoul A, Juan A, Zare H, Feng X, Clermont D, Koulnis M, Gutierrez-Cruz G, Fulco M, Sartorelli V (2015). The NAD(+)-dependent SIRT1 deacetylase translates a metabolic switch into regulatory epigenetics in skeletal muscle stem cells. *Cell Stem Cell*. **16**, 171-183.

Ryan MT, Hoogenraad NJ (2007). Mitochondrial-nuclear communications. *Annu Rev Biochem*. **76**, 701-722.

Safdar A, Bourgeois JM, Ogborn DI, Little JP, Hettinga BP, Akhtar M, Thompson JE, Melov S, Mocellin NJ, Kujoth GC, Prolla TA, Tarnopolsky MA (2011). Endurance exercise rescues progeroid aging and induces systemic mitochondrial rejuvenation in mtDNA mutator mice. *Proc Natl Acad Sci U S A*. **108**, 4135-4140.

Safdar A, Hamadeh MJ, Kaczor JJ, Raha S, Debeer J, Tarnopolsky MA (2010). Aberrant mitochondrial homeostasis in the skeletal muscle of sedentary older adults. *PLoS One*. **5**, e10778.

Saks VA, Belikova YO, Kuznetsov AV, Khuchua ZA, Branishte TH, Semenovsky ML, Naumov VG (1991). Phosphocreatine pathway for energy transport: ADP diffusion and cardiomyopathy. *Am J Physiol*. **261**, 30-38.

Saks VA, Veksler VI, Kuznetsov AV, Kay L, Sikk P, Tiivel T, Tranqui L, Olivares J, Winkler K, Wiedemann F, Kunz WS (1998). Permeabilized cell and skinned fiber techniques in studies of mitochondrial function in vivo. *Mol Cell Biochem*. **184**, 81-100.

Sambasivan R, Yao R, Kissenpfennig A, Van Wittenberghe L, Paldi A, Gayraud-Morel B, Guenou H, Malissen B, Tajbakhsh S, Galy A (2011). Pax7-expressing satellite cells are indispensable for adult skeletal muscle regeneration. *Development*. **138**, 3647-3656.

Seo AY, Joseph AM, Dutta D, Hwang JC, Aris JP, Leeuwenburgh C (2010). New insights into the role of mitochondria in aging: mitochondrial dynamics and more. *J Cell Sci*. **123**, 2533-2542.

Scarpulla RC (2008). Transcriptional paradigms in mammalian mitochondrial biogenesis and function. *Physiol Rev*. **88**, 611-638.

Schiavi A, Maglioni S, Palikaras K, Shaik A, Strappazzon F, Brinkmann V, Torgovnick A, Castelein N, De Henau S, Braeckman BP, Cecconi F, Tavernarakis N, Ventura N (2015). Iron-Starvation-Induced Mitophagy Mediates Lifespan Extension upon Mitochondrial Stress in C. elegans. *Curr Biol*. **25**, 1810-1822.

Schmalbruch H, Hellhammer U (1977). The number of nuclei in adult rat muscles with special reference to satellite cells. *Anat Rec*. **189**, 169-175.

Schultz E (1974). A quantitative study of the satellite cell population in postnatal mouse lumbrical muscle. *Anat Rec*. **180**, 589-595.

Schultz E, Lipton BH (1982). Skeletal muscle satellite cells: changes in proliferation potential as a function of age. *Mech Ageing Dev*. **20**, 377-383.

Schwerzmann K, Hoppeler H, Kayar SR, Weibel ER (1989). Oxidative capacity of muscle and mitochondria: correlation of physiological, biochemical, and morphometric characteristics. *Proc Natl Acad Sci U S A*. **86**, 1583-1587.

Sczelecki S, Besse-Patin A, Abboud A, Kleiner S, Laznik-Bogoslavski D, Wrann CD, Ruas JL, Haibe-Kains B, Estall JL (2014). Loss of Pgc-1α expression in aging mouse muscle potentiates glucose intolerance and systemic inflammation. *Am J Physiol Endocrinol Metab*. **306**, E157-167.

Seale P, Sabourin LA, Girgis-Gabardo A, Mansouri A, Gruss P, Rudnicki MA (2000). Pax7 is required for the specification of myogenic satellite cells. *Cell*. **102**, 777-786.

Sebastián D, Sorianello E, Segalés J, Irazoki A, Ruiz-Bonilla V, Sala D, Planet E, Berenguer-Llergo A, Muñoz JP, Sánchez-Feutrie M, Plana N, Hernández-Álvarez MI, Serrano AL, Palacín M, Zorzano A (2016). Mfn2 deficiency links age-related sarcopenia and impaired autophagy to activation of an adaptive mitophagy pathway. *EMBO J*. **35**, 1677-1693.

Serrano AL, Quiroz-Rothe E, Rivero JL (2000). Early and long-term changes of equine skeletal muscle in response to endurance training and detraining. *Pflugers Arch*. **441**, 263-274.

Shadrach JL, Wagers AJ (2011). Stem cells for skeletal muscle repair. *Philos Trans R Soc Lond B Biol Sci*. **366**, 2297-2306.

Sharpless NE, DePinho RA (2007). How stem cells age and why this makes us grow old. *Nat Rev Mol Cell Biol*. **8**, 703-713.

Shefer G, Van de Mark DP, Richardson JB, Yablonka-Reuveni Z (2006). Satellite-cell pool size does matter: defining the myogenic potency of aging skeletal muscle. *Dev Biol*. **294**, 50-66.

Shigenaga MK, Hagen TM, Ames BN (1994). Oxidative damage and mitochondrial decay in aging. *Proc Natl Acad Sci U S A*. **91**, 10771-10778.

Shirendeb UP, Calkins MJ, Manczak M, Anekonda V, Dufour B, McBride JL, Mao P, Reddy PH (2012). Mutant huntingtin's interaction with mitochondrial protein Drp1 impairs mitochondrial biogenesis and causes defective axonal transport and synaptic degeneration in Huntington's disease. *Hum Mol Genet*. **21**, 406-420.

Short KR, Bigelow ML, Kahl J, Singh R, Coenen-Schimke J, Raghavakaimal S, Nair KS (2005). Decline in skeletal muscle mitochondrial function with aging in humans. *Proc Natl Acad Sci U S A*. **102**, 5618-5623.

Short KR, Vittone JL, Bigelow ML, Proctor DN, Nair KS (2004). Age and aerobic exercise training effects on whole body and muscle protein metabolism. *Am J Physiol Endocrinol Metab*. **286**, E92-101.

Short KR, Vittone JL, Bigelow ML, Proctor DN, Rizza RA, Coenen-Schimke JM, Nair KS (2003). Impact of aerobic exercise training on age-related changes in insulin sensitivity and muscle oxidative capacity. *Diabetes*. **52**, 1888-1896.

Siegel MP, Kruse SE, Percival JM, Goh J, White CC, Hopkins HC, Kavanagh TJ, Szeto HH, Rabinovitch PS, Marcinek DJ (2013). Mitochondrial-targeted peptide rapidly improves mitochondrial energetics and skeletal muscle performance in aged mice. *Aging Cell*. **12**, 763-771.

Sin J, Andres AM, Taylor DJ, Weston T, Hiraumi Y, Stotland A, Kim BJ, Huang C, Doran KS, Gottlieb RA (2016). Mitophagy is required for mitochondrial biogenesis and myogenic differentiation of C2C12 myoblasts. *Autophagy*. **12**, 369-380.

Smits P, Smeitink J, van den Heuvel L (2010). Mitochondrial translation and beyond: processes implicated in combined oxidative phosphorylation deficiencies. *J Biomed Biotechnol*. **2010**, 737385.

Snow MH (1983). A quantitative ultrastructural analysis of satellite cells in denervated fast and slow muscles of the mouse. *Anat Rec*. **207**, 593-604.

Sousa-Victor P, Gutarra S, García-Prat L, Rodriguez-Ubreva J, Ortet L, Ruiz-Bonilla V, Jardí M, Ballestar E, González S, Serrano AL, Perdiguero E, Muñoz-Cánoves P (2014). Geriatric muscle stem cells switch reversible quiescence into senescence. *Nature*. **506**, 316-321.

Speakman JR, Talbot DA, Selman C, Snart S, McLaren JS, Redman P, Krol E, Jackson DM, Johnson MS, Brand MD (2004). Uncoupled and surviving: individual mice with high metabolism have greater mitochondrial uncoupling and live longer. *Aging Cell*. **3**, 87-95.

Spinazzi M, Casarin A, Pertegato V, Salviati L, Angelini C (2012). Assessment of mitochondrial respiratory chain enzymatic activities on tissues and cultured cells. *Nat Protoc*. **7**, 1235-1246.

Staunton L, O'Connell K, Ohlendieck K (2011). Proteomic Profiling of Mitochondrial Enzymes during Skeletal Muscle Aging. *J Aging Res*. **2011**, 908035.

Stein LR, Imai S (2014). Specific ablation of Nampt in adult neural stem cells recapitulates their functional defects during aging. *EMBO J*. **33**, 1321-1340.

Su J, Ekman C, Oskolkov N, Lahti L, Ström K, Brazma A, Groop L, Rung J, Hansson O (2015). A novel atlas of gene expression in human skeletal muscle reveals molecular changes associated with aging. *Skelet Muscle*. **5**, 35.

Sugiura T, Matoba H, Miyata H, Kawai Y, Murakami N (1992). Myosin heavy chain isoform transition in ageing fast and slow muscles of the rat. *Acta Physiol Scand*. **144**, 419-423.

Sugiyama S, Takasawa M, Hayakawa M, Ozawa T (1993). Changes in skeletal muscle, heart and liver mitochondrial electron transport activities in rats and dogs of various ages. *Biochem Mol Biol Int*. **30**, 937-944.

Sullivan VK, Powers SK, Criswell DS, Tumer N, Larochelle JS, Lowenthal D (1995). Myosin heavy chain composition in young and old rat skeletal muscle: effects of endurance exercise. *J Appl Physiol (1985)*. **78**, 2115-2120.

Sun N, Youle RJ, Finkel T (2016). The Mitochondrial Basis of Aging. *Mol Cell*. **61**, 654-666.

Talmadge RJ, Roy RR (1993). Electrophoretic separation of rat skeletal muscle myosin heavy-chain isoforms. *J Appl Physiol (1985)*. **75**, 2337-2340.

Tanaka A, Cleland MM, Xu S, Narendra DP, Suen DF, Karbowski M, Youle RJ (2010). Proteasome and p97 mediate mitophagy and degradation of mitofusins induced by Parkin. *J Cell Biol*. **191**, 1367-1380.

Tanaka Y, Guhde G, Suter A, Eskelinen EL, Hartmann D, Lüllmann-Rauch R, Janssen PM, Blanz J, von Figura K, Saftig P (2000). Accumulation of autophagic vacuoles and cardiomyopathy in LAMP-2-deficient mice. *Nature*. **406**, 902-906.

Taylor CR, Maloiy GM, Weibel ER, Langman VA, Kamau JM, Seeherman HJ, Heglund NC (1981). Design of the mammalian respiratory system. III Scaling maximum aerobic capacity to body mass: wild and domestic mammals. *Respir Physiol*. **44**, 25-37.

Terman A (1995). The effect of age on formation and elimination of autophagic vacuoles in mouse hepatocytes. *Gerontology*. **41 Suppl 2**, 319-326.

Terman A, Kurz T, Navratil M, Arriaga EA, Brunk UT (2010). Mitochondrial turnover and aging of long-lived postmitotic cells: the mitochondrial-lysosomal axis theory of aging. *Antioxid Redox Signal*. **12**, 503-535.

Thompson LV, Brown M (1999). Age-related changes in contractile properties of single skeletal fibers from the soleus muscle. *J Appl Physiol (1985)*. **86**, 881-886.

Toledo M, Busquets S, Ametller E, López-Soriano FJ, Argilés JM (2011). Sirtuin 1 in skeletal muscle of cachectic tumour-bearing rats: a role in impaired regeneration? *J Cachexia Sarcopenia Muscle*. **2**, 57-62.

Twig G, Elorza A, Molina AJ, Mohamed H, Wikstrom JD, Walzer G, Stiles L, Haigh SE, Katz S, Las G, Alroy J, Wu M, Py BF, Yuan J, Deeney JT, Corkey BE, Shirihai OS (2008). Fission and selective fusion govern mitochondrial segregation and elimination by autophagy. *EMBO J*. **27**, 433-446.

Twig G, Shirihai OS (2011). The interplay between mitochondrial dynamics and mitophagy. *Antioxid Redox Signal*. **14**, 1939-1951.

Valberg S (2013). Muscle anatomy, physiology and adaptations to exercise and training. In: *The Athletic Horse: Principles and Practice of Equine Sports Medicine*, St. Louis, MO: Elsevier/Saunders. 174-201.

van den Hoven R, Wensing T, Breukink HJ, Meijer AE, Kruip TA (1985). Variation of fiber types in the triceps brachii, longissimus dorsi, gluteus medius, and biceps femoris of horses. *Am J Vet Res*. **46**, 939-941.

van der Bliek AM, Shen Q, Kawajiri S (2013). Mechanisms of mitochondrial fission and fusion. *Cold Spring Harb Perspect Biol*. **5**.

Verdijk LB, Koopman R, Schaart G, Meijer K, Savelberg HH, van Loon LJ (2007). Satellite cell content is specifically reduced in type II skeletal muscle fibers in the elderly. *Am J Physiol Endocrinol Metab*. **292**, E151-157.

Verdijk LB, Snijders T, Drost M, Delhaas T, Kadi F, van Loon LJ (2014). Satellite cells in human skeletal muscle; from birth to old age. *Age (Dordr)*. **36**, 545-547.

Vermulst M, Wanagat J, Kujoth GC, Bielas JH, Rabinovitch PS, Prolla TA, Loeb LA (2008). DNA deletions and clonal mutations drive premature aging in mitochondrial mutator mice. *Nat Genet*. **40**, 392-394.

Verney J, Kadi F, Charifi N, Féasson L, Saafi MA, Castells J, Piehl-Aulin K, Denis C (2008). Effects of combined lower body endurance and upper body resistance training on the satellite cell pool in elderly subjects. *Muscle Nerve*. **38**, 1147-1154.

Villani G, Attardi G (1997). In vivo control of respiration by cytochrome c oxidase in wild-type and mitochondrial DNA mutation-carrying human cells. *Proc Natl Acad Sci U S A*. **94**, 1166-1171.

Villani G, Greco M, Papa S, Attardi G (1998). Low reserve of cytochrome c oxidase capacity in vivo in the respiratory chain of a variety of human cell types. *J Biol Chem*. **273**, 31829-31836.

Villeda SA, Luo J, Mosher KI, Zou B, Britschgi M, Bieri G, Stan TM, Fainberg N, Ding Z, Eggel A, Lucin KM, Czirr E, Park JS, Couillard-Després S, Aigner L, Li G, Peskind ER, Kaye JA, Quinn JF, Galasko DR, Xie XS, Rando TA, Wyss-Coray T (2011). The ageing systemic milieu negatively regulates neurogenesis and cognitive function. *Nature*. **477**, 90-94.

Viña J, Gomez-Cabrera MC, Borras C, Froio T, Sanchis-Gomar F, Martinez-Bello VE, Pallardo FV (2009). Mitochondrial biogenesis in exercise and in ageing. *Adv Drug Deliv Rev*. **61**, 1369-1374.

Votion DM, Fraipont A, Goachet AG, Robert C, van Erck E, Amory H, Ceusters J, de la Rebière de Pouyade G, Franck T, Mouithys-Mickalad A, Niesten A, Serteyn D (2010). Alterations in mitochondrial respiratory function in response to endurance training and endurance racing. *Equine Vet J Suppl*, 268-274.

Votion DM, Gnaiger E, Lemieux H, Mouithys-Mickalad A, Serteyn D (2012). Physical fitness and mitochondrial respiratory capacity in horse skeletal muscle. *PLoS One*. **7**, e34890.

Wagatsuma A, Kotake N, Yamada S (2011). Muscle regeneration occurs to coincide with mitochondrial biogenesis. *Mol Cell Biochem*. **349**, 139-147.

Wagatsuma A, Sakuma K (2013). Mitochondria as a potential regulator of myogenesis. *ScientificWorldJournal*. **2013**, 593267.

Wagers AJ, Conboy IM (2005). Cellular and molecular signatures of muscle regeneration: current concepts and controversies in adult myogenesis. *Cell*. **122**, 659-667.

Wagner AL, Urschel KL, Betancourt A, Adams AA, Horohov DW (2013). Effects of advanced age on whole-body protein synthesis and skeletal muscle mechanistic target of rapamycin signaling in horses. *Am J Vet Res*. **74**, 1433-1442.

Wai T, Langer T (2016). Mitochondrial Dynamics and Metabolic Regulation. *Trends Endocrinol Metab*. **27**, 105-117.

Wallace DC (2005). A mitochondrial paradigm of metabolic and degenerative diseases, aging, and cancer: a dawn for evolutionary medicine. *Annu Rev Genet*. **39**, 359-407.

Walsh B, Tonkonogi M, Söderlund K, Hultman E, Saks V, Sahlin K (2001). The role of phosphorylcreatine and creatine in the regulation of mitochondrial respiration in human skeletal muscle. *J Physiol*. **537**, 971-978.

Wang Y, Michikawa Y, Mallidis C, Bai Y, Woodhouse L, Yarasheski KE, Miller CA, Askanas V, Engel WK, Bhasin S, Attardi G (2001). Muscle-specific mutations accumulate with aging in critical human mtDNA control sites for replication. *Proc Natl Acad Sci U S A*. **98**, 4022-4027.

Wang Y, Pessin JE (2013). Mechanisms for fiber-type specificity of skeletal muscle atrophy. *Curr Opin Clin Nutr Metab Care*. **16**, 243-250.

Warren GL, Hulderman T, Jensen N, McKinstry M, Mishra M, Luster MI, Simeonova PP (2002). Physiological role of tumor necrosis factor alpha in traumatic muscle injury. *FASEB J*. **16**, 1630-1632.

Welle S, Bhatt K, Shah B, Needler N, Delehanty JM, Thornton CA (2003a). Reduced amount of mitochondrial DNA in aged human muscle. *J Appl Physiol (1985)*. **94**, 1479-1484.

Welle S, Bhatt K, Thornton CA (2000). High-abundance mRNAs in human muscle: comparison between young and old. *J Appl Physiol (1985)*. **89**, 297-304.

Welle S, Brooks AI, Delehanty JM, Needler N, Thornton CA (2003b). Gene expression profile of aging in human muscle. *Physiol Genomics*. **14**, 149-159.

Welle S, Thornton C, Jozefowicz R, Statt M (1993). Myofibrillar protein synthesis in young and old men. *Am J Physiol*. **264**, E693-698.

Wenz T (2013). Regulation of mitochondrial biogenesis and PGC-1α under cellular stress. *Mitochondrion*. **13**, 134-142.

Westermann B (2010). Mitochondrial fusion and fission in cell life and death. *Nat Rev Mol Cell Biol*. **11**, 872-884.

White SH, Warren LK, Li C, Wohlgemuth S (2015). Mitochondrial adaptations to submaximal exercise training in the gluteus medius and triceps brachii of young equine athletes. *J Equine Vet Sci*. **35**, 395.

Wohlgemuth SE, Seo AY, Marzetti E, Lees HA, Leeuwenburgh C (2010). Skeletal muscle autophagy and apoptosis during aging: effects of calorie restriction and life-long exercise. *Exp Gerontol*. **45**, 138-148.

Wojtysiak D, Połtowicz K (2014). Carcass quality, physico-chemical parameters, muscle fibre traits and myosin heavy chain composition of m. longissimus lumborum from Puławska and Polish Large White pigs. *Meat Sci*. **97**, 395-403.

Wozniak AC, Anderson JE (2007). Nitric oxide-dependence of satellite stem cell activation and quiescence on normal skeletal muscle fibers. *Dev Dyn*. **236**, 240-250.

Wu JJ, Liu J, Chen EB, Wang JJ, Cao L, Narayan N, Fergusson MM, Rovira II, Allen M, Springer DA, Lago CU, Zhang S, DuBois W, Ward T, deCabo R, Gavrilova O, Mock B, Finkel T (2013). Increased mammalian lifespan and a segmental and tissue-specific slowing of aging after genetic reduction of mTOR expression. *Cell Rep*. **4**, 913-920.

Wu JJ, Quijano C, Chen E, Liu H, Cao L, Fergusson MM, Rovira II, Gutkind S, Daniels MP, Komatsu M, Finkel T (2009). Mitochondrial dysfunction and oxidative stress mediate the physiological impairment induced by the disruption of autophagy. *Aging (Albany NY)*. **1**, 425-437.

Wu Z, Puigserver P, Andersson U, Zhang C, Adelmant G, Mootha V, Troy A, Cinti S, Lowell B, Scarpulla RC, Spiegelman BM (1999). Mechanisms controlling mitochondrial biogenesis and respiration through the thermogenic coactivator PGC-1. *Cell*. **98**, 115-124.

Xie Z, Klionsky DJ (2007). Autophagosome formation: core machinery and adaptations. *Nat Cell Biol*. **9**, 1102-1109.

Yarasheski KE (2003). Exercise, aging, and muscle protein metabolism. *J Gerontol A Biol Sci Med Sci*. **58**, M918-922.

Yarasheski KE, Welle S, Nair KS (2002). Muscle protein synthesis in younger and older men. *JAMA*. **287**, 317-318.

Yoon YS, Yoon DS, Lim IK, Yoon SH, Chung HY, Rojo M, Malka F, Jou MJ, Martinou JC, Yoon G (2006). Formation of elongated giant mitochondria in DFO-induced cellular senescence: involvement of enhanced fusion process through modulation of Fis1. *J Cell Physiol*. **209**, 468-480.

Youle RJ, Narendra DP (2011). Mechanisms of mitophagy. *Nat Rev Mol Cell Biol*. **12**, 9-14.

Zhang H, Ryu D, Wu Y, Gariani K, Wang X, Luan P, D'Amico D, Ropelle ER, Lutolf MP, Aebersold R, Schoonjans K, Menzies KJ, Auwerx J (2016). NAD^+ repletion improves mitochondrial and stem cell function and enhances life span in mice. *Science*. **352**, 1436-1443.

Zhou J, Chong SY, Lim A, Singh BK, Sinha RA, Salmon AB, Yen PM (2017). Changes in macroautophagy, chaperone-mediated autophagy, and mitochondrial metabolism in murine skeletal and cardiac muscle during aging. *Aging (Albany NY)*. **9**, 583-599.

Zhu J, Wang KZ, Chu CT (2013). After the banquet: mitochondrial biogenesis, mitophagy, and cell survival. *Autophagy*. **9**, 1663-1676.

BIOGRAPHICAL SKETCH

Chengcheng Li was born in Qingdao, Shandong, People's Republic of China. She finished her high school at her hometown, where she was an honor student and received scholarships several times. In 2005, she attended the Shandong Agricultural University with a major in animal science. In the four years she spent in college, she received continued Academic Excellence Scholarship and graduated in 2009. Following that, Chengcheng pursued a Master of Science degree in animal nutrition and feed science program, where she started to get interested in the cellular and molecular biology. In 2012, she graduated with an Outstanding Graduate Student Award. After taking a year off from school, Chengcheng was admitted at the University of Florida under the Doctor of Philosophy in Animal Molecular & Cellular Biology program. During her PhD life, Chengcheng received Graduate Assistanship fellowship. She was also awarded Outstanding Academic Achievement and Susan Meg Weinstein Animal Sciences Graduate Scholarship, and she completed her PhD in the summer of 2017. Upon completion of her PhD degree, Chengcheng plans to continue biology research as a post-doctoral scholar in United States and explore more in the molecular and cellular biology related fields.